NUREG/CR-2331
BNL-NUREG-51454
VOL. 4, NO. 4

SAFETY RESEARCH PROGRAMS SPONSORED BY OFFICE OF NUCLEAR REGULATORY RESEARCH

QUARTERLY PROGRESS REPORT
OCTOBER 1 — DECEMBER 31, 1984

Date Published — May 1985

DEPARTMENT OF NUCLEAR ENERGY, BROOKHAVEN NATIONAL LABORATORY
UPTON, NEW YORK 11973

Prepared for the U.S. Nuclear Regulatory Commission
Office of Nuclear Regulatory Research
Contract No. DE-AC02-76CH00016

NUREG/CR-2331
BNL-NUREG-51454
VOL. 4, NO. 4
AN, R-1,4,5,7,8, RD

SAFETY RESEARCH PROGRAMS SPONSORED BY OFFICE OF NUCLEAR REGULATORY RESEARCH

QUARTERLY PROGRESS REPORT
OCTOBER 1 — DECEMBER 31, 1984

Herbert J.C. Kouts, Department Chairman
Walter Y. Kato, Deputy Chairman

Principal Investigators:

R.A. Bari	J.N. O'Brien
J.L. Boccio	W.T. Pratt
R.J. Cerbone	M. Reich
T. Ginsberg	P. Saha
G.A. Greene	C. Sastre
J.G. Guppy	J.H. Taylor
R.E. Hall	D. van Rooyen
W.J. Luckas, Jr.	W. Wulff

Compiled by: Allen J. Weiss
Manuscript Completed March 1985

DEPARTMENT OF NUCLEAR ENERGY
BROOKHAVEN NATIONAL LABORATORY, ASSOCIATED UNIVERSITIES, INC.
UPTON, NEW YORK 11973

Prepared for the
OFFICE OF NUCLEAR REGULATORY RESEARCH
U.S. NUCLEAR REGULATORY COMMISSION
CONTRACT NO. DE-AC02-76CH00016
FIN NOS. A-3014,-3015,-3016,-3024,-3208,-3215,-3226,-3227,-3242,
-3266,-3268,-3270,-3271,-3272,-3274,-3275,-3277

Available from
Superintendent of Documents
U.S. Government Printing Office
P.O. Box 37082
Washington, DC 20013-7982
and
National Technical Information Service
Springfield, Virginia 22161

FOREWORD

The Advanced and Water Reactor Safety Research Programs Quarterly Progress Reports have been combined and are included in this report entitled, "Safety Research Programs Sponsored by the Office of Nuclear Regulatory Research - Quarterly Progress Report." This progress report will describe current activities and technical progress in the programs at Brookhaven National Laboratory sponsored by the Division of Accident Evaluation, Division of Engineering Technology, and Division of Risk Analysis and Operations of the U. S. Nuclear Regulatory Commission, Office of Nuclear Regulatory Research.

The projects reported are the following: High Temperature Reactor Research, SSC/MINET Development, Validation and Application, Thermal-Hydraulic Reactor Safety Experiments, Plant Analyzer, Code Assessment and Application, Code Maintenance (RAMONA-3B), Calculational Quality Assurance in Support of PTS; Stress Corrosion Cracking of PWR Steam Generator Tubing, Probability Based Load Combinations for Design of Category I Structures, Soil-Structure Interaction Evaluations, Identification of Age Related Failure Modes; Application of HRA/PRA Results to Resolve Human Reliability and Human Factors Safety Issues, PRA Technology Transfer Program, Emergency Action Levels, and Protective Action Decisionmaking. The previous reports have covered the period October 1, 1976 through September 30, 1984.

TABLE OF CONTENTS

TABLE OF CONTENTS (Cont'd.)

TABLE OF CONTENTS (Cont'd.)

FIGURES

FIGURES (Cont'd.)

FIGURES (Cont'd.)

TABLES

I. DIVISION OF ACCIDENT EVALUATION

SUMMARY

High Temperature Reactor Research

The No. 4, medium sized (7.62 cm ϕ x 15.24 cm L) 2020 graphite specimen, which was oxidized for 260 days in the HIL, was cut perpendicular to the axis to make five 1.27 cm thick slices. These graphite slices were x-ray radiographed, and density maps will be made from the radiographs.

A new oxidation profiling technique was developed and tested successfully, and oxidation profiles were generated from the middle part of the No. 4, 2020 graphite specimen utilizing this technique.

The oxidation rate measurements, with a large sized (5.97 cm x 5.72 cm x 15.24 cm) TS-1621 graphite block, have been completed. The effect of gas composition on the oxidation rate was also studied.

Two tensile strength measurement techniques (ASTM method using dogbone specimens and a technique employed by GA and BNL using glued cylindrical specimens), were compared by testing with unoxidized 2020 graphite. The tensile strength values from the ASTM method were ~1.5 times higher than those from the BNL method. However, more study is needed to make conclusions.

One more IFPT experimental run, incorporating 24 grams of silver, was conducted at 1600°C. It was observed that the plate-out occurred during the run, not during the cooldown period. At 1600°C (susceptor temperature), the amount of silver plate-out was 145 mg/hr and the aerosol generated was 0.77 mg/hr; while at 1500°C, the amount of plate-out and aerosol formation were 41.6 mg/hr and 0.067 mg/hr, respectively.

A scoping analysis of the gas exchange between the reactor vessel, the confinement cavity, and the open atmosphere was made, using previously computed core transient temperatures, for a depressurized core heatup transient with passively operating Rector Cavity Cooling System. The results show that after the initial blowdown only very little gas (about .02%) from the reactor vessel ever reaches the environment. Thus, the fission product discharge during such an accident may be dominated by the release of circulating inventory at the time of blowdown.

An extension of our previous core heatup accident studies to the case without operating Reactor Cavity Cooling System was made. While the resulting scenario indicates no significant consequences for the first 100 hrs, the metal components, and in particular the reactor vessel, reach excessive temperatures after 300 to 400 hrs, which could result in vessel failure. Therefore, it appears that the Reactor Cavity Cooling System design must clearly stress reliability and redundancy to eliminate such accidents from consideration.

SSC/MINET Improvement, Validation and Application

The SSC/MINET Improvement, Validation and Application Program encompasses a series of computer codes. The prefix SSC denotes the Super System Code, where: (1) SSC-L is for system transients in loop-type liquid metal-cooled reactors (LMRs); (2) SSC-P is for system transients in pool-type LMRs and (3) SSC-S is for long term shutdown transients. In addition to these code development and application efforts, validation of these codes is an ongoing task.

Another component of this program is the generic balance of plant (BOP) modeling effort. It provides for the development and validation of models to represent and link together BOP components that are generic to all types of nuclear power plants. This system transient analysis package is designated MINET to reflect the generality of the models and methods, which are based on a momentum integral network method.

Under SSC related activities, the previously developed intra-assembly heat transfer model has been incorporated as a user selectable option into the base program library. An additional significant extension of the capabilities of SSC is nearing completion, with the inclusion of an inter-assembly heat transfer model. This heat transfer model is based on an adaptation of a seven assembly cluster representation. Testing and validation are almost completed. Implementation of the two-dimensional improved upper plenum model into SSC is continuing.

Work on the balance of plant code (MINET) continued with the addition of helium gas as the fifth fluid option; inclusion of a trapped cover gas region capability in tanks containing quantities of sub-cooled fluids; improvement to the present turbine model and; on-going effort to provide a drift-flux representation, in addition to the present homogeneous equilibrium model of two-phase flow. Application work continues to focus on test calculations using the recently completed RAMONA/MINET composite code to study the effect of improved feedwater flow and temperature boundary condition values for their effect on the transient response.

Thermal-Hydraulic Reactor Safety Experiments

The effect of steam superheat on the top-flood debris bed quench characteristics was investigated. This work continues that reported in an earlier quarterly report. Calculations are presented for the bed heat flux and the superficial vapor velocity at the top of the bed. Results indicate that the effect of steam superheat on heat flux during bed quench is a significant one, especially for small particles and under conditions of large steam superheat.

A second series of bottom-reflood experiments was initiated. Special thermocouples with the thermocouple junction inside the 3.18-mm stainless steel spheres were used to monitor the actual solid-fluid heat transfer rates. The thermocouple responses are currently being evaluated.

The CORCON and VANESA codes were implemented as part of an audit of source term calculations. The part of the audit reported here was directed towards demonstration that the two codes could be made operational and that BMI-2104 calculations could be reproduced. Aspects of the codes are discussed and selected calculations are presented.

Plant Analyzer

The LWR Plant Analyzer Program is being conducted to develop an engineering plant analyzer capable of performing accurate, real-time and faster than real-time simulations of plant transients and Small-Break Loss of Coolant Accidents (SBLOCAs) in LWR power plants. The first program phase was carried out earlier to establish the feasibility of achieving faster than real-time simulations and faster than mainframe, general-purpose computer (CDC-7600) simulations through the use of modern, interactive, high-speed, special-purpose minicomputers, which are specifically designed for interactive time-critical systems simulations. It has been successfully demonstrated that special-purpose minicomputers can compete with, and outperform, mainframe computers in reactor simulations. The current program phase is being carried out to provide a complete BWR simulation capability, including on-line, multicolor graphic display of safety-related parameters.

The plant analyzer program is directed primarily toward reactor safety analyses, but it is also useful for on-line plant monitoring and accident diagnosis, for accident mitigation, further for developing operator training programs and for assessing and improving existing and future training simulators. Major assets of the simulator under development are its low cost, unsurpassed convenience of operation and high speed of simulation. Major achievements of the program are summarized below.

Existing training simulator capabilities and limitations regarding their representation of the Nuclear Steam Supply system have been assessed previously. Simulators reviewed at the time have been found to be limited to steady-state simulations and to restricted quasi-steady transients within the range of normal operating conditions.

A special-purpose, high-speed peripheral processor had been selected for the plant analyzer, which is specifically designed for efficient systems simulations at real-time or faster computing speeds. The processor is the AD10 from Applied Dynamics International (ADI) of Ann Arbor, Michigan. A PDP-11/34 Minicomputer serves as the host computer to program and control the AD10 peripheral processor. Both the host computer and the peripheral processor have been operating at BNL since March 15, 1982.

A four-equation model for nonequilibrium, nonhomogeneous, two-phase flow in a typical BWR/4 had been implemented on the AD10 processor. It is called HIPA-BWR/4 for High-Speed Interactive Plant Analysis of a BWR/4 power plant. The implementation of HIPA-BWR/4 had been carried out in the high-level language MPS10 of the AD10.

It had been demonstrated during the last quarter of 1982 that the AD10 special-purpose peripheral processor can produce accurate simulations of a BWR design base transient at computing speeds up to 10 times faster than real-time and 110 times faster than the CDC-7600 mainframe computer carrying out the same simulation.

After the successful completion of the feasibility demonstration, work has continued to expand the simulation capability to simulating the dynamics of the entire nuclear steam supply system as well as the entire balance of plant (steam lines, turbines, condensers and feedwater trains).

Models have been developed and implemented for point neutron kinetics with seven feedback mechanisms and seven automatic scram trip initiations, for thermal conduction in fuel elements, for steam line dynamics capable of simulating acoustical effects from sudden valve actions, for turbines, condensers, feedwater preheaters and feedwater pumps and for emergency cooling systems.

The software systems of both the PDP-11/34 host computer and the AD10 special-purpose peripheral processor have been upgraded to achieve greater computing speed and a larger number of analog input/output channels. Two AD10s are coupled via a direct bus-to-bus interface to compute in parallel.

Models have been developed and implemented for the feedwater controller, the pressure regulator and the recirculation flow controller. Twenty-eight parameters for initiating control systems and valve failures and for selecting set points can be changed on-line from a 32-channel control panel. Sixteen dedicated analog output lines are provided for the simultaneous display of 15 selected parameters versus time. All input-output channels are addressed approximately 200 times per second.

All program modules have been combined into the HIPA-BWR/4 code. The entire BWR power plant simulation, including the nuclear steam supply system, the steam lines with all valves, the turbines, condensers, feedwater preheater and pumps, and the control and plant protection systems, has been executed. Fifteen selected parameters can be stored simultaneously in the IBM Personal Computer and then displayed as functions of time in labelled diagrams. A silent movie has been produced to show how the plant analyzer is operated and how it responds to on-line analog signals.

During the first reporting period of 1984, we presented the comparison of plant analyzer results with published results from GE for 10 different ATWS events as a part of developmental assessment. The assessment showed that the plant analyzer is capable of simulating ATWS. The plant analyzer has been generalized to simulate any BWR-4 power plant in response to input data changes from the keyboard.

During the second reporting period of 1984, we continued the developmental assessment of the plant analyzer by comparisons against GE, TRAC-BD1, RELAP-5, and RAMONA-3B code results. The results showed that the plant analyzer is capable of realistically simulating a large class of plant transients efficiently at very low cost.

During the last reporting period, we implemented the capability of simulating flow reversal, continued the implementation of the level tracking model with the drift flux model, and demonstrated successfully the simulation of boron injection and the subsequent cessation of fission power. Several transients were simulated to demonstrate the plant response to manual depressurization and HPCI flow reduction during an ATWS event. These simulations were carried out to assess the efficacy of proposed emergency procedure guidelines. The results indicate that the fission power can be reduced without boron injection and core uncovery, by lowering the pressure and by lowering the coolant level in the downcomer and thereby reducing the core flow rate.

The previously distributed draft report documenting the BWR plant analyzer was updated as a final report [Wulff, Cheng, Lekach and Mallen, 1984] and submitted for printing.

During the current reporting period we have demonstrated that the plant analyzer can simulate, in less than four days, thirty-seven different transients, induced by both single and multiple failures or events. We have started to develop the capability of accessing and operating the plant analyzer remotely via commercial telephone. We have achieved the ability to operate the plant analyzer remotely from an IBM Personal Computer, equipped with 128 Kbyte memory, an RS-232 serial port, a 1200 baud modem, a Plantronics PC+ Colorplus color graphics adapter card and a standard R-G-B color monitor. An order was placed for a Tektronix 4115B graphics terminal

The interest in the Plant Analyzer Development Program continues to be high, both in domestic and foreign institutions. Six presentations with demonstrations were given at BNL to visitors from the U.S., from Spain and from Sweden. An invited paper was presented at the International Conference on Power Plant Simulation in Mexico, and two additional invited papers have been submitted for presentation.

Code Assessment and Application

A preliminary calculation has been performed for the FIST Test 4PMC1 (BWR/4MSIV Closure ATWS) using the TRAC-BD1/MOD1 code. The code prediction up to 28 seconds into the transient agreed very well with the experimental data. However, some noding changes seem to be necessary to obtain a better steady-state and a more reasonable computer run time. The final calculation will be performed after these changes are made.

A second EM-type calculation has been performed for the 200% cold leg break of the Westinghouse 4-loop RESAR-3S plant using the TRAC-PD2/MOD1 code. In this calculation, the reactor coolant pumps were assumed to experience a locked rotor condition during the reflood phase of the accident. Because of the increased loop resistances, the core cooling was somewhat impaired, and the peak clad temperature ws 81ɑK higher than in the smaller situation with no locked rotor assumption.

Code Maintenance (RAMONA-3B)

A new version of RAMONA-3B, i.e., RAMONA-3B/MODO/Cycle 8, has been generated by incorporating many improvements in the hydraulic and neutronic sections of the code since the creation of Cycle 7 in February 1984. Modifications required to generate 1-D cross sections by using the auxiliary 3-D to 1-D collapser code FRAM, have also been incorporated.

A pure thermal-hydraulic calculation bypassing the neutronics has been run to verify the changes made to correctly calculate the possible flow reversal situations in the core.

Calculational Quality Assurance in Support of PTS

The quantitative in-depth review of the remaining two selected PTS thermal-hydraulic calculations for the H. B. Robinson-2 plant performed at INEL using the RELAP5 code has been completed. These transients were: (1) steam generator tube rupture at hot zero power, and (2) loss of secondary heat sink with primary system feed-and-bleed recovery at hot full power. A simple method based on mass and energy balances was used in the review process. The RELAP5 results for both of the above transients seem reasonable.

This concludes the BNL assignment under the NRC PTS program.

1. High Temperature Reactor Research

1.1 Graphite and Ceramics (B. S. Lee, J. H. Heiser, III, D. R. Wales and C. C. Finfrock)

1.1.1 Nondestructive Measurements

The No. 4 medium sized (7.62 cm ϕ x 15.24 cm L) 2020 graphite specimen, which was oxidized for 260 days in the HIL, was cut perpendicular to the axis to make five 1.27 cm thick slices. These graphite slices were x-ray radiographed along with 11 standards which ranged between 50 and 100% of 2020 graphite density. Density maps will be made after densities are estimated, utilizing a microbeam densitometer. The radiographs show that the top part of the specimens oxidized significantly more compared to the bottom part (these cylindrical specimens were laid down with the axes of the specimens parallel to the axis of the tube furnace), which is probably caused by different flow conditions at the top, the sides and the bottom of the specimens. This will give different oxidation profiles at different parts of the specimen (oxidation profile is a function of an angle from the top).

The profile results will show the effect of oxidant level/flow rate of coolant on oxidation profile.

1.1.2 Oxidation Profile Measurement

Due to the oxidation mode in the long term, medium sized specimens, a new profiling method has been developed. A strip which is parallel to the axis of the specimen is milled at every 9° (40 strips per layer), weighed, and the density calculated. The thickness of each layer was 0.51 mm. With this method, the profiles from different portions of the specimen can be compared, and the effects of oxidant level and flow rate can be studied. The middle part of the No. 4 medium sized 2020 graphite sample was profiled, and some of the early results are shown in Figure 1.1. The profiles, 1,2,3,4 and 5 are from 0°, 45°, 90°, 135 and 180°, respectively (the most oxidized part is 0°). These profiles will be analyzed with oxidation profile computer codes in the future.

1.1.3 Oxidation Kinetics Measurements

The oxidation rate runs, with larger size (5.97 cm x 5.72 cm x 15.24 cm) TS-1621 graphite, have been completed. So far, we have measured oxidation rates for 2020, PGX and TS-1621 graphites. H-451 graphite is being prepared for rate measurements.

The purpose of this study is to obtain F_b (burnoff factor) values for these graphites and to compare the oxidation rates under the same experimental conditions. We are studying the effects of gas compositions on the oxidation rates at the same time.

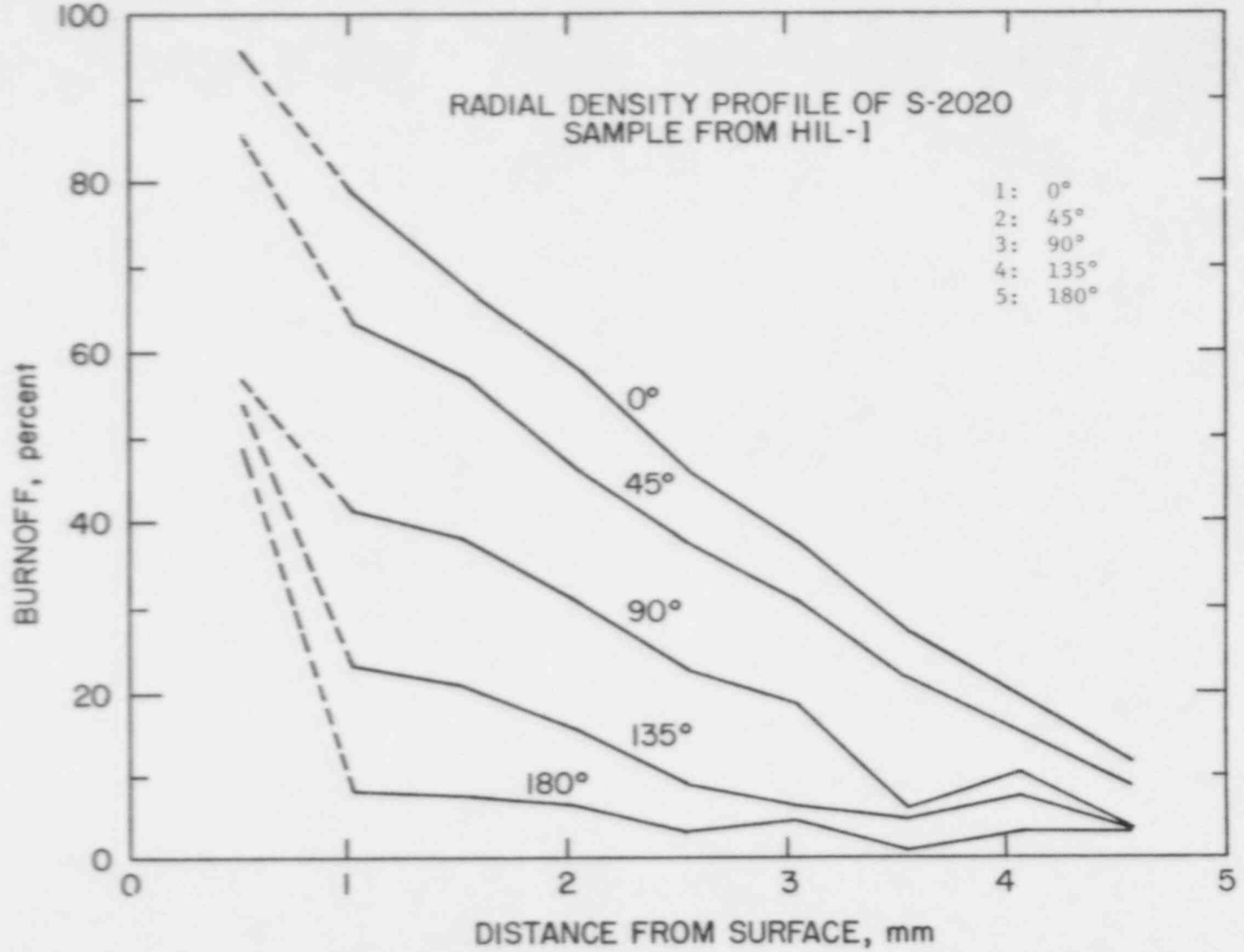

Figure 1.1 Oxidation Profiles from the No. 4 Medium Sized S-2020 Sample Oxidized for 260 Days

The oxidation rates for 2020, PGX and TS-1621 graphites are compared in Table 1.1 As shown in this Table, TS-1621 graphite is comparable to 2020 graphite in oxidation rate. The oxidation rates for TS-1621 graphite as a function of the accumulated oxidation time are shown in Figure 1.2.

The initial oxidation rate was ~450 ppm, and the rate decreased down to ~250 ppm/hr ($CO + CO_2$) after ~200 hours. After 438 hours of oxidation, the H_2 and H_2O levels were lowered to 211 and 39 ppm, respectively, for 6 hours (see the arrow in Figure 1.2). As shown in Figure 1.2, the oxidation rate at the normal impurities level (~5,000 ppm H_2, ~500 H_2O) after this treatment was higher than the one before the treatment. The next runs showed the oxidation rates decreased to the level of those before the treatment.

This indicates that the catalysts in the graphite become oxidized at the impurities levels of ~5,000 ppm H_2 and ~500 H_2O, and the oxidation rate decreases. However, when the catalysts are reduced by carbon due to the low oxidant level, the oxidation rate increases.

Table 1.1

Oxidation Rates for 2020, PGX and TS-1621 Graphites at 850° With 500 ppm H_2O/5000 ppm H_2 (Balance He)

Graphite	Oxidation Rate (ppm ($CO+CO_2$)/hr)		
	Initial Rate	After 50 hrs	After 440 hrs
2020	278	239	262
PGX	673	1273	3746
TS-1621	451	340	242

1.1.4 Tensile Strength Measurement

The ASTM recommended tensile strength test specimen is a dogbone specimen with reduced gauge cross section. However, these specimens are difficult to machine and cause large amounts of material loss. Thus, GA and BNL decided to use glued cylindrical specimens (GCS). Later, GA found that the GCS technique gives far lower tensile strengths than those from "dogbone" specimens for fine grained graphite like 2020 graphite. GA's dogbone specimens produced values almost twice as high as those from the GCS.

During the last quarter, the tensile strength values from BNL's GCS technique (which is believed to be better than GA's) were compared to those generated with the dogbone technique, and the strengths from the dogbone specimens (gauge diameter: 6.4 mm) are ~1.5 times higher than those from GCS

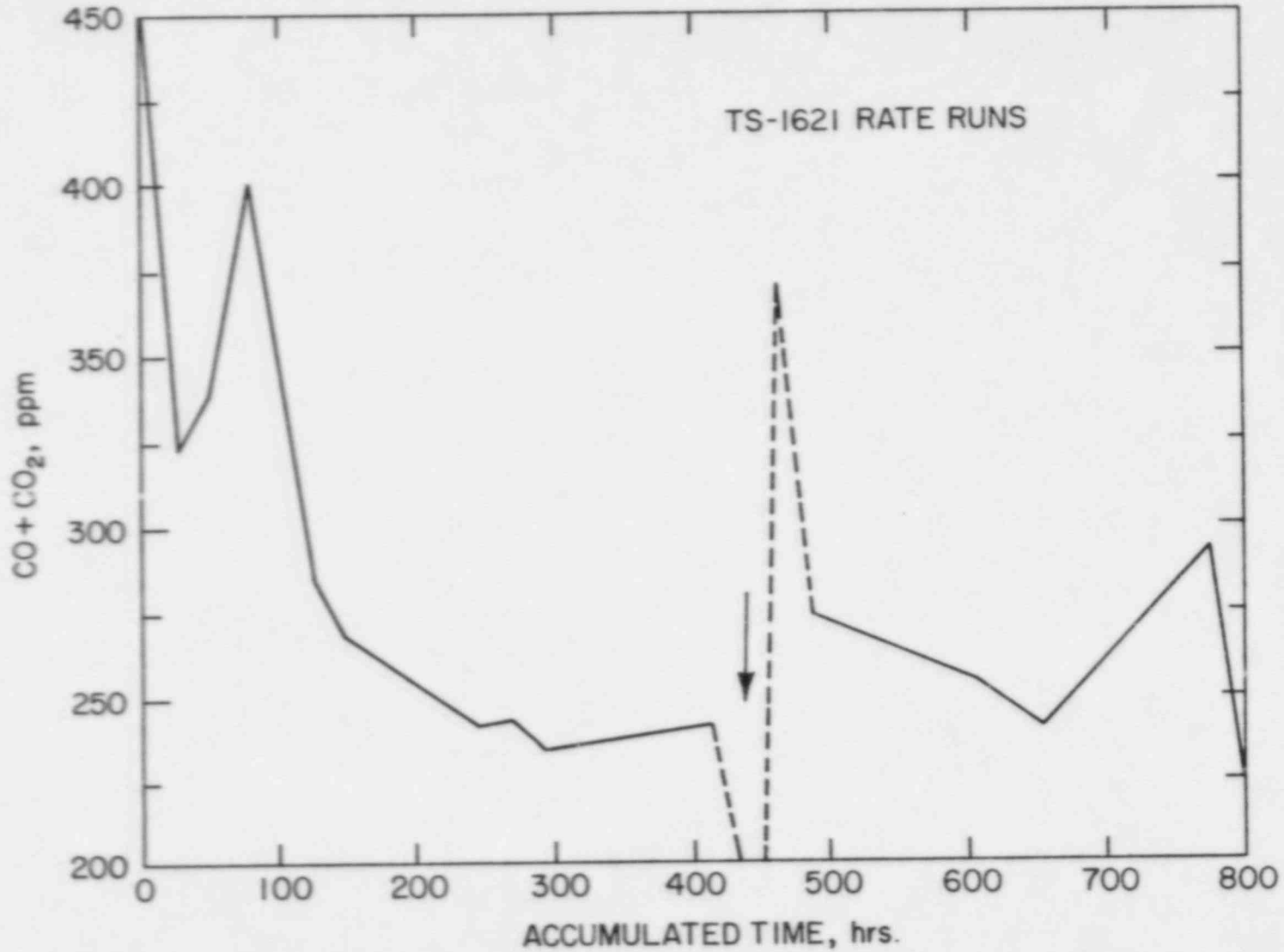

Figure 1.2 Oxidation Rate for TS-1621 Graphite at 850° C in ~5000 ppm H_2/~500 ppm H_2O/He

(gauge diameter: 12.8 mm), as shown in Figure 1.3. However, this work should be extended to dogbone specimens of gauge diameter of 12.8 mm, because smaller diameter specimens usually give higher strengths.

It is also believed that oxidized specimens should make less differences between these two techniques than the unoxidized specimens.

1.2 Fission Product Transport (B. S. Lee, J. H. Heiser, III, and C. C. Finfrock)

During the last quarter, one more integrated fission product transport (IFPT) experimental run (#103084) incorporating silver was conducted. The run was at 1600°C for 5.5 hours with 24 grams of Ag in the fuel channels.

In this run, the temperature gradient in the chimney was monitored throughout the experiment, and the temperature profile is shown in Figure 1.4. The temperature gradient is linear between 4 cm and 10 cm from the susceptor and is -56°K/cm.

From this profile, it was learned that the silver plate-out started at a position where the temperature was ~1220°C (m.p. of Ag is 962°C, and b.p. of Ag is 2212°C). With the use of a video camera equipped with a telescopic lens, it was shown that the plate-out occurred during the run, not during the cooldown period.

The chimney from the run #103084 was sectioned in 1.27 cm intervals, and was analyzed for Ag with an atomic absorption technique, and the silver plate-out is plotted as a function of distance from the susceptor in Figure 1.5. The total amount of silver plate-out was 798 mg (145 mg/hr) and the filter collected 4.21 mg (0.77 mg/hr) of silver, while the earlier experiment at 1500°C with the same flow rate showed 41.6 mg/hr of plate-out and 0.067 mg/hr of aerosol formation.

1.3 Analytical

1.3.1 Gas Release During Severe Accident Transients in Modular Pebble Bed Reactors (P. G. Kroeger)

In the previous Quarterly Report (Kroeger, 1984) reactor temperatures and heat flows were presented for a depressurized core heatup transient with the Reactor Cavity Cooling System (RCCS) functioning in the passive, gravity fed mode. Figure 1.6 shows several reactor temperatures and heat flows, indicating that the maximum core temperature peaks at about 1820C at about 90 hrs.

Using the core and confinement cavity temperatures from this transient, a scoping assessment of gas exchange rates to be expected between the core and the confinement cavity, as well as between the confinement and the open atmosphere, was made.

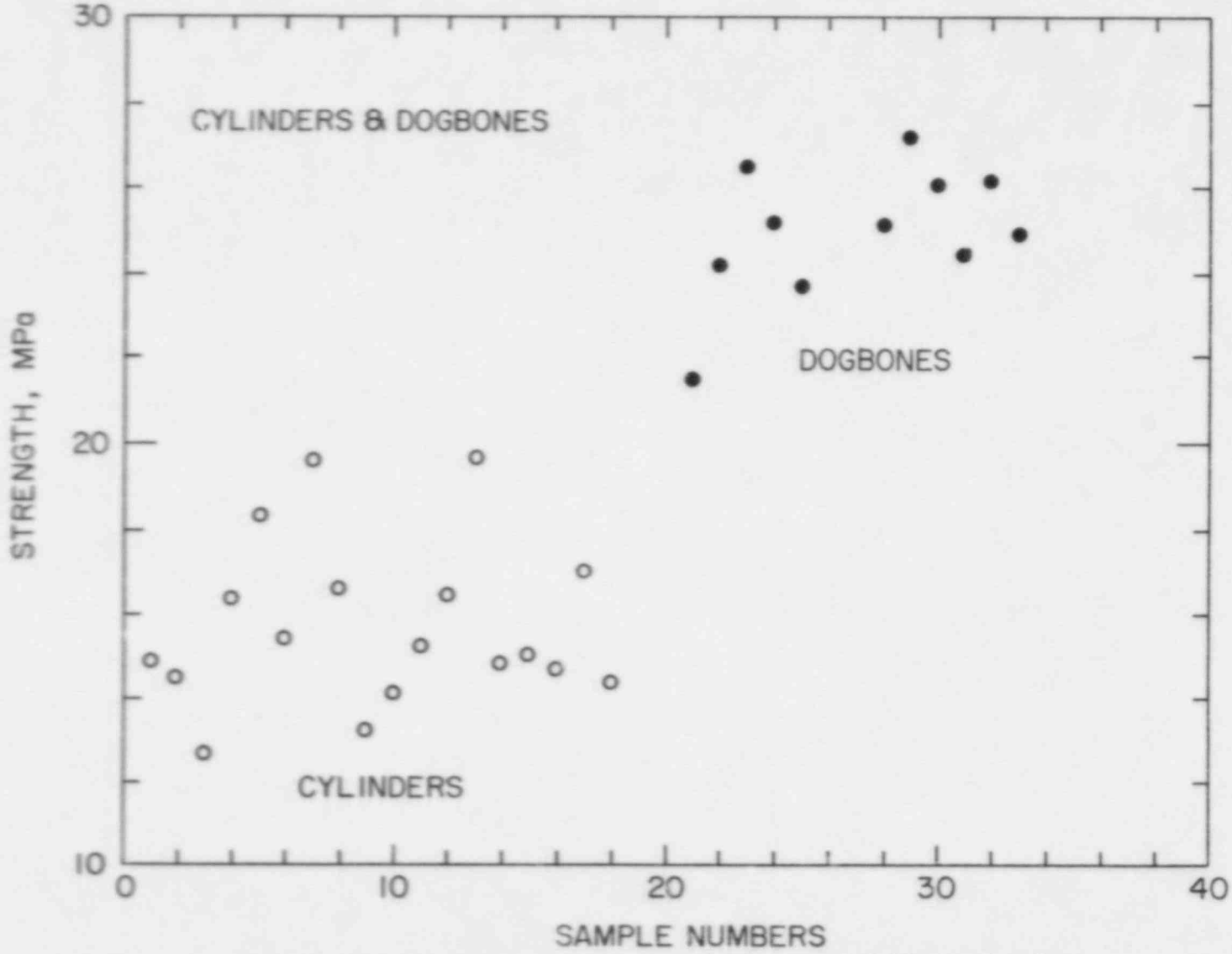

Figure 1.3 Tensile Strengths from Dogbone and Cylinder Specimens

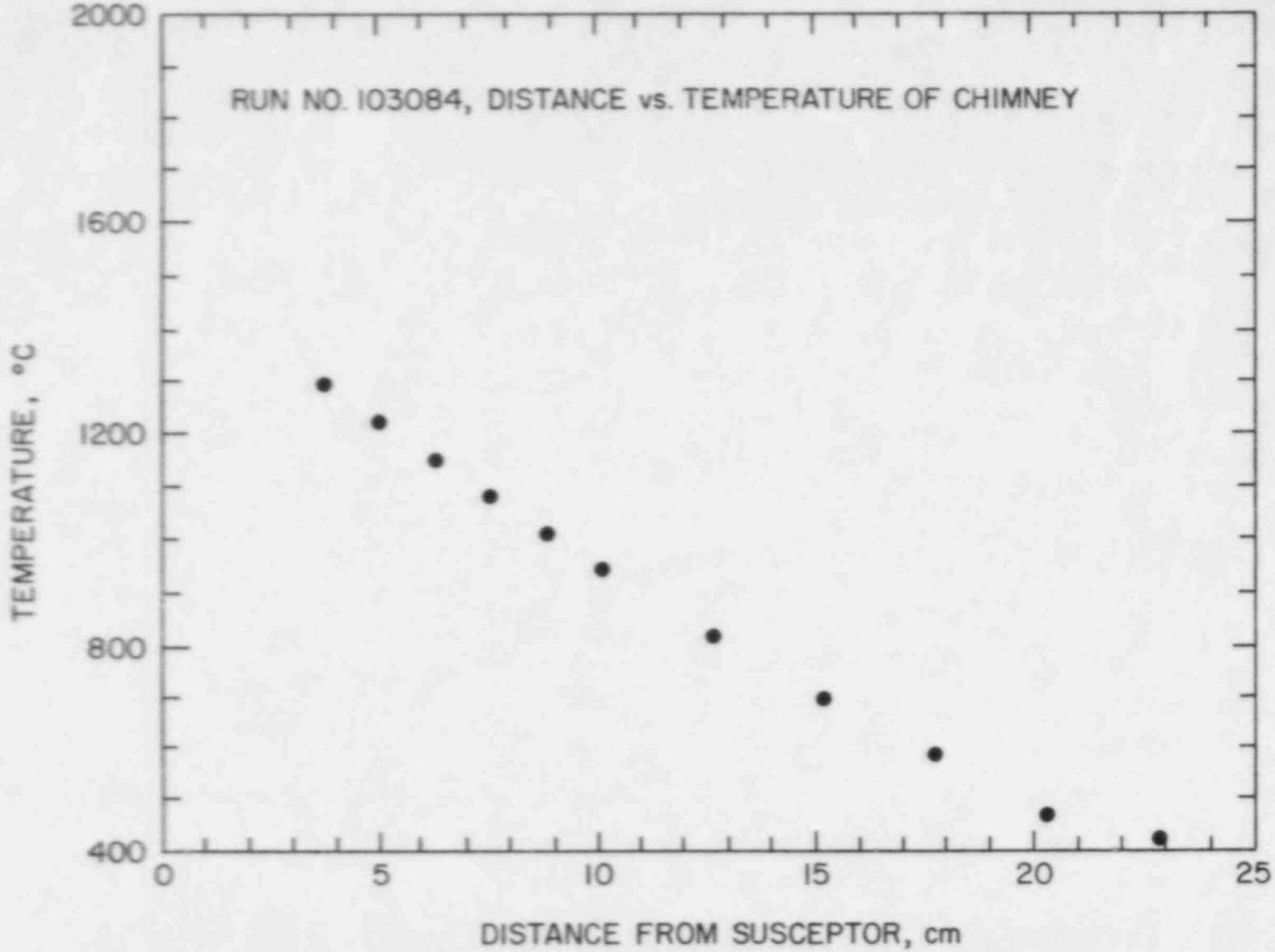

Figure 1.4 Temperature Gradient in the Chimney for Run # 103084

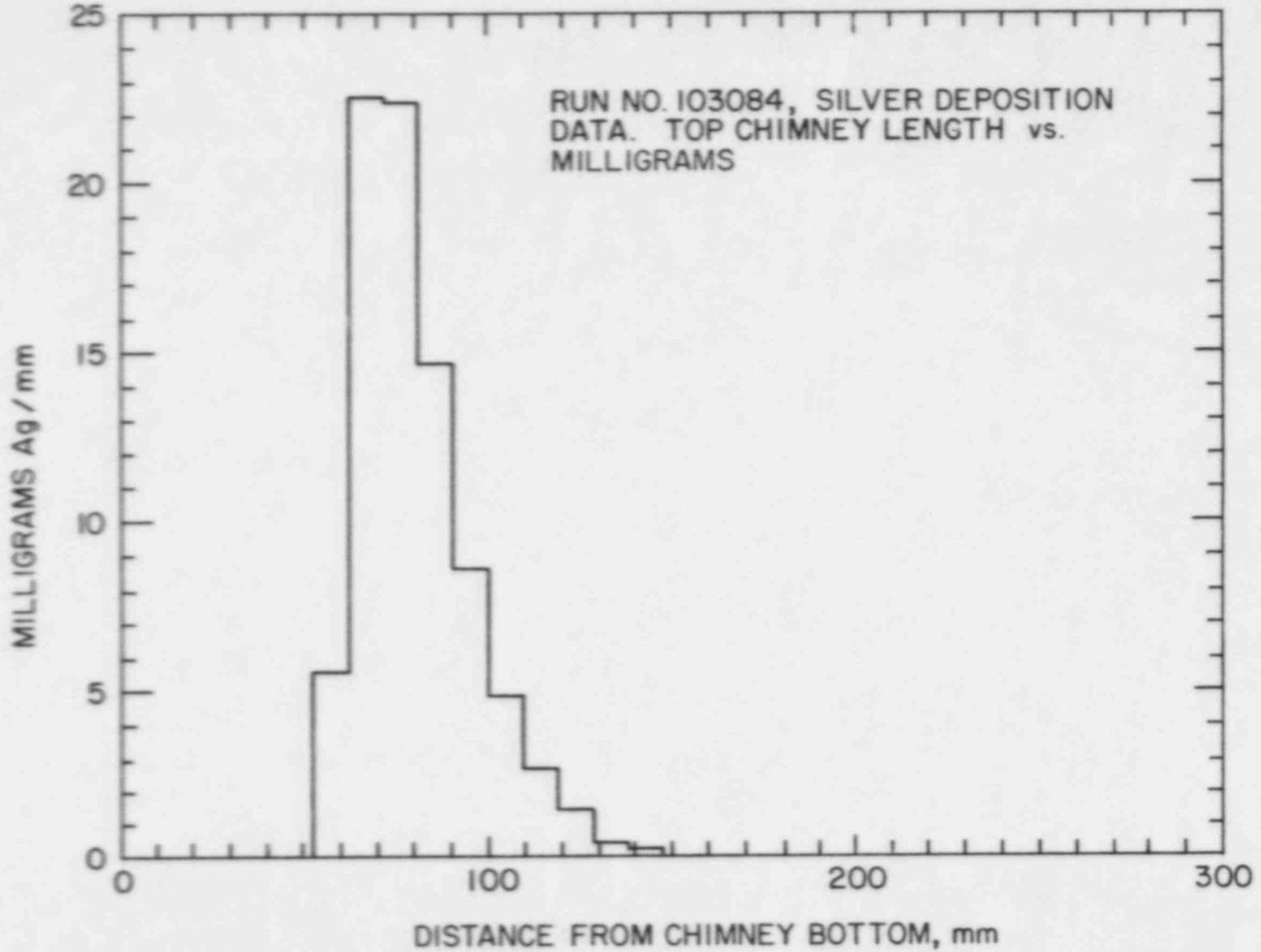

Figure 1.5 Silver Plate-Out as a Function of Distance from the Susceptor for Run # 103084

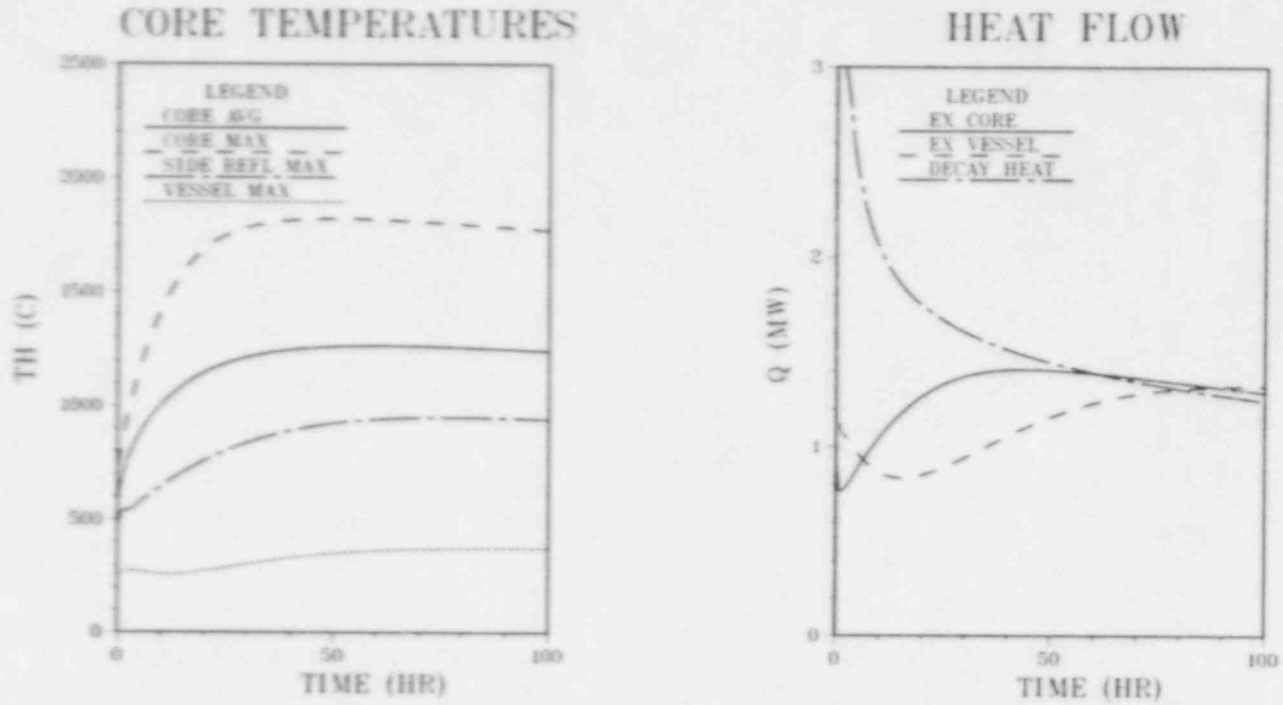

Figure 1.6 Reactor Temperatures and Heat Flow During Depressurized Core Heatup Transient with RCCS Functioning in the Passive Mode

At the initial assumed depressurization from 70 bar operating pressure to atmospheric pressure a total of about 330 kg mol of helium would be discharged from the vessel to the confinement, with about an equal release of 330 kg mol of helium and air from the confinement to the atmosphere.

After the initial blowdown, the confinement contains about 80 kg mol of helium/air mixture and the reactor vessel contains about 5 kg mol of helium.

Figure 1.7 includes the gas contained in the lower part of the reactor vessel during the first 100 hrs of the transient. During this time the total gas content in the core does not change appreciably. With a net cooldown on the primary side of the steam generator during the first two hrs, there is a net gas inflow into the reactor vessel of about .4 kg mol during this time.

From 2 to about 20 hrs, due to lower plenum gas cooldown, there is a small net inflow of gas into the reactor vessel of about 0.1 kg mol. From 20 to 100 hrs there is an outflow of about 0.1 kg mol from the reactor vessel. This is the time where the core reaches peak temperatures and where fuel failures occur. After 100 hrs there is a very small net inflow into the reactor vessel. Thus, even if escaping fission products were well mixed within the reactor vessel gas, only .1 of 5 kg mol or 2% would escape from the vessel to the confinement.

Similarly, for the confinement building there is a net outflow during the first 2 hrs of about 2 to 3 kg mol to the atmosphere, due to gas expansion in the upper and lower regions. Thereafter a minor inflow of about 1 kg mol is observed for the period of 2 to 20 hrs, followed by a net outflow of about 1.2 kg mol between 20 and 100 hrs, with a net inflow thereafter. Thus, only about 1.2/80 or about 1% of the confinement gas is discharged to the environment during and after the time of fuel failure.

While these computations are of a scoping nature, they indicate that gas discharge from the core to the environment during the time of some fuel failure appears to remain very small, and the discharge of some of the circulating inventory during the initial blowdown may be more significant. Future, more detailed calculations are required for confirmation.

1.3.2 Core Heatup Accident Transients in Modular Pebble Bed Reactors without Reactor Cavity Cooling System (P. G. Kroeger)

While the passive operating mode of the RCCS and the typical use of two parallel independent cooling systems makes an RCCS failure highly unlikely, its potential consequences should still be considered.

Our scoping analyses were therefore applied to such a transient. Typical results are shown in Figure 1.8. The maximum core temperature again peaks at about 1830 C at about 50 hrs, similar to the case with RCCS. The average core temperature is also not very much higher than in the case with RCCS. About 16% of the core will exceed a temperature of 1600 C at 60 hrs, versus 14% at 50 hrs in the case with RCCS.

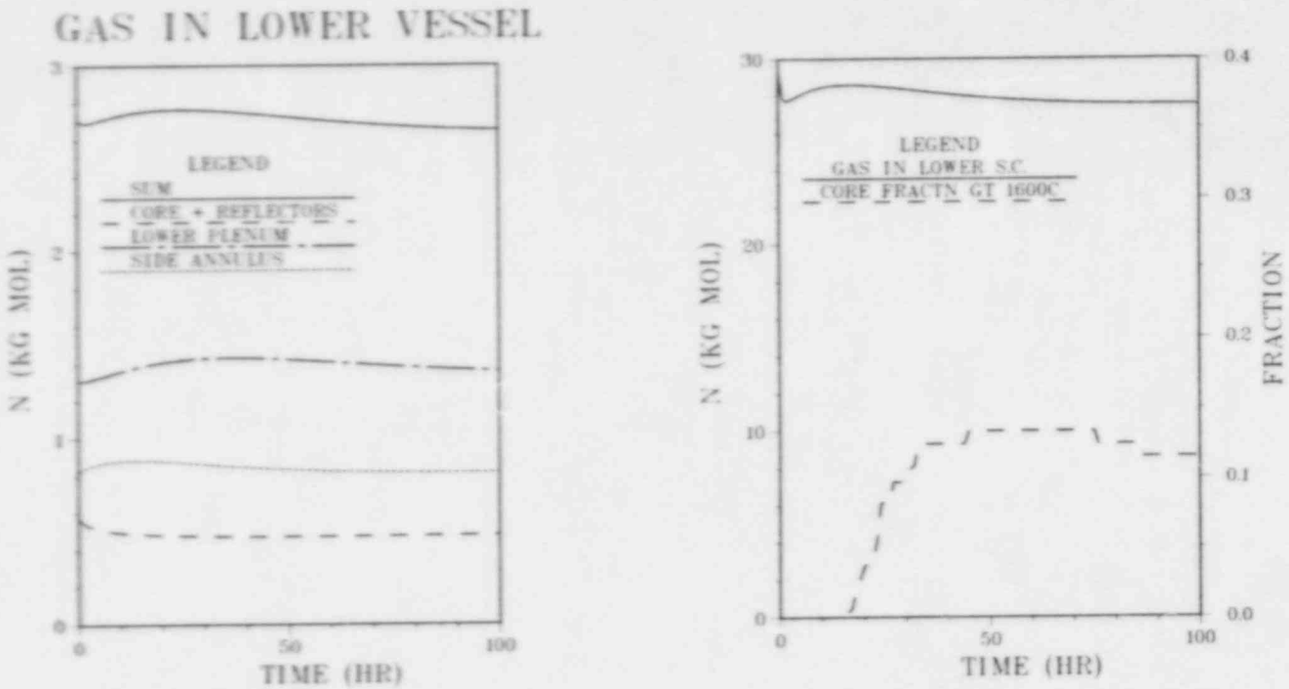

Figure 1.7 Gas Content in Lower Port of Reactor Vessel and Confinement During Depressurized Core Heatup Transient with RCCS and Fraction of Core Exceeding 1600 C During Transient

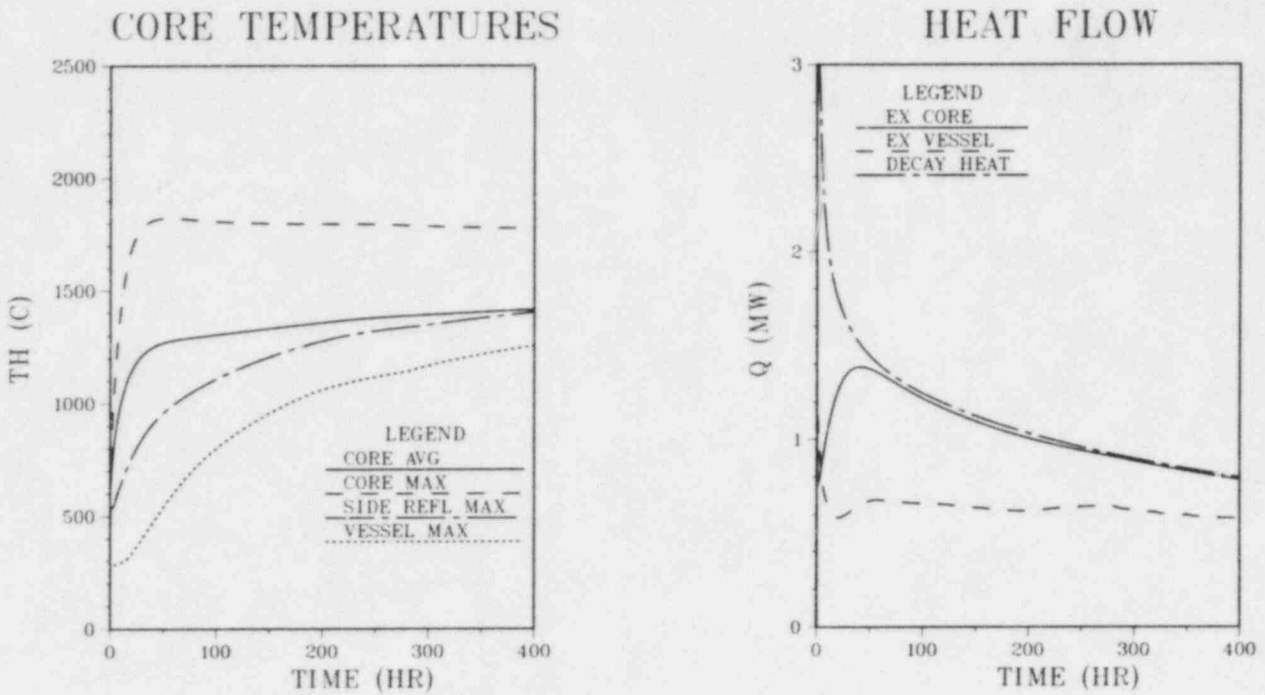

Figure 1.8 Reactor Temperatures and Heat Flows for Core Heatup Transient Without Operating Reactor Cavity Cooling System

However, with the ultimate heat rejection now going into the cavity concrete and the surrounding soil, which are typically media of low thermal diffusivity, the metal components, and in particular the reactor vessel, are being exposed to excessive temperatures. The highest vessel temperatures reach about 800 C at 100 hrs and 1200 C at 400 hrs. If the accident transient cannot be terminated by supplying means for decay heat removal, it must be expected that physical vessel failure will result at these temperatures. The side cavity cooling panels and the cavity concrete will also deteriorate, with concrete surface temperatures exceeding 900 C. These results were obtained for typical concrete and soil properties (thermal diffusivity, $\alpha \approx 10^{-6}$ m^2/s*). Assuming a higher conductivity soil ($\alpha \approx 2 \times 10^{-6}$ m^2/s), about 200 C lower vessel temperatures were obtained.

Thus, paying attention to the local soil conditions can somewhat reduce the consequences of such an accident. However, for the system to be truly "inherently safe" the RCCS design must be such that the probability of a failure is far beyond the region of concern. These were scoping calculations, and if one were interested in an analysis of this accident, further design details would have to be available and some of the modelling should be refined.

REFERENCES

KROEGER, P. G., Quarterly Progress Report, Brookhaven National Laboratory, July - Sept., 1984, BNL-NUREG-51454, Vol. 4, No. 3.

PUBLICATIONS

CHAN, B. C. and KENNETT, R. J., "HTGR Containment Building Thermal Analysis", Brookhaven National Laboratory Report to be published.

*Reference value only; actual soil and concrete properties used are temperature dependent.

2. SSC/MINET Improvement, Validation and Application (J. G. Guppy)

The SSC/MINET Improvement, Validation and Application Program deals with advanced thermohydraulic codes to simulate transients in liquid metal-cooled reactors (LMRs). During this reporting period, work continued on three codes in the Super System Code (SSC) series. These codes are: (1) SSC-L for simulating short-term transients in loop-type LMRs; (2) SSC-P which is analogous to SSC-L except that it is applicable to pool-type designs and (3) SSC-S for long-term (shutdown) transients occurring in either loop- or pool-type LMRs. In addition to these code development and application efforts, validation of these codes is an ongoing task. Reference is made to the previous quarterly progress report (Guppy, 1984) for a summary of accomplishments prior to the start of the current period.

Additionally, this program deals with a generic balance of plant (BOP) modeling effort, which encompasses the development of safety analysis tools for system simulation of nuclear power plants. It provides for the development and validation of models to represent and link together BOP components (e.g., steam generator components, feedwater heaters, turbine/generator, condensers) that are generic to all types of nuclear power plants. This system transient analysis package is designated MINET to reflect the generality of the models and methods, which are based on a momentum integral network method. The code is fast-running and capable of operating as a self-standing code or to be easily interfaced to other system codes.

2.1 SSC-L Code (W. C. Horak)

2.1.1 Intra-Assembly Heat Transfer (W. C. Horak, R. J. Kennett)

Intra-assembly heat transfer has now been added as an option to SSC. The intra-assembly module, which is a revised version of the previously developed TWIST code, uses a two-dimensional porous body approach. Transverse momentum is considered negligible, permitting the calculations to be done in a marching fashion. As coded, the module is limited to only one assembly for a particular core model. Additionally, due to computer core storage limitations, the quantities calculated by the intra-assembly module (velocities,temperatures, and pressure) are stored in large core memory (LCM). The module is accessed from subroutines OPTN6S in the steady-state and subroutine FUEL5T in the transient. In the steady-state, the module can currently only be used with the fixed flow fraction option for SSC.

The module is currently being tested on a scram-to-natural circulation transient.

2.1.2 Inter-Assembly Heat Transfer Model

2.1.2.1 Introduction

SSC has been developed to be a fast-running, system-wide transient analysis code. Thus, the inter-assembly model developed for SSC utilized certain

assumptions and features so that an adequate portrayal of the important processes involved was accomplished, while minimizing computation. The model also was designed to easily interface with the previously developed low heat flux boiling model and the intra-assembly heat transfer model.

Initially, a survey was made of the inter-assembly models used in other computer codes. These models were found to be of two main types: 1) seven assembly cluster model and 2) three-assembly in-line model (Fig. 2.1).

In the seven-assembly cluster model (Fig.2.1a) inter-assembly heat transfer is modeled by a central assembly transferring heat to the adjacent ring of six assemblies. The six outer assemblies are assumed not to transfer heat to the next ring, i.e., the outer surfaces are assumed to be adiabatic. Usually in this model, each edge of the duct wall is assumed to be at its own temperature. This means there are 42 duct wall temperatures to be calculated per axial level, per cluster. Since there are usually ten or more axial levels modeled in SSC, implementation of such a seven assembly model for a systems code such as SSC would involve prohibitive computational costs.

The three-assembly in-line model consists of three adjacent assemblies usually arranged radially out from the core. The outer surfaces of the two outer assemblies can be considered adiabatic. The duct walls can be split into two temperature regions. Therefore, this model needs to calculate only six duct wall temperatures per axial level per cluster, and would not involve prohibitive computational costs for a systems code such as SSC. The model is usually used for simulations where the heat transfer is predominantly in one direction (usually radially out from the core center), but would not be adequate in other situations where this does not occur, i.e., a fuel assembly surrounded by three or more colder assemblies.

In order to adequately model inter-assembly heat transfer, while maximizing the computational efficiency, a simplified seven-assembly cluster model was developed. In the simplified model, a full seven assembly cluster is analyzed, but the duct wall is divided into only two constant temperature regions (Fig. 2.2). This reduces the number of duct wall temperatures to be calculated to fourteen per axial level per cluster. Moreover, the two temperature region duct wall model is fully compatible with the previously developed intra-assembly model, which also calculates two duct wall temperatures.

The assemblies are numbered as shown in Fig. 2.2. The two duct wall regions per assembly are separated by the dashed line. The six outer surfaces are considered to be adiabatic. The sodium in the interstices between the assemblies is assumed to be stagnant. The heat capacity of the interstitial sodium is lumped with that of the duct wall, permitting the interstices to be represented as thermal resistances between the duct walls.

The model is currently restricted to the specified flow fraction option in SSC. Also, the model as coded is restricted to use with an assembly represented by an average fuel rod. Additionally, although the module can represent more than one cluster at a time, each cluster is analyzed separately. Therefore, it is not possible to overlap clusters.

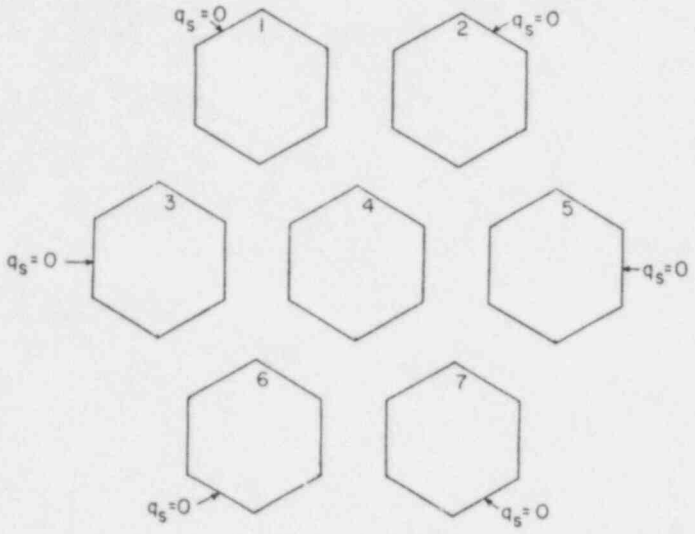

Fig. 2.1a - Seven Assembly Cluster Model

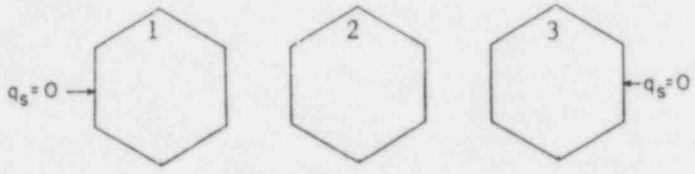

Fig. 2.1b - Three Assembly In-Line Model

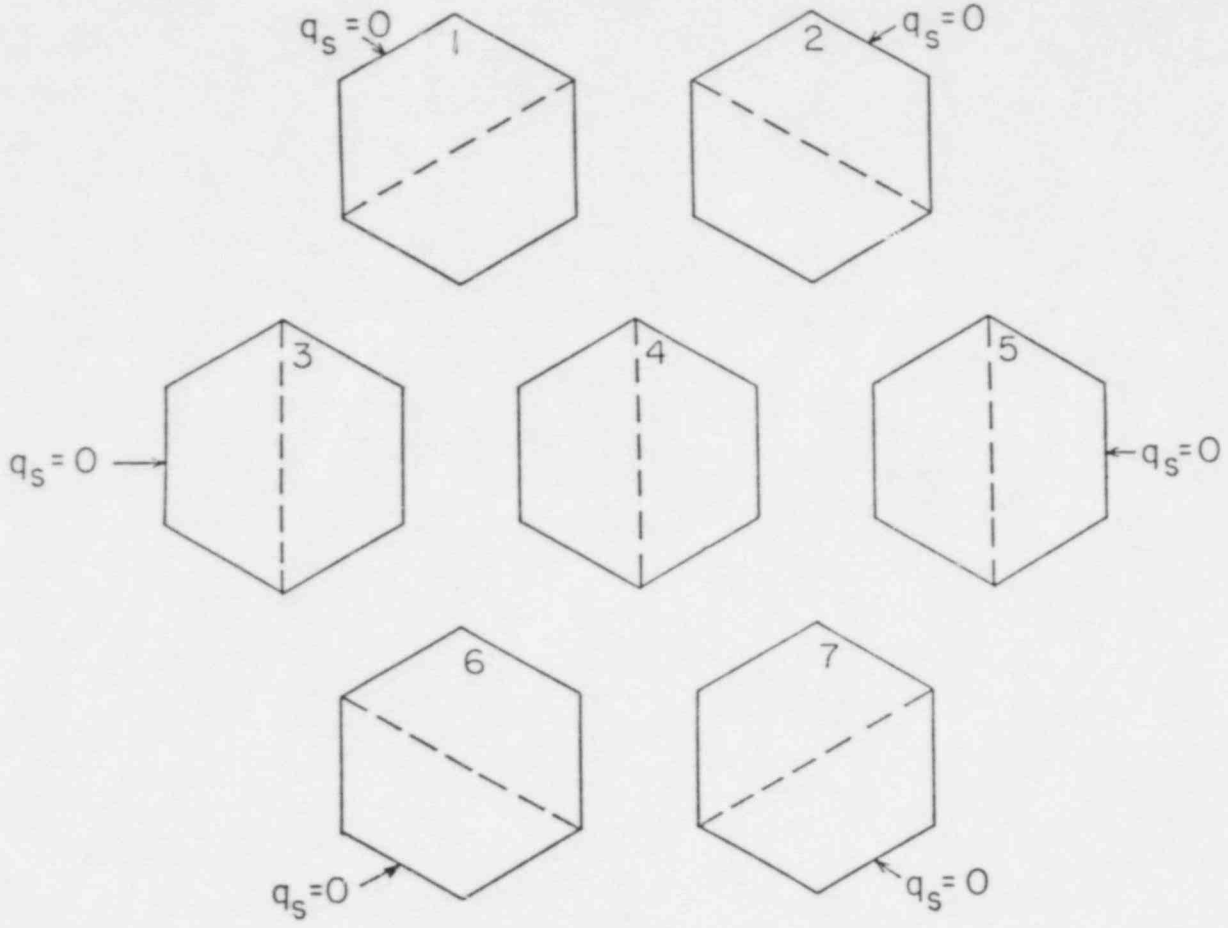

Fig. 2.2 Seven-Assembly Cluster Model for Inter-Assembly Heat Transfer

2.1.2.2 Steady-State Module

In the SSC core module, heat conduction in the axial direction is ignored. This enables the core temperatures to be determined on an axial level basis in a marching fashion. Additionally, since all heat generated in a particular axial location of a fuel pin must be deposited into the adjacent coolant, the coolant and duct wall temperatures can be solved for independently of the fuel rod temperatures. (The fuel rod temperatures are solved for after the coolant temperatures are determined.)

In the steady-state, all the duct wall temperatures and assembly coolant temperatures at a particular axial level are solved for simultaneously using matrix methods. Since the heat transfer coefficients and material properties are temperature dependent, an iterative procedure is employed. Once the temperatures are converged, the procedure is then repeated for the next axial level, marching in the direction of flow.

For the six outer (adiabatic) surfaces (Fig. 2.2), the temperatures are given by:

$$UC\ [TD - \overline{\overline{TC}}] = QD \qquad (2.1)$$

where, TD = duct wall temperature

$\overline{\overline{TC}}$ = assembly average coolant temperature

QD = power deposited directly into the duct, and

UC = overall heat transfer coefficient between the duct and coolant

The duct wall temperatures for the eight inner surfaces (Fig. 2.2) are given by

$$UC\ [TD - \overline{\overline{TC}}] + \sum_{j=1}^{3} UI_j\ (TD - TD_j) = QD \qquad (2.2)$$

where the summation is over the three adjacent duct walls and UI is the overall heat transfer coefficient from duct wall to duct wall across the interstices.

The overall heat transfer coefficient from duct wall to duct wall across the interstice is given by:

$$UI = A/\left\{ \frac{x_i}{2k_i} + \frac{\delta}{k_I} + \frac{x_j}{2k_j} \right\} \qquad (2.3)$$

where,

A = heat transfer area

x_i = i-th duct wall thickness

k_i = i-th duct wall conductivity

δ = interstice thickness

k_I = conductivity of the sodium in the interstice

The overall heat transfer coefficient from the duct wall to the bulk coolant temperature is given by:

$$UC = AW/RW + AD/RD \tag{2.4}$$

where,

AW = heat transfer area of the associated wire wrap
RW = thermal resistance of wire
AD = heat transfer area of the duct wall
RD = thermal resistance of the duct wall

and

$$RW = DW/4\ k_w + 1/h \tag{2.5a}$$

$$RD = XD/2k_D + 1/h \tag{2.5b}$$

where,

DW = wire diameter

k_w = thermal conductivity of the wire

h = convective heat transfer coefficient

XD = duct wall thickness

k_D = duct wall thermal conductivity

The coolant exit temperature is given by:

$$(Wc_p)\ (TC - TC^{-}) = Q_{co}$$

$$+ \sum_{i=1}^{2} UC_i\ [TD_i - TC] \tag{2.6}$$

where, TC = coolant exit temperature

$\overline{TC}$ = coolant inlet temperature

Q_{co} = energy deposited directly into coolant (includes energy generated in associated fuel pin).

Equations 2.1, 2.2 and 2.6 form a banded matrix (see Fig. 2.3) in the unknown duct wall temperatures and coolant exit temperatures. This banded matrix is solved using standard techniques. Since the overall heat transfer coefficients are temperature dependent, an iterative procedure is employed at each axial level until the temperatures are converged.

At the conclusion of the steady-state, the heat fluxes between the duct walls are stored for use in the transient.

The heat flux is given by

$$QS = \sum_{j=1}^{3} UI_j \, (TD_j - TD), \tag{2.7}$$

where the summation is over the three adjacent surfaces.

2.1.2.3 Transient Formalism

In the transient, the fuel rod temperature calculation and the coolant temperature calculation cannot be separated. In SSC, these temperatures are solved for implicitly using a weighted-residuals procedure. In order to retain this procedure, which is computationally efficient, it was decided to handle the duct wall to duct wall heat flux explicitly. An explicit treatment of the heat fluxes does limit the time step, but an analysis of the limiting time constant showed it to be on the order of 4 seconds for typical designs, which is not overly restrictive for the analysis of most transients. Axial heat conduction was neglected as in the steady-state, permitting the calculations to be done on an axial level basis in a marching fashion.

The only equations that were modified for the transient were the duct wall temperature equations. These equations were given modified source terms which accounted for the duct wall to duct wall heat fluxes. The modified equation is

$$(mc_p) \, (TD - \overline{TD}) / \Delta t = QD + \overline{QS} \tag{2.8}$$

where

(mc_p) = lumped duct wall thermal mass

Δt = timestep size,

and the superscripted values are evaluated at the previous timestep.

		1	2	3	4	5	6	7	8	9	10	11	12	13	14	15	16	17	18	19	20	21
TD(1,1)	1	X	X																			
TC(1)	2	X	X	X																		
TD(1,2)	3		X	X	X					X	X											
TD(2,1)	4			X	X	X							X	X								
TC(2)	5				X	X	X															
TD(2,2)	6					X	X															
TD(3,1)	7							X	X													
TC(3)	8							X	X	X												
TD(3,2)	9			X					X	X	X								X			
TD(4,1)	10			X						X	X	X							X			
TC(4)	11										X	X	X									
TD(4,2)	12				X							X	X	X						X		
TD(5,1)	13				X								X	X	X					X		
TC(5)	14													X	X	X						
TD(5,2)	15														X	X						
TD(6,1)	16																X	X				
TC(6)	17																X	X	X			
TD(6,2)	18									X	X							X	X	X		
TD(7,1)	19												X	X					X	X	X	
TC(7)	20																			X	X	X
TD(7,2)	21																				X	X

Fig. 2.3 Banded Matrix for Steady-State Inter-Assembly Heat Transfer

These equations, along with the equations for the coolant and fuel pin temperatures, described in Sec. 3.1.2.6 of (Guppy, et al., 1983), are solved using standard banded matrix inversion routines. The order of the matrix is increased by one since there are now two duct wall temperatures per axial level per assembly. The formulation is compatible with the previously developed boiling model.

After the core temperatures have been advanced, the duct wall to duct wall heat fluxes are updated using Eq. 2.7.

2.1.2.4. Numerical Example

As a test of the inter-assembly model, SSC was used to simulate a scram from 100% power, 100% flow to natural circulation transient, that was performed at the Fast Flux Test Facility (FFTF).

To assess the inter-assembly model, the scram-to-natural circulation transient was simulated using SSC, both with and without inter-assembly heat transfer. The Row 6 fuel open test assembly (FOTA) coolant temperatures were taken as the main parameters of interest, since this assembly is adjacent to the colder reflector assemblies and should be more affected by inter-assembly heat transfer. A 10 channel core model was developed for SSC consisting of the Row 2 FOTA, average fuel channel, average reflector channel, and a seven assembly cluster centered on the Row 6 FOTA. This cluster consisted of five fuel assemblies and two reflector assemblies (assemblies 5 and 7 in Fig. 2.4).

Figure 2.4 also shows the exit coolant temperatures as calculated at steady-state with inter-assembly heat transfer (the lower figure on each assembly) and without inter-assembly heat transfer (the upper, underlined figure). As can be seen, with inter-assembly heat transfer, there is heat flow to the colder assemblies, raising their temperatures, and lowering the temperatures of the center assembly, as expected.

The transient was simulated for 360(s). The coolant temperatures at two axial locations, at the top of the fuel (heated section) and the top of the pin, as calculated by SSC were compared to the experimental data. The results from SSC without inter-assembly heat transfer are shown in Figs. 2.5-2.8. As can be seen, SSC is in good agreement with the Row 2 FOTA throughout the transient. However, SSC overpredicts the peak temperatures for the Row 6 FOTA, which, being adjacent to the colder reflector assemblies, should be more affected by inter-assembly heat transfer.

Figures 2.9-2.12 show the transient simulation by SSC with inter-assembly heat transfer. The Row 6 FOTA was the center of an inter-assembly cluster. As can be seen, the peak coolant temperatures for the Row 6 FOTA are now decreased and the agreement with the experimental data improved. The Row 2 FOTA was modeled without inter-assembly heat transfer; therefore, the results are the same.

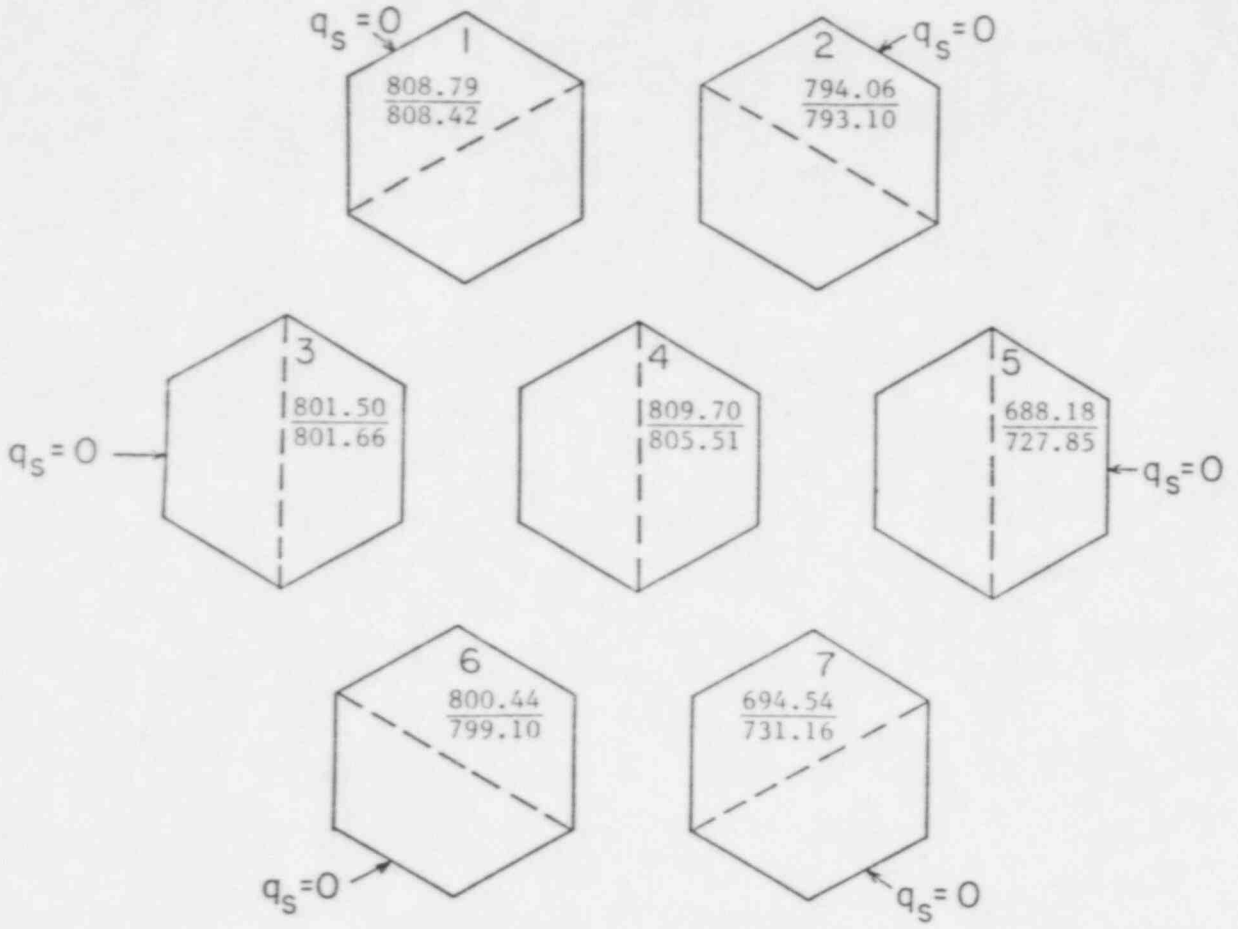

Fig. 2.4 Coolant Exit Temperatures for a Seven-Assembly Cluster With (lower figure) and Without (upper figure) Inter-Assembly Heat Transfer

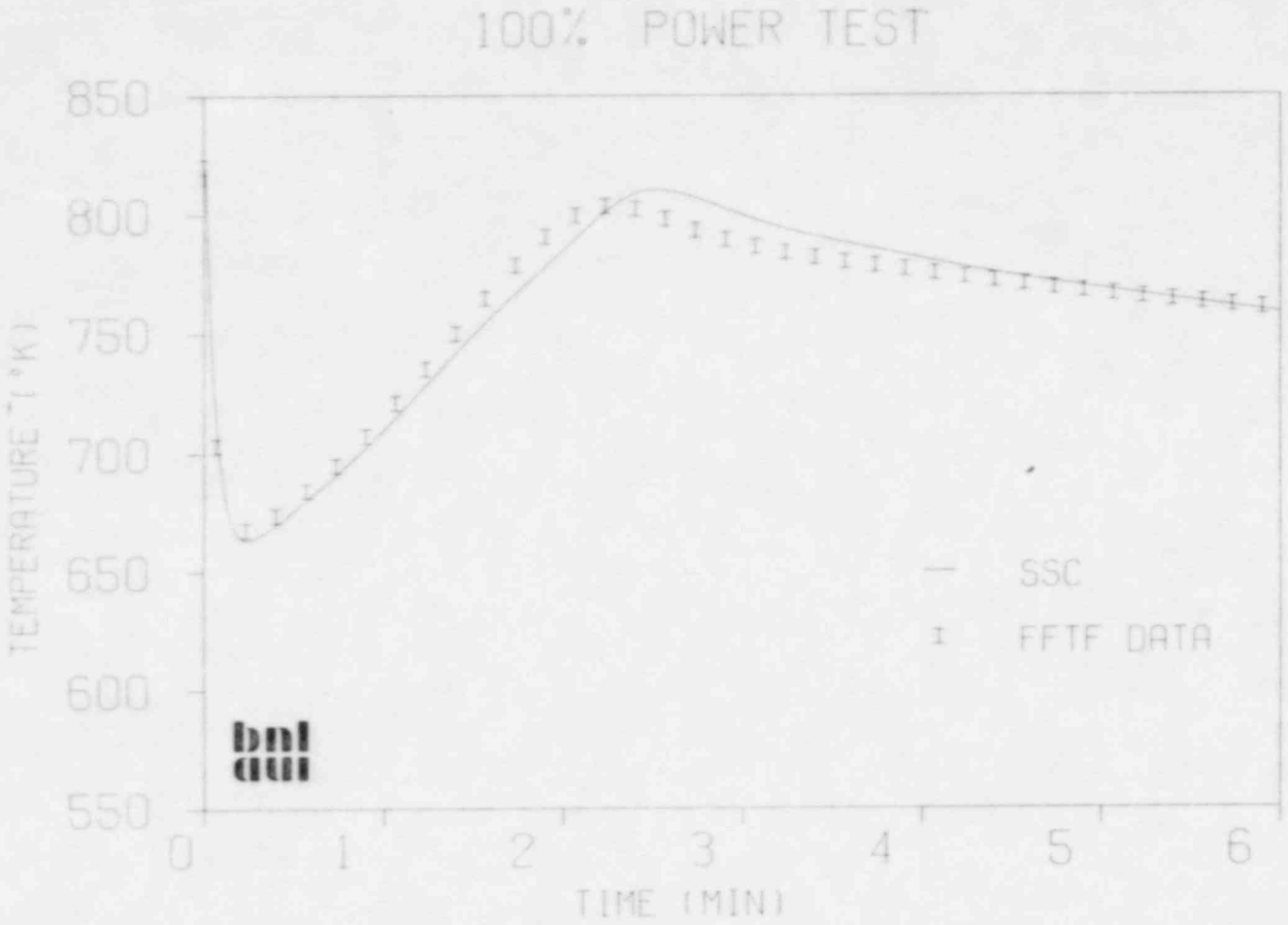

Fig. 2.5

No Inter-Assembly Heat Transfer

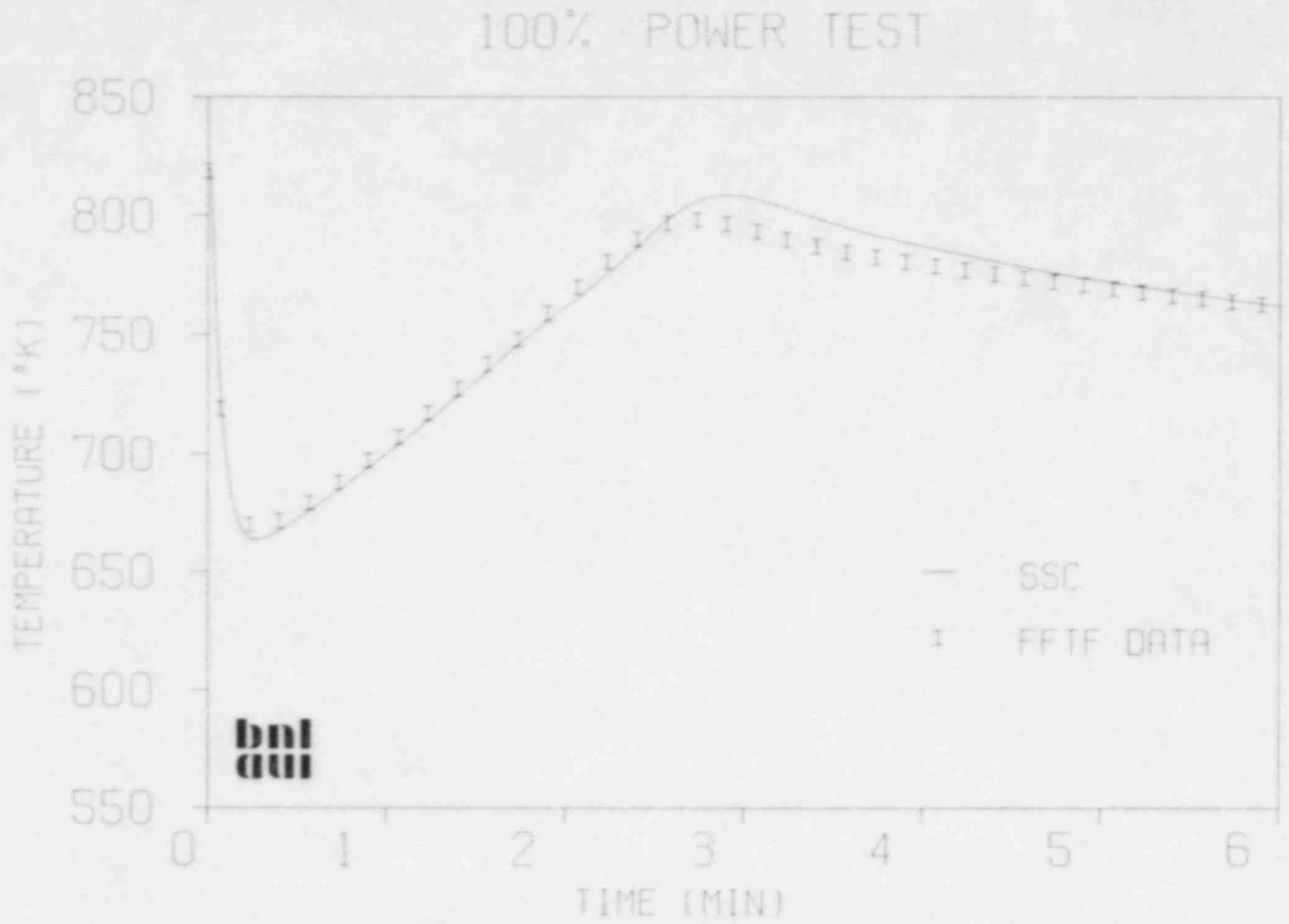

Fig. 2.6 ROW 2 FOTA, TOP OF PIN,

No Inter-Assembly Heat Transfer

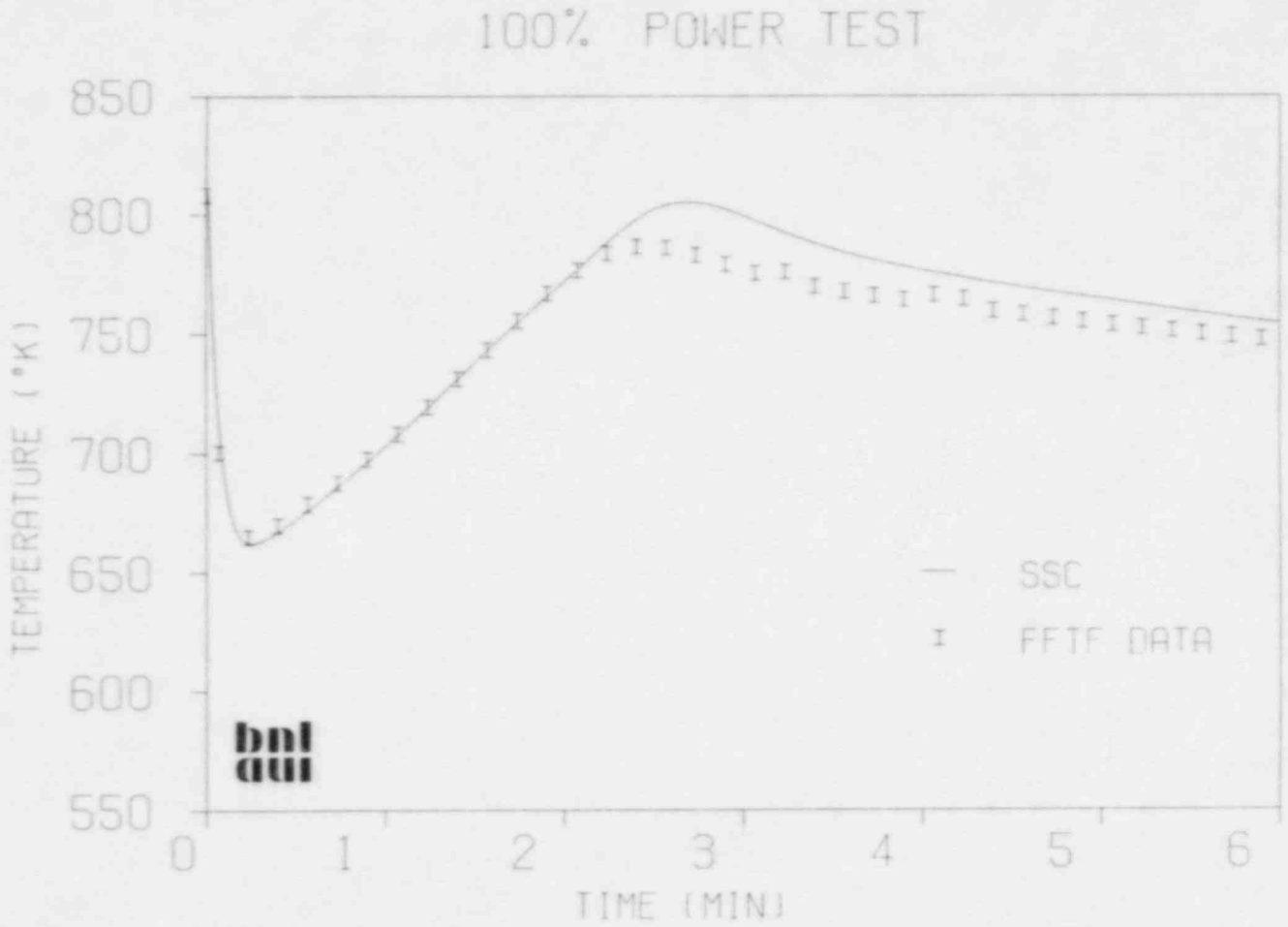

Fig. 2.7

No Inter-Assembly Heat Transfer

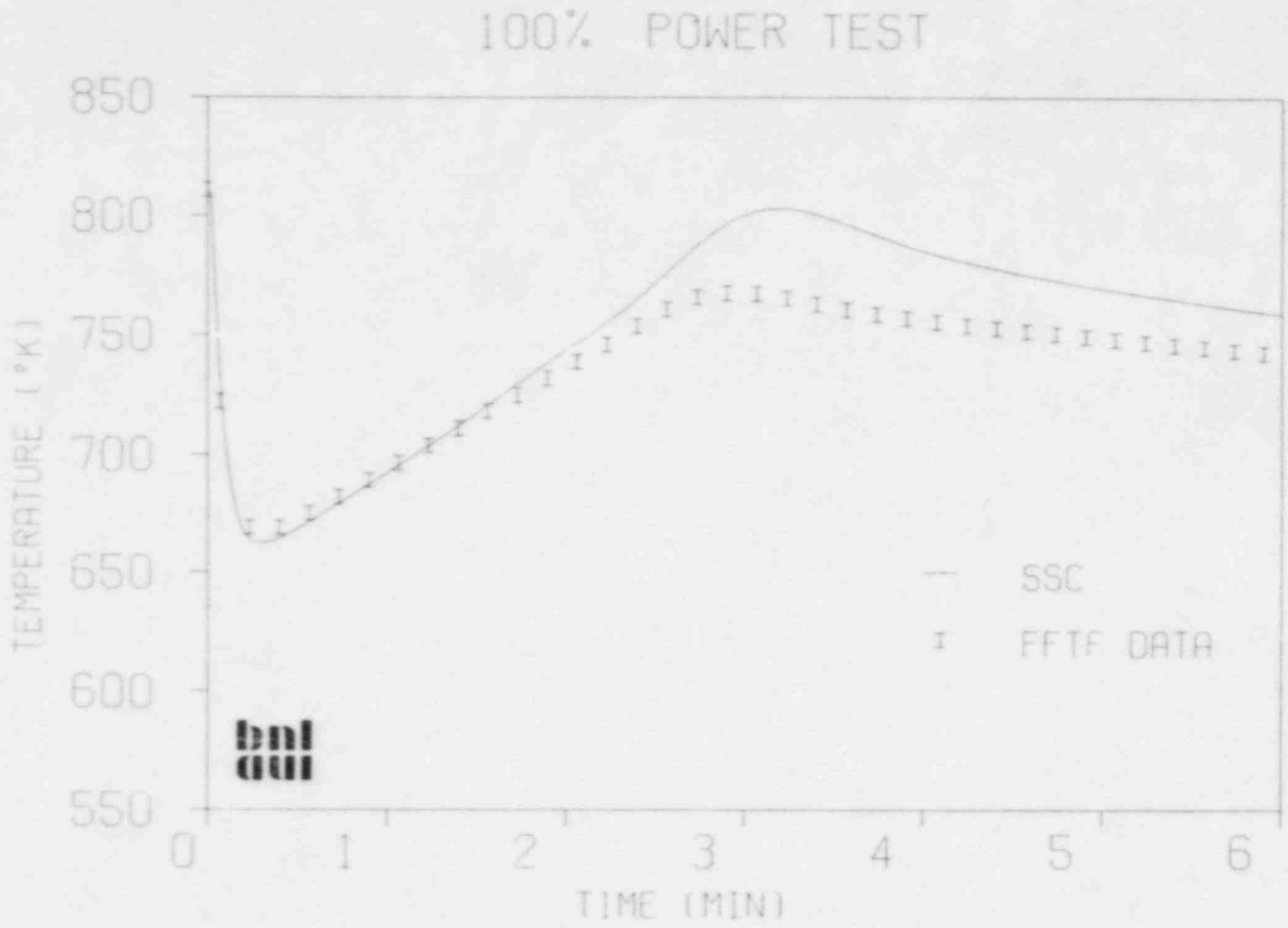

Fig. 2.8 No Inter-Assembly Heat Transfer

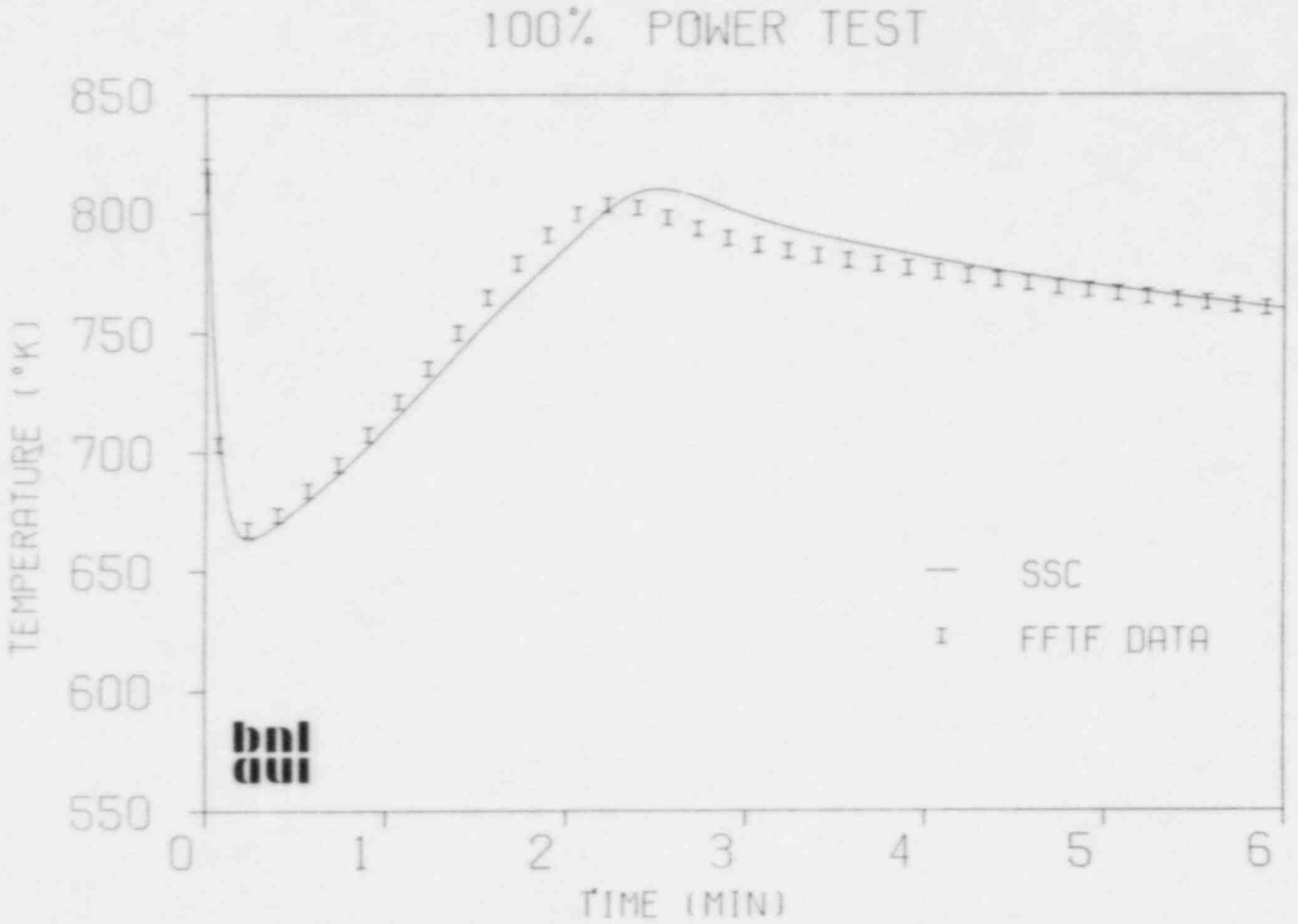

Fig. 2.9 Inter-Assembly Heat Transfer

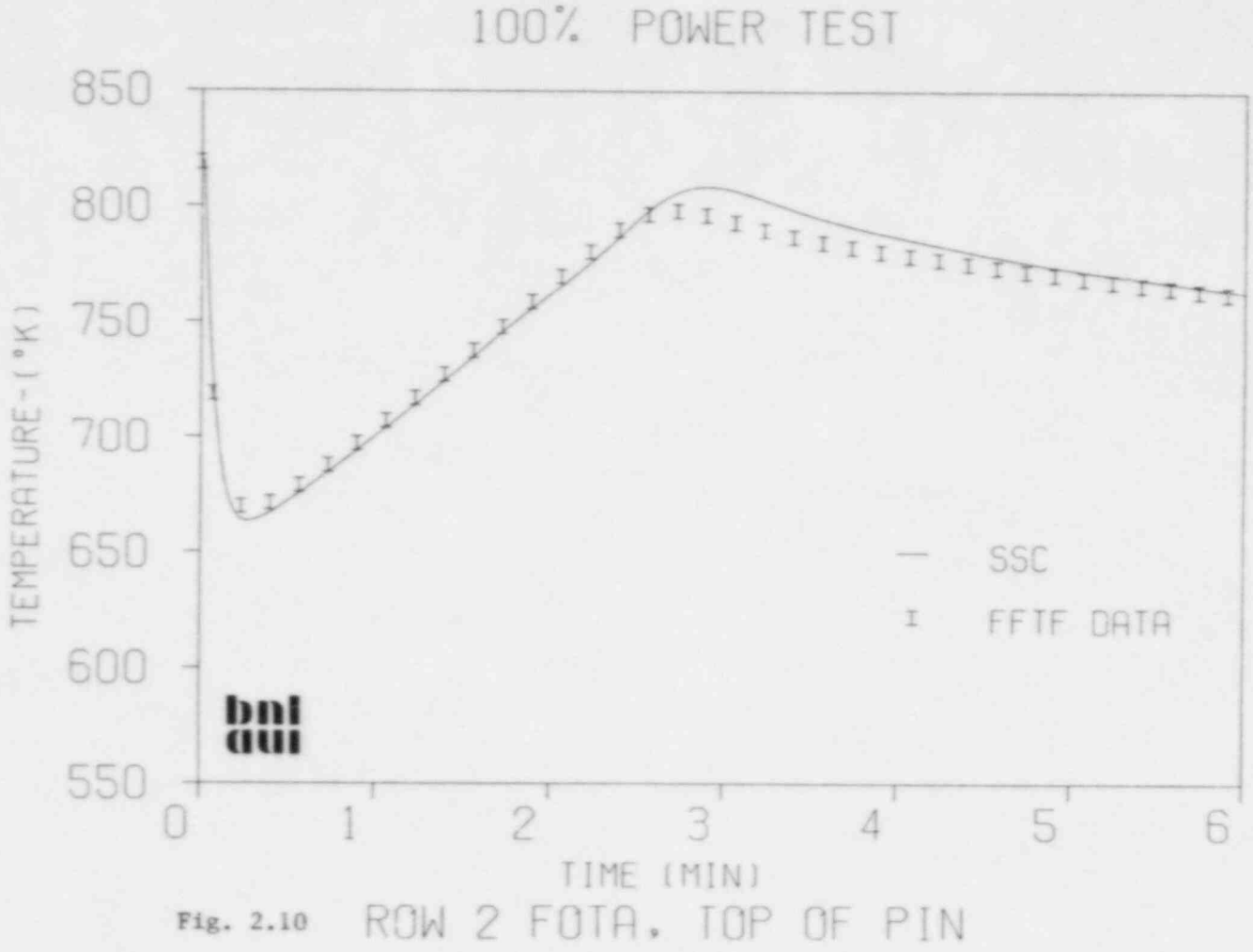

Fig. 2.10 Inter-Assembly Heat Transfer

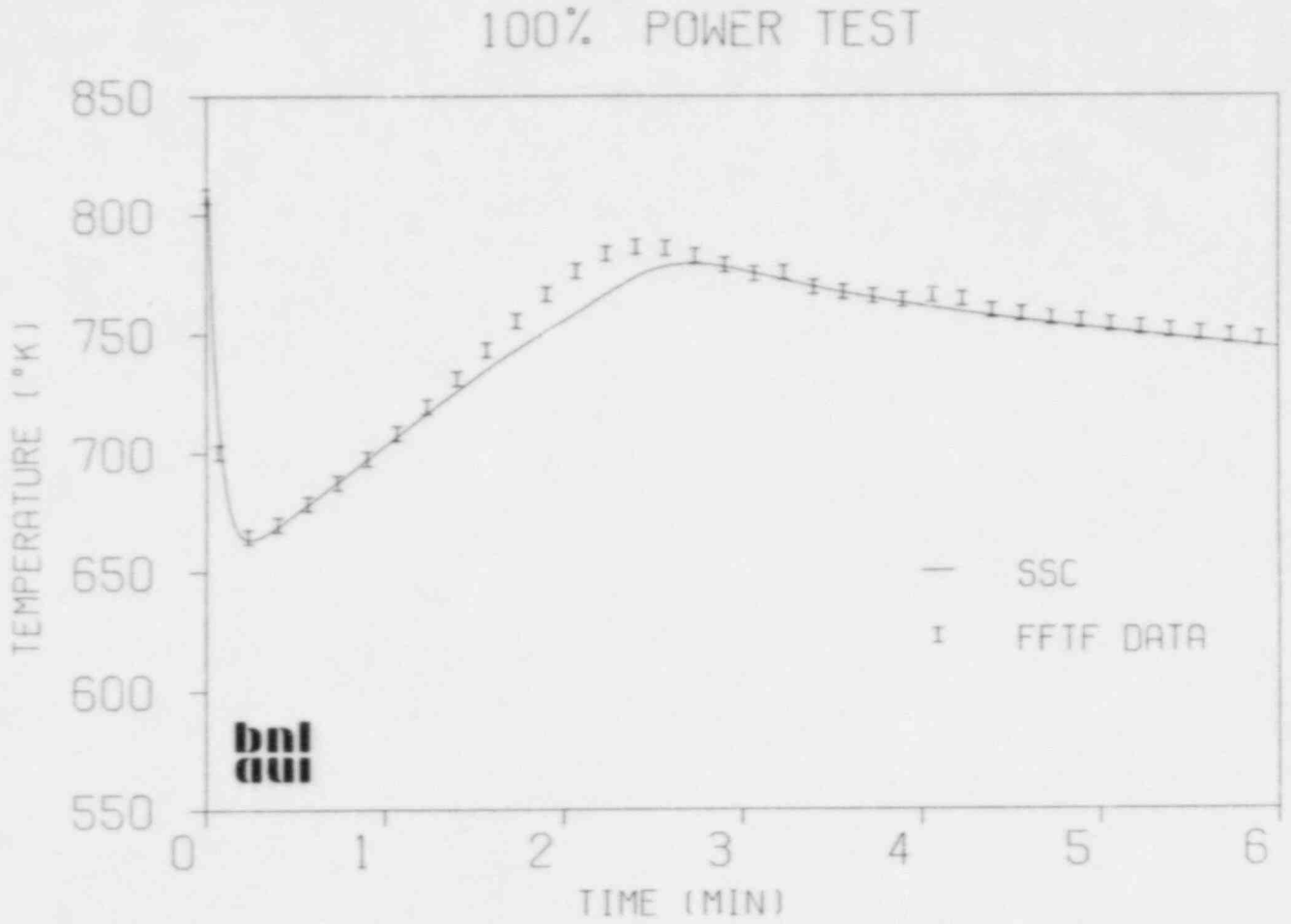

Fig. 2.11

Inter-Assembly Heat Transfer

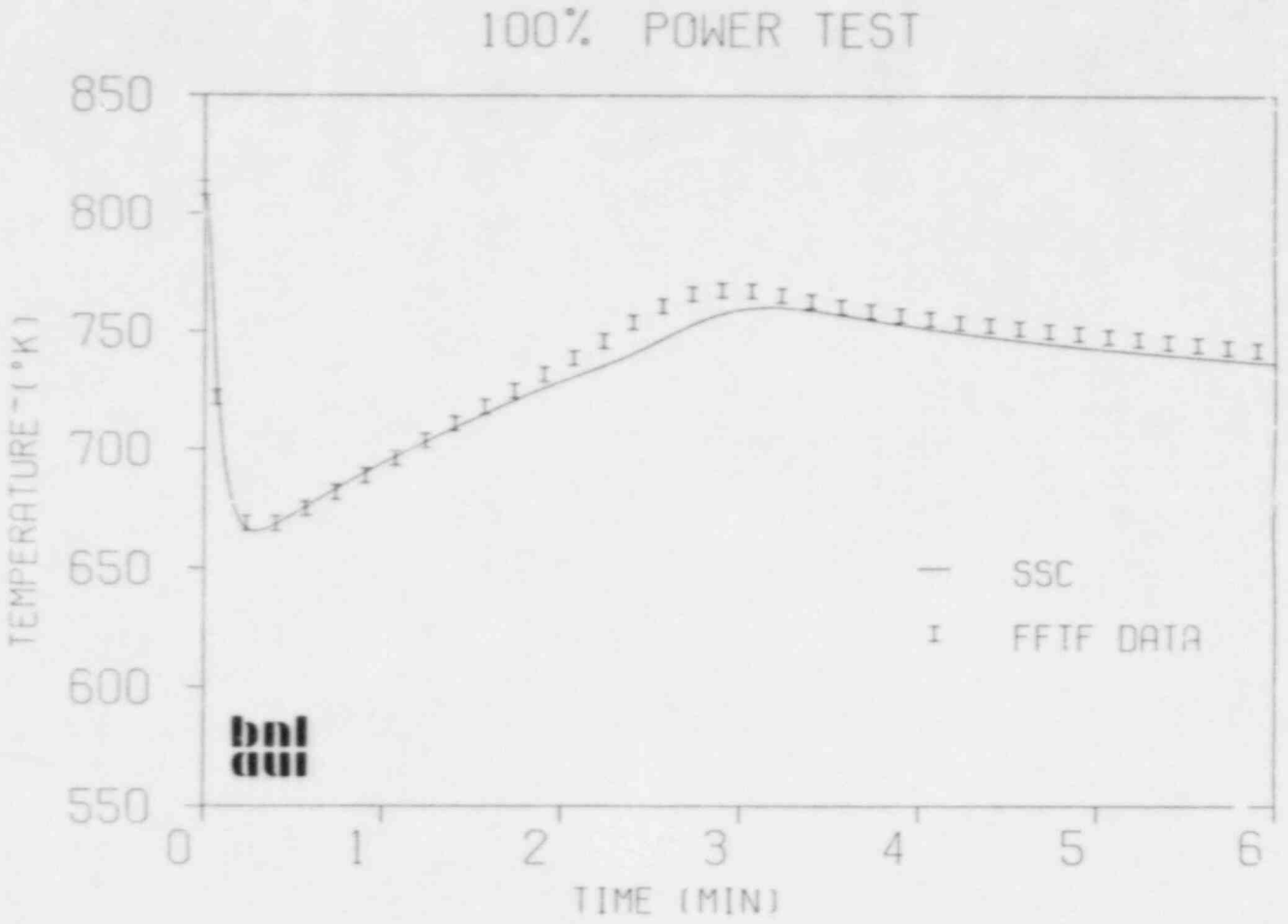

Fig. 2.12 ROW 6 FOTA, TOP OF PIN

Inter-Assembly Heat Transfer

2.1.2.5. Conclusions and Recommendations for Future Work

An inter-assembly heat transfer model has been developed and coded into SSC. The model is for a simplified seven assembly cluster, with each assembly having a two region duct wall temperature. More than one cluster can be represented at one time. The module makes extensive use of matrix techniques to attain the high computational efficiency necessary for a systems code such as SSC. The module was tested by simulating a scram-to-natural circulation transient using SSC with and without inter-assembly heat transfer. The inter-assembly heat transfer module significantly improved the SSC calculated coolant temperatures in an assembly adjacent to the reflector.

The module as coded is restricted to the SSC channel flow fraction specified steady-state option. Extension to the specified ΔP option should be done in the future. The coolant in the interstices is currently assumed to be stagnant. In certain cases, natural convection of this interstitial sodium may be possible. Future research into this possible heat removal mechanism should be done.

2.2 SSC-S Code (B. C. Chan)

2.2.1 Upper Plenum Model Coupling (B. C. Chan, R. J. Kennett)

The upper plenum data structure has been modified and implemented into the SSC program library. The resulting reduction in code and data structure is quite significant. The module has been debugged of Fortran errors and tested against previous calculations.

A 200 second transient test case is being run. In this transient, a reactor plenum similar to FFTF is used. The inlet temperature and velocity profiles used in this calculation are supplied from the results of an SSC four channel core model simulation. Complex flow patterns and transient temperature responses develop within the plenum for this reactor scram transient, which is followed by a reactor coolant pump coastdown. All results are in agreement with expectations. Further testing is in progress.

2.3 Generic Balance of Plant Modeling (MINET) (G. J. Van Tuyle)

2.3.1 Balance of Plant Models (G. J. Van Tuyle)

Models for Version 1 of MINET were completed several months ago. Major new models for the plant control system and the rotor module are planned for incorporation into Version 2 of MINET. In the meantime, various enhancements to Version 1 are to be made, so as to improve on the system modeling capabilities. This intermediate version of MINET will be designated Version 1A, as the name "Version 2" is to be reserved for the version that includes the control system models.

Thermodynamic and heat transfer properties for helium gas have been developed for application in MINET as the fifth fluid option. Preliminary testing indicates these properties are accurate over a wide range of temperatures

and pressures, and that the fitted functions execute quickly in the MINET calculations. A more extensive testing program should be undertaken before these properties are applied to modeling HTGR plant systems.

There is often a cover gas region in tanks containing quantities of subcooled fluids. When the subcooled fluid is drawn from the tank, the fluid level drops, and the gas expands as the pressure is reduced. In order to represent this trapped cover gas situation, a model was developed and incorporated into MINET 1A.

The MINET turbine model is based largely on basic thermodynamics and known performance characteristics. An important parameter in the turbine model is the efficiency of the turbine stage(s) in converting fluid energy into mechanical energy. In comparing the efficiency expressions currently in MINET to those used in the BNL Plant Analyzer (W. Wulff, et al., 1984), we have determined that the expressions in the latter are preferable in terms of both convenience and generality. A set of code modifications has been developed to incorporate the alternate set of efficiency expressions into MINET 1A.

Various drift-flux models were considered for incorporation into MINET as an optional representation of two-phase flow. An approach was developed to factor the unequal phase velocities into the calculation of the mixture density, via the void fraction. The fundamental approach is based on the original (Zuber and Findlay, 1965) model, and is similar to models incorporated in the MMS (EPRI) Two-Phase modules (Snidow and Wilson, 1984).

In this approach, the mixture density, ρ_m, is calculated from the void fraction, α, and densities of the liquid and gas phases, ρ_ℓ and ρ_g, respectively:

$$\rho_m = (1-\alpha)\ \rho_\ell + \alpha\ \rho_g \ . \qquad (2.9)$$

Void fraction α is evaluated from quality (X), mass velocity (G), drift velocity (V_{gj}), distribution parameter (C_o), and the phase densities:

$$\alpha = \frac{X}{C_o \left[\left(1 - \frac{\rho_g}{\rho_\ell}\right) X + \rho_g/\rho_\ell\right] + \rho_g\ V_{gj}/G} \ . \qquad (2.10)$$

The package of drift velocity correlations was taken from the TRAC-PD2 code (Rohatgi, et al., 1982) and includes bubbly and slug flow models from (Zuber and Findlay, 1965) and an annular flow model from (Ishii, 1977). As there are numerous drift velocity models for various conditions, it is likely that this initial MINET package will be upgraded in the future.

In the incorporation of a drift flux model into MINET , we are attempting to correctly account for the unequal velocities of the gas and liquid phases. This behavior can be important in a steam generator under low flow conditions, for example. We continue to treat both phases as having equal (saturation) temperatures, consistent with our application of MINET to the longer, slower, system-wide transients. The MINET drift-flux representation is, therefore, not nearly as detailed as the two-phase representations in TRAC and RELAP5, but is sufficient for anticipated MINET applications.

2.3.2 MINET Code Improvements (G. J. Van Tuyle, T. C. Nepsee, K. Lexing)

An updated version of MINET (Version 1.10) has been constructed. Enhancements to the input data error testing include:

- Data range testing for discrete-valued data on both INTEGER and REAL types
- Listing of field name and expected data range for all input data fields which are out-of-range
- Network connectivity tests to identify unconnected module ports
- Tests for missing data

Other enhancements include:

- Optional data records with default data values
- Reorganized formatted input data printout which groups records on a per-module basis

A new version of ABEND (the analysis package used for debug purposes in MINET code development) has been written to comply with CDC FORTRAN VERSION 5. It is currently under test with the FORTRAN 77 MINET.

Revisions to produce a 1977 FORTRAN compatible version of MINET have now been completed. The code is now being tested using CDC FORTRAN VERSION 5.

Work is progressing on Version 1A of MINET, which will be an extension of Version 1. The control system model and the rotor module will go into Version 2, but until that is accomplished, smaller improvements will go into Version 1A.

Wide range helium property functions have been developed and tested in code update form. The functions appear to work quickly and accurately, although a detailed study has not yet been performed.

The trapped cover gas option has been incorporated in the MINET update set, and some testing has been performed. We have determined that mass is being conserved, and that all trends appear correct and consistent.

For MINET Version 1A, a set of code modifications to incorporate the revised turbine efficiency expressions was developed and tested. Two sets of default parameters were incorporated into the input processor for options 1 (high pressure turbine) and 2 (low pressure turbine). In addition we plan to provide a third option, where the user can input a set of efficiency parameters for whatever alternate turbine type is under consideration.

A set of code modifications was developed to substitute the new drift-flux representation for the homogeneous equilibrium model of two-phase flow. Eventually this would be changed to a user-input option. The principal change is that the calculation of flow segment nodal density and density derivatives becomes dependent on the drift velocity, via the void fraction. Thus far, the only difficulty has been in getting convergence on the void fraction for a void-fraction-dependent drift velocity correlation. This was resolved by introducing a back-up iterative scheme based on bisection.

2.3.3 MINET Standard Input Decks (G. J. Van Tuyle)

MINET input decks currently in use were updated to execute with Version 1.10. Changes were made in two areas. First, because the subroutine line numbers were re-sequenced (for export), update commands had to be revised slightly. Second, the improved error diagnostics in the input processor began to reject certain un-used (i.e., "dummy") input parameters, so more physically sound values had to be substituted.

MINET input deck BF4 (see Fig. 2.13) includes representations for parts of the Brown's Ferry feedwater and ECCS systems, and is soon to be used in our RAMONA/MINET representation of the BWR system. We have recently conducted a detailed quality check on the input data, working to evaluate exactly where the uncertainties (due to lack of specific plant information) were located and how serious these uncertainties were. It now appears that the principal guesswork is in the area of response time, particularly for the pumps and valves. Because system response time has to be estimated regardless of how the system is represented, such guesswork in BF4 should not preclude its application.

Several decks used for earlier code validation work have been restored for testing of the drift-flux model. These include decks for EBR-II, the once-through and U-tube steam generator decks, and the helical coil heat exchanger deck. Current standard decks BF3 and BF4 do not normally contain two-phase flow, but remain active for application with RAMONA for BWR analysis.

2.3.4 MINET Validations and Applications (G. J. Van Tuyle, E. G. Cazzoli)

The initial RAMONA/MINET interface, through the feedwater line, has been completed and we are beginning to look at differences in the results between RAMONA/MINET and those generated by RAMONA alone. In applying RAMONA stand-alone, the user either specifies the feedwater flow and temperature vs. time or requests a control system representation. When the RAMONA control system option is invoked, the feedwater temperature (into the vessel) is switched (to room temperature) as soon as HPCI and RCIC come on line. Essentially, this

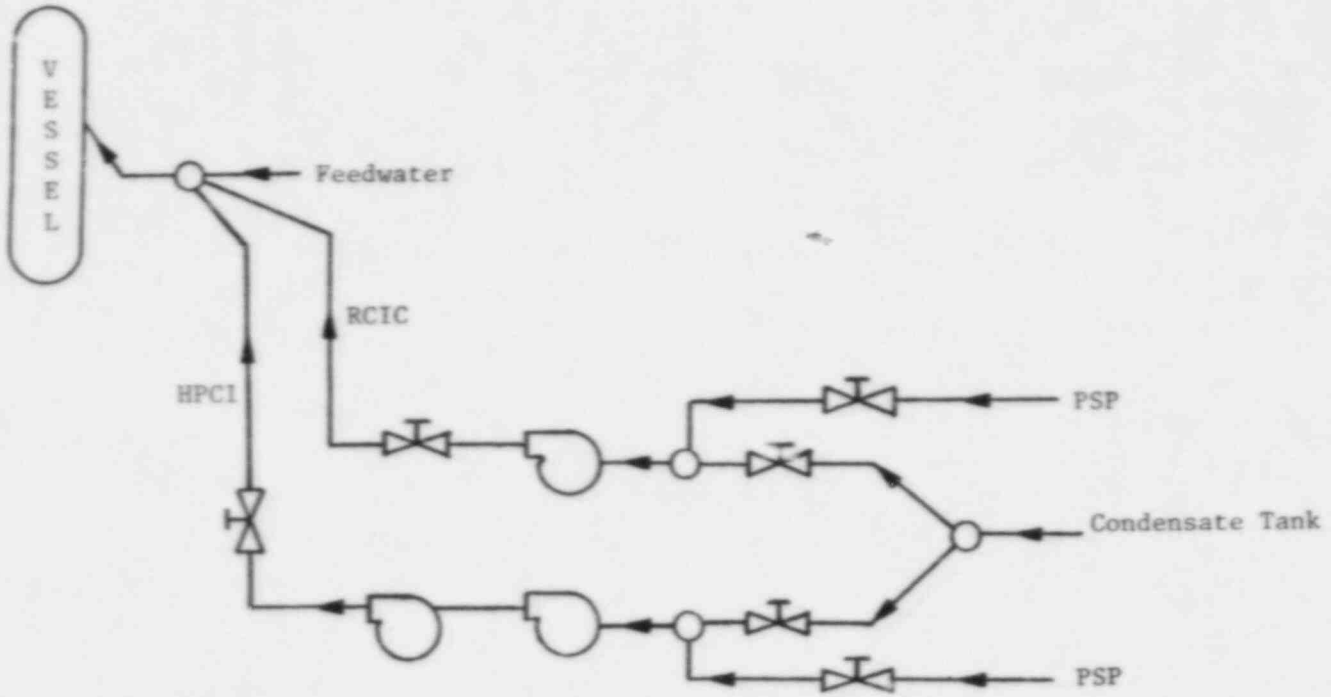

Fig. 2.13 MINET Deck BF4, HPCI and RCIC Systems from BROWNS FERRY

instantly converts all the water in the feedwater line from 464 K to 293 K. In Browns Ferry, this piping run is 70 meters long, and it causes a transport delay of nearly 1-1/2 minutes at combined HPCI and RCIC flow rates. When using the RAMONA/MINET combined representation, we have developed MINET Deck BF3 to account for this delay. We are still working to quantify the results of this change in the representation. It should be noted that much of the important SASA work performed using RAMONA was done with table-driven feedwater flows and temperatures obtained from more detailed thermal hydraulic analysis. Thus, these runs were not affected by the missing transport delay.

We have completed a preliminary design for the second RAMONA/MINET interface through the safety/relief valve line. Once this interface is completed, representation of the pressure suppression pool will be possible.

We are currently repeating our MINET validation tests in order to test the drift-flux model under development. The results for the once-through steam generator cases appear to be quite similar to our previous results, although this is not surprising, given the near full-flow conditions of the tests. However, there are discernable changes in the results, and they are in the right direction in terms of physical reasoning and in proximity to the experimental data.

2.3.5 User Support (G. J. Van Tuyle, T. C. Nepsee)

A copy of MINET Version 1.10 was sent to the New York Power Authority (NYPA), to be used in simulating the Fitzpatrick plant (a BWR). A second copy was sent to Babcock & Wilcox, for use in their plant simulator development effort.

Additional input verification has been implemented and tested. These improvements should make it easier for our initial users to debug their first MINET input decks.

REFERENCES

GUPPY, J. G., et al., (1984), "SSC Development, Validation and Application," Safety Research Programs Sponsored by Office of Nuclear Regulatory Research Quarterly Progress Report, July 1 - Sept 30, 1984, Brookhaven National Laboratory Report to be published.

GUPPY, J. G., et al., (1983), "Super System Code (SSC. Rev. 0) An Advanced Thermohydraulic Simulation Code for Transients in LMFBRs," Brookhaven National Laboratory Report, BNL/CR-3169, BNL-NUREG-51650, April 1983.

WULFF, W., et al., (1984), "The BWR Plant Analyzer," Brookhaven National Laboratory Report, BNL/CR-3943, BNL-NUREG-51812, July 1984.

ZUBER, N. and FINDLAY, J. A., "An Average Volumetric Concentration in Two Phase Flows," Transactions of ASME Journal of Heat Transfer, Vol. 87, p. 453, Nov. 1965.

SNIDOW, N. L. and WILSON, T. L., "U-Tube Steam Generator for the Modular Modeling System," Proceedings of the International Conference on Power Plant Simulation, Cuernavaca, Morelos, Mexico, Nov. 1984.

ROHATGI, U. S., et al., "Constitutive Relations in TRAC-PD2," Brookhaven National Laboratory Report, BNL/CR-3073, BNL-NUREG-51616, Sept. 1982.

ISHII, M., "One Dimensional Drift-Flux Model and Constitutive Equations for Relative Motion Between Phases in Various Two-Phase Flow Regimes," ANL-77-47, Oct. 1977.

PUBLICATIONS

HORAK, W. C. and GUPPY, J. G., "Improved Inter-Assembly Heat Transfer Modeling Under Low Flow Conditions for the Super System Code," Brookhaven National Laboratory Report to be published.

VAN TUYLE, G. J., "MINET Validation Study Using Steam Generator Test Data," Proceedings of the International Conference on Power Plant Simulation, Cuernavaca, Mexico, November 19-21, 1984. To be published.

3. Thermal-Hydraulic Reactor Safety Experiments

3.1 Core Debris Thermal-Hydraulic Phenomenology: Ex-Vessel Debris Quenching
(T. Ginsberg, J. Klein, J. Klages and C. E. Schwarz)

This task is directed towards development and experimental evaluation of analytical models for prediction of the rate of steam generation during quenching of core debris under postulated LWR core meltdown accident conditions. This program is designed to support development of LWR containment analysis computer codes.

3.1.1 On the Effect of Steam Superheating on Debris Bed Quenching

In the April-June 1984 Quarterly Progress Report (Ginsberg, 1984) an analysis was presented of the influence of steam superheat on debris bed heat removal. The following discussion expands upon the previous work and corrects an error in the result presented earlier.

Figure 3.1 is a schematic diagram of a superheated packed bed during a transient quench process. The model is discussed by Ginsberg (1984). The heat flux at the quench front, q_{QF}, was shown to be

$$q''_{QF} = (\rho_g j_g)_{TB} h_{fg} \tag{1}$$

where ρ_g and j_g are the density and vapor volume flux, respectively, both evaluated at conditions local to the top of the bed (TB). h_{fg} is the latent heat of vaporization. The heat flux at the top of the bed is given by

$$q''_{TB} = (\rho_g j_g)_{TB} h_{fg} \left[1 + \frac{c_g (T_g - T_{SAT})}{h_{fg}}\right] \tag{2}$$

where both c_g and T_g are the steam specific heat and temperature, both evaluated at the top of the bed. T_{SAT} is the water saturation temperature.

An error was made, however, in calculations leading to Fig. 4.2 of the April-June 1984 quarterly report. A corrected calculation is shown in Fig. 3.2, in which the quench front and debris bed heat fluxes are shown as a function of steam exit temperature for quench cooling of a superheated bed of porosity 0.4 and height of 1 m. Note that the heat flux at zero steam superheat is approximately that at the intercept. As indicated above, the quench front heat flux is smaller than the overall bed heat flux as a result of the assumption that the steam is superheated as it flows up the channels of unquenched particles. The advance of the quench front would be determined by the quench front heat flux. Note that for small particles the effect of superheat is significant, both for the quench front and the overall bed heat fluxes. For the large particles the effect of steam superheat is less pronounced.

The effect of steam superheating on the quench front and debris bed heat fluxes can be understood with the aid of Eqs. (1) and (2) and Fig. 3.3, which

shows the behavior of the steam volume flux computed using the Lipinski model with steam superheat. The parameters affecting the heat fluxes are the steam density, the volume flux of steam at the top of the bed and the steam superheat. The steam density is a decreasing function of steam temperature. The dependence of volume flux of steam on temperature comes about through the effects of density and steam viscosity. For beds of particles in the range of millimeters in diameter, the volume flux of vapor is a relatively weak function of steam temperature, as shown in Fig. 3.3. For small particles (~1-mm diameter), the vapor flux from the bed decreases with temperature as a result of the dependence on the viscosity, whereas for the large particles (~2-mm diameter), the vapor flux increases with temperature due to the effect of decreasing vapor density. Since both the steam density and volume flux decrease with temperature for small diameter particles, the quench front heat flux also decreases relatively strongly with temperature. For the large particles the steam flux increases with temperature and the combined effect with vapor density is a weaker dependence of quench front heat flux on steam temperature. The heat flux at the top of the bed is influenced by the superheat multiplier given in Eq. (2). This leads to the weaker dependence on temperature than computed for the quench front heat flux.

The above calculations indicate that the effect of steam superheat on heat flux during bed quench is a significant one, especially for small particles and under conditions of large steam superheat.

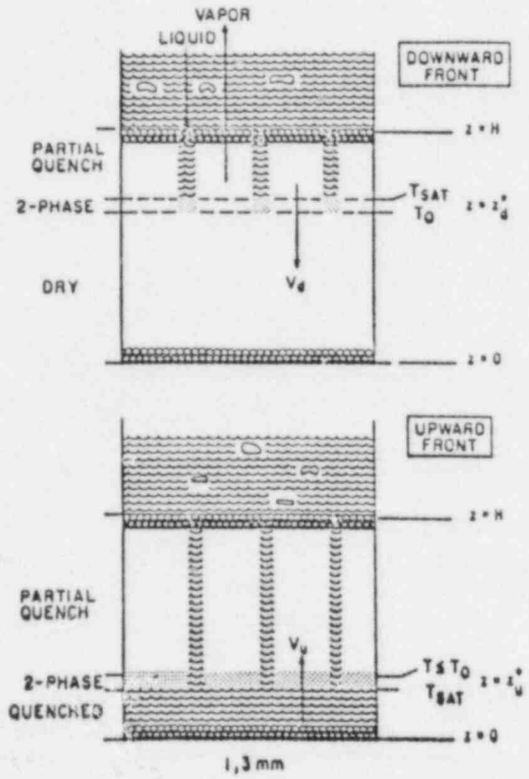

Figure 3.1 Schematic of Superheated Packed Bed Quench Process.

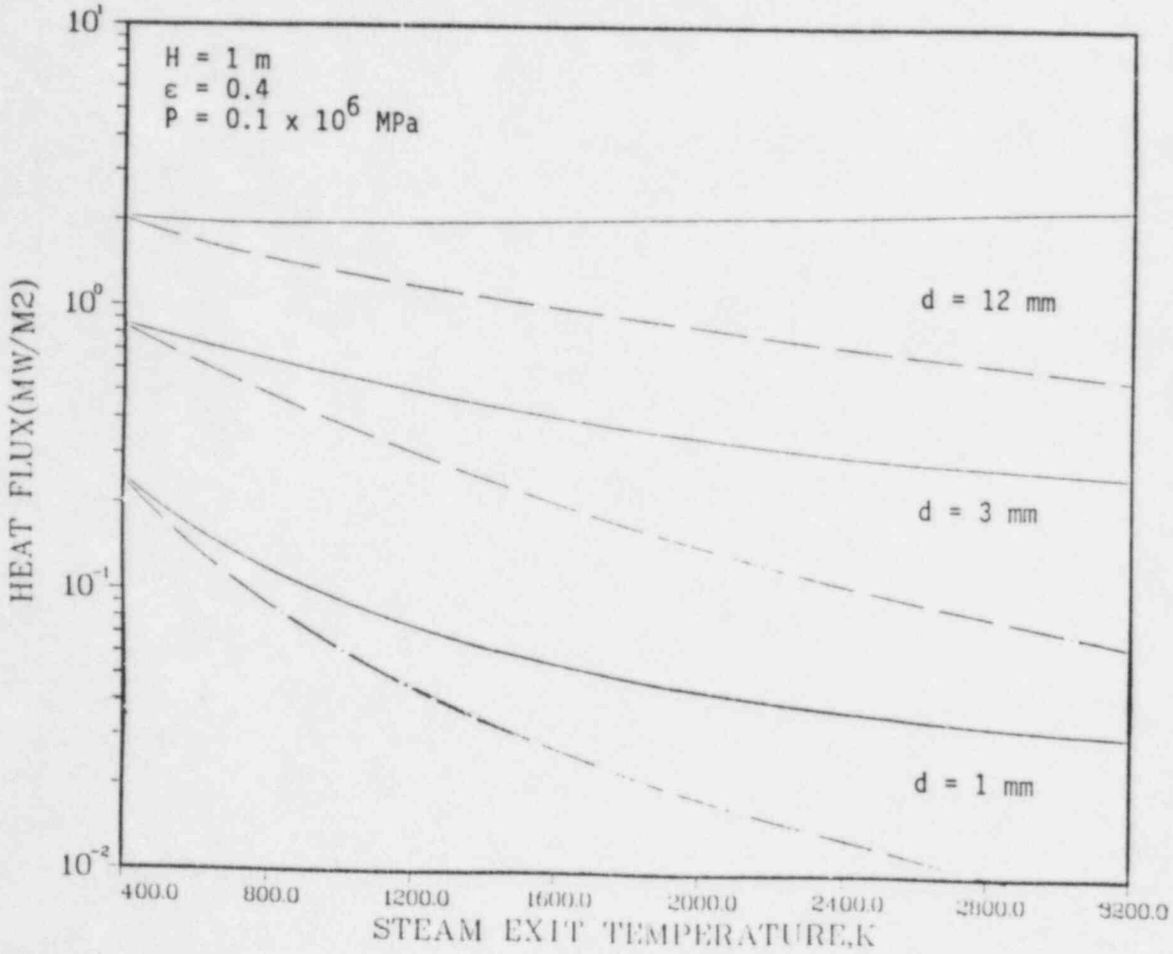

Figure 3.2 Variation of Bed Heat Flux With Steam Temperature During Quench Process.

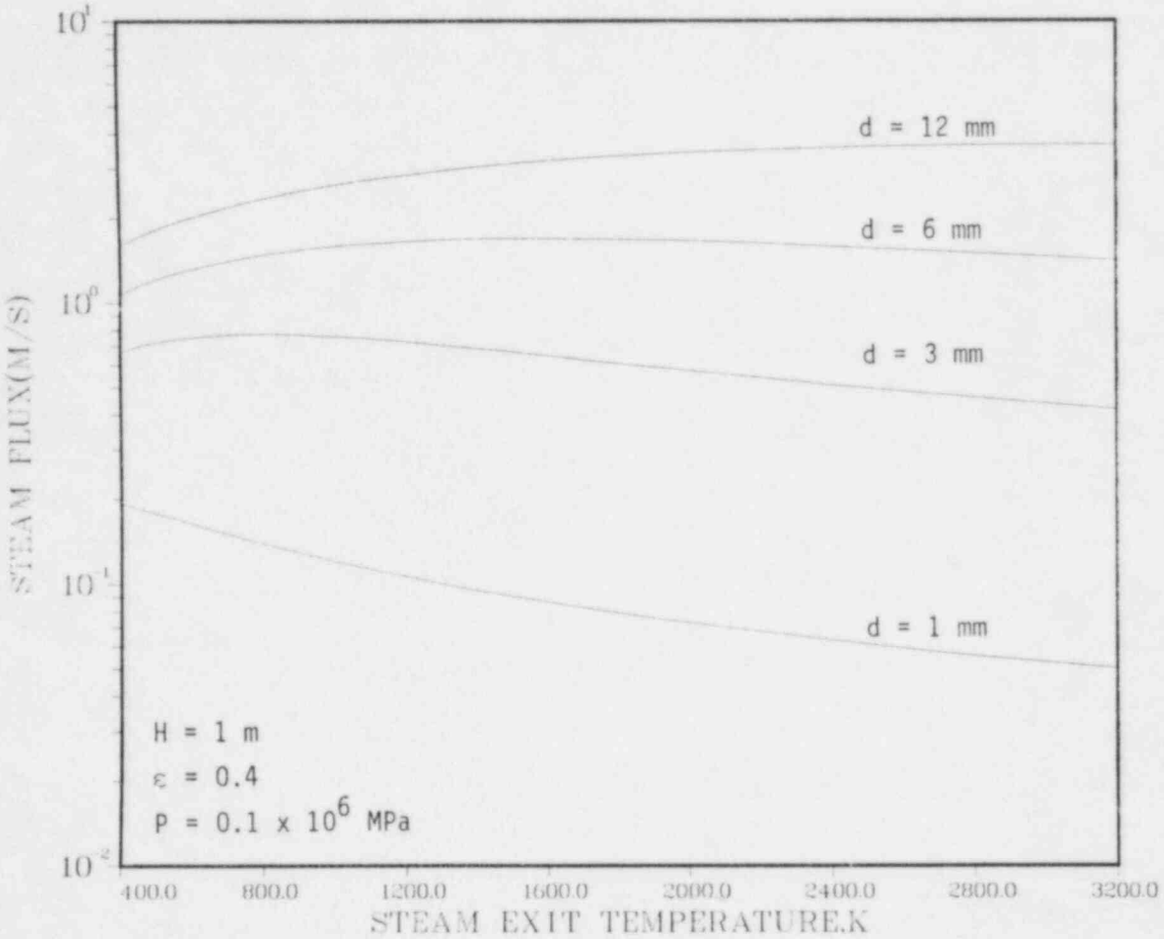

Figure 3.3 Effect of Steam Superheat on Steam Volume Flux.

3.2 Core Debris Thermal-Hydraulic Phenomenology: In-Vessel Debris Quenching

(N.K. Tutu, T. Ginsberg, J. Klein, J. Klages and C.E. Schwarz)

The purpose of this task is to develop an understanding of the transient quenching of in-vessel debris beds (formed in the reactor core region) when the coolant is injected from below. The experimental results would, in addition, generate a data base for verifying the transient thermal-hydraulic models for the quenching process. The present experimental and model development effort is directed towards the case where the coolant is being injected at a constant rate.

3.2.1 Experimental Program

The second series of debris bed quench experiments was begun. Special thermocouple probes, with the thermocouple junction inside the 3.18-mm stainless steel sphere (particle thermocouple), were placed within the debris bed to monitor the actual solid-fluid heat transfer rates. Preliminary results from the 10 runs performed to date indicate that only one of the "particle thermocouples" within the bed shows the "expected" quench behavior. It is suspected that the "particle thermocouples" being used might be defective. Therefore, a second batch of "particle thermocouples" has been fabricated using a different and more reliable technique of internal spot welding. These have been installed in the test section.

3.3 Core-Concrete Heat Transfer Studies (G.A. Greene)

The purpose of this task is to study the mechanisms of liquid-liquid boiling heat transfer and its effect on the ex-vessel attack of molten core debris on concrete. This effort is in support of the CORCON and VANESA development programs at Sandia National Laboratories.

3.3.1 Ex-Vessel Aerosol and Source Term Audit Study

The Accident Source Term Program Office has sponsored the development of a suite of severe accident phenomenology codes intended to describe how a nuclear reactor core might degrade without adequate cooling and release radioactive fission products. The codes follow the subsequent transport of the fission products from the damaged core to the environment if the containment fails or is bypassed. These codes therefore focus on the release and transport of fission products and were applied to model selected severe accidents for six representative reactor designs. The results of this code application effort are reported in BMI-2104 (Gieseke et al., 1984).

This methodology has received extensive peer review and is also under review by the American Physical Society. As a result of questions raised during the review, it was decided to demonstrate that the suite of codes, in particular CORCON (Muir et al., 1981) and VANESA (Powers et al., 1983), could be exported to an independent organization and that, by using similar input parameters and intercode data transfer, similar results to those reported in BMI-2104 for ex-vessel aerosol and fission product release to containment could be obtained. BNL was selected by the NRC to be the independent organization. The accident sequences that were chosen for this audit were the Peach Bottom AE, Surry TMLB' and Surry S2D sequences.

The primary objective of this effort was to demonstrate that the two codes used for the calculations of the ex-vessel source term, CORCON and VANESA, could be made operational at BNL and that the results in BMI-2104 could be reproduced.

3.3.2 Calculational Models

The codes used to analyze the ex-vessel release of aerosols and fission products to the containment in these audit calculations were CORCON/MOD1-C2

and VANESA. It was requested that no modifications be made either to the codes themselves or to their input, and that the same versions of the codes be used. With respect to CORCON, this meant determining that all official Fortran updates to the code be identified and attached for the calculation. One update was identified which had only been transmitted to BNL informally and this was used in the audit. With respect to VANESA, this meant getting the code running on the BNL computer, running a sample problem, and identifying errors in transcribing the Fortran version from the original SNL version. Errors and inconsistencies in the VANESA model sent to BNL were identified in this fashion and corrected. This ensured that the SNL and BNL versions of both CORCON/MOD1-C2 and VANESA were the same.

A discussion of both CORCON and VANESA as utilized in these audit calculations follows.

3.3.3 CORCON

The CORCON code was used to calculate the ex-vessel attack of molten core debris on the basemat, and this calculation drives the ex-vessel aerosol and fission product source term calculation. The CORCON code is a model for the analysis of the interaction between molten fuel and structural materials with concrete. Typical output of CORCON calculations are the concrete erosion rate, generation rates of concrete decomposition gases, and the core-melt temperature history. These three quantities are necessary input to the VANESA code for the calculation of the ex-vessel release of fission products and aerosols into the containment during a core melt accident.

The version of the CORCON code used in all the BMI-2104 accident sequence source term calculations was CORCON/MOD1 with two official Fortran update packages documenting changes made to the original code by Sandia National Laboratories. This code is heretofore referred to as CORCON/MOD1-C2. A third update which was not distributed was identified during this audit calculation and was used in the BNL calculations.

The input to the CORCON code consists primarily of concrete composition data (user input), core melt composition (MARCH output), cavity geometry (plant specifications/FSAR), surroundings temperature history (user input or MARCH), initial melt temperature and time after SCRAM at start of core/concrete interaction (MARCH), and melt/concrete/surroundings radiative emissivity vs. time (user input). Those input variables which are "user input" are left to the discretion and scientific judgment of the user. There are no internal parametric model variations possible through input. A more complete assessment of this computer code may be found in ORNL/TM-8842, Chap. V.

The input and results of the three sets of CORCON/MOD1-C2 calculations for the Peach Bottom AE, Surry TMLB', and Surry S2D sequences are shown in Reference 5 and will be omitted here. They consist of melt temperature history vs. time, integrated gas generation rates vs. time, and vertical and lateral erosion depths vs. time. These results, along with the integrated concrete erosion mass vs. time, were input to the VANESA model for calculation of the ex-vessel aerosol and fission product release rates.

3.3.4 VANESA

In order to account for the ex-vessel release of aerosols and fission products into the containment during the thermal interaction between molten core debris and structural concrete, the VANESA model was used. The VANESA model is a mechanistic description of the aerosol generation and fission product release during ex-vessel core-concrete interactions.

The version of VANESA used in these audit calculations was the first exportable Fortran version. This version was adapted from the original non-Fortran version written at SNL and used in the BMI-2104 study. The code was first received at BNL on November 15, 1984. It was successfully compiled and a sample problem executed on November 19, 1984. In the process of familiarization with the code, several minor transcription errors were identified in the Fortran version by the SNL and BNL staff and were corrected. A more complete description of the VANESA model may be found in ORNL/TM-8842, Chapter VI. The VANESA model accepts as input the output of the CORSOR and CORCON computer codes.

From CORSOR, VANESA will get the mass of all species in the core melt inventory. At the present state of development, VANESA can accept explicitly 32 species; other species are surrogates of one of the 32 species. In addition, it is required to input the inventory of Nb as the equivalent mass of Nb_2O_5 directly into VANESA. These variations on melt species input reflect the ongoing development of the VANESA model as new species were identified as important during the Accident Source Term Reassessment Study.

From CORCON, VANESA receives the following information at each time step as calculated:

oxide melt temperature (K)
integrated gas release rates (kg)

H_2
H_2O
CO
CO_2

maximum radial erosion radius (m)
SiO_2 content of melt (kg)

In this study, the two codes were linked and these variables were transferred automatically.

A detailed description of the output from VANESA has been documented elsewhere (Powers et al., 1983) and will not be repeated here. The most important of the output quantities for subsequent use in the calculation of the ex-vessel source term are:

1. aerosol mass generation rate,
2. chemical composition of aerosolized mass,
3. aerosol mean particle size, and
4. aerosol density.

3.3.5 Summary of Results and Comments

A summary of the ex-vessel release rates of aerosols and fission products from the BMI CORCON/VANESA calculations is presented in Reference 5 for the Peach Bottom AE, Surry TMLB', and Surry S2D sequences. The calculated source rates are generally in agreement with the BMI-2104 results within $\pm 5\%$, often closer to $\pm 1\%$. Calculated melt temperatures have been found to be in agreement generally within ± 5-10 K. The fractional composition of each species in the aerosol was calculated by BNL to be nearly identical to the results presented in BMI-2104, disagreeing by no more than 2-3%. This level of agreement between the results of the BNL audit calculations and the results presented in BMI-2104 is generally found in all three of the cases examined. (The Peach Bottom AE ex-vessel source term was recalculated by SNL and the new results supercede those presented in BMI-2104, Volume II.)

The release fractions for five selected species were integrated over 10 hours of core/concrete interactions and the BNL and SNL results are presented in Table 3.1. The SNL figures reflect the recent recalculation referred to above; the BNL figures reflect the results from the audit calculation. From the table, it is clear that the BNL and SNL (BMI-2104) results are in excellent agreement when integrated over 10 hours. The results from the two sets of calculations differ, in fact, by no more than round off error.

Table 3.1 Comparison of Total Ex-Vessel Release Fractions (%) of Selected Species for Peach Bottom AE Sequence Calculation by SNL and BNL*

	La_2O_3	SrO	BaO	Te	CeO
SNL	1.8	67	48	69	2.9
BNL	1.9	68	49	68	3.0

*Integrated release from ex-vessel core/concrete interaction over 10 hours.

This comparison demonstrates that the CORCON and VANESA codes can be successfully exported to an independent organization, and that the results in BMI-2104 can be reproduced if the same versions of the codes and identical input and modeling assumptions are used. This assessment is in no way to be interpreted as an endorsement of the methodology used in the BMI-2104 study. The audit calculations have demonstrated that some inconsistencies exist in BMI-2104 regarding inter-code data transfer. However, for the particular sequences examined, these inconsistencies did not strongly influence the predicted ex-vessel aerosol and fission product release rates.

REFERENCES

GINSBERG, T., et al., (1984), "Thermal-Hydraulic Reactor Safety Experiments," Ch. 4 in Safety Research Programs Sponsored by Office of Nuclear Regulatory Research, Quarterly Progress Report, compiled by Allen J. Weiss, April 1 - June 30, 1984, NUREG/CR-2331, BNL-NUREG-51454, Vol. 4, No. 2 (1984).

GIESEKE, J.A., CYBULSKIS, P., DENNING, R.S., KUHLMAN, M.R., LEE, K.W., and CHEN, H., "Radionuclide Release Under Specific LWR Accident Conditions," BMI-2104 (July 1984).

MUIR, J.F., COLE, R.K., CORRADINI, M.L., and ELLIS, M.A., "CORCON-MOD1: An Improved Model for Molten Core-Concrete Interactions," SAND80-2415 (1981).

POWERS, D.A. and BROCKMAN, J.E., "Status of VANESA Validation," Chap. VI, in "Review of the Status of Validation of the Computer Codes Used in the NRC Accident Source Term Reassessment Study," ORNL/TM-8842 (November 1983).

GREENE, G.A., "Status of Validation of the CORCON Computer Code," Chap. V, in "Review of the Status of Validation of the Computer Codes Used in the NRC Accident Source Term Reassessment Study," ORNL/TM-8842 (November 1983).

GREENE, G.A., et al., "Audit Calculations of Ex-Vessel Fission Product and Aerosol Release to Containment for Selected Accident Sequences," BNL Informal Report to J. Rosenthal (USNRC), (January 10, 1985).

4. Plant Analyzer
(W. Wulff)

4.1 Introduction

This program is being conducted to develop an engineering plant analyzer, capable of performing accurate, real-time and faster than real-time simulations of plant transients and Small-Break Loss of Coolant Accidents (SBLOCAs) in LWR power plants. The engineering plant analyzer is being developed by utilizing a modern, interactive, high-speed, special-purpose peripheral processor, which is designed for time-critical systems simulations. The engineering plant analyzer primarily supports safety analyses, but it also serves as the basis of technology development for nuclear power plant monitoring, for on-line accident diagnosis and mitigation, and for upgrading operator training programs and existing training simulators.

Originally, there were three activities related to the LWR Plant Analyzer Development Program; namely, (1) the assessment of the capabilities and limitations of existing simulators for nuclear power plants, (2) the selection and acquisition of a special-purpose, high-speed peripheral processor suitable for real-time and faster than real-time simulation of power plant transients, and (3) the development of mathematical models and the software for this peripheral processor.

Below is a brief summary of previous results and a detailed summary of achievements during the current reporting period.

4.2 Assessment of Existing Training Simulators (W. Wulff and H. S. Cheng)

The assessment of then current simulator capabilities consisted of evaluating qualitatively the thermohydraulic modeling assumptions in the training simulator and comparing quantitatively the predictions from the simulator with results from the detailed systems code RETRAN.

The results of the assessment have been published earlier in three reports (Wulff, 1980; Wulff, 1981a; Cheng and Wulff, 1981). It had been found that the reviewed training simulators were limited to the simulation of steady-state conditions and quasi-steady transients within the parameter range of normal operations. Most PWR simulators delivered before 1980 cannot simulate two-phase flow conditions in the primary reactor coolant loops, nor the motion of the two-phase mixture level beyond the narrow controls range in the steam generator secondary side. Most BWR simulators delivered before 1980 cannot simulate two-phase flow conditions in the recirculation loops or in the downcomer and lower plenum, nor can they simulate coolant level motions in the steam dome, the lower regions of the downcomer (below the separators), or in the riser and core regions. These limitations arise from the lack of thermohydraulic models for phase separation and mixture level tracking (Wulff, 1980; 1981a).

The comparison between PWR simulator and corresponding RETRAN results, carried out for a reactor scram from full power, showed significant discrepancies for primary and secondary system pressures and for mean coolant temperatures of the primary side. The discrepancies were found even after the

elimination of differences in fission power, feedwater flow and rate of vapor discharge from the steam dome. Good agreement was obtained between simulator and RETRAN calculations for only the early part (narrow control range) of the water level motion in the steam generator. The differences between simulator and RETRAN calculations have been explained in terms of modeling differences (Cheng and Wulff, 1981).

4.3 Acquisition of Special-Purpose Peripheral Processor and Ancillary Equipment (A.N. Mallen, R.J. Cerbone and S.V. Lekach)

The AD10 had been selected earlier as the special-purpose peripheral processor for high-speed, interactive systems simulation through integrating large systems of nonlinear ordinary differential equations. A brief description of the processor has been published in a previous Quarterly Progress Report (Wulff, 1981b). A PDP-11/34 DEC computer serves as the host computer. An IBM Personal Computer is used for graphics displays and for remote access via commercial telephone lines.

Two AD10 units, coupled directly to each other by a bus-to-bus interface and equipped with a total of one megaword of memory, have been installed with the PDP-11/34 host computer, two 67 megabyte disc drives, a tape drive and a line printer. On-line access is facilitated by a model 4012 Tektronix oscilloscope terminal and a 28-channel signal generator. The system is accessed remotely via up to four ADDS CRT terminals and two DEC Writer terminals, one also equipped with a line printer. An IBM Personal Computer is also used to access the PDP-11/34 host computer and to generate labeled, multicolored graphs from AD10 results. A Tektronix 4115B multicolor graphics terminal has been ordered, however, for on-line display of simulated parameters generated by the AD10 at real-time or faster computing speeds.

4.4 Model Implementation on AD10 Processor and Developmental Assessment

A four-equation model for nonhomogeneous, nonequilibrium two-phase flow had been formulated and supplemented by constitutive relations from an existing BWR reference code, then scaled and adapted to the AD10 processor to simulate the Peach Bottom-2 BWR power plant (Wulff, 1982a). The resulting High-Speed Interactive Plant Analyzer code (HIPA-PB2) has been programmed in the high-level language MPS10 (Modular Programming System) of the AD10. After implementing the thermohydraulics of HIPA-PB2 on the AD10, we compared the computed results and the computing speed of the AD10 with those of the CDC-7600 mainframe computer, to demonstrate the feasibility of achieving engineering accuracy at high simulation speeds with the low-cost AD10 minicomputer (Wulff, 1982b).

It has been demonstrated (Wulff, 1982b) that (i) the high-level, state equation-oriented systems simulation language MPS10 compressed 9,950 active FORTRAN statements into 1,555 calling statements to MPS10 modules, (ii) the hydraulics simulation occupies one-fourth of available program memory, (iii) the difference between AD10 and CDC-7600 results is only approximately $\pm 5\%$ of total parameter variations during the simulation of a severe licensing base transient, (iv) the AD10 is 110 times faster than the CDC-7600 for the same transient, and (v) the AD10 simulates the BWR hydraulics transients up to 10 times faster than real-time process speed. It has been demonstrated that even after the inclusion of models for neutron kinetics, conduction, balance of

plant dynamics and controls, the AD10 still achieves 10 times real-time simulation speed for all transients reported earlier (Wulff, 1983c).

The HIPA-PB2 hydraulics program used earlier for the feasibility demonstration has been expanded to simulate neutron kinetics (point kinetics), thermal conduction in fuel elements and the thermohydraulics of the components of the balance of plant shown in Figure 4.1. Previously used slip formulations for simulating nonhomogeneous two-phase flow have been replaced by drift flux formulations. Condensation of vapor on subcooled liquid has been modeled. The expanded version is called HIPA-BWR/4 and is capable of simulating all BWR/4 reactor plants.

The stand-alone program modules for neutron kinetics with reactivity feedback and automatic reactor trips, for thermal conduction in fuel elements, for compressible flows in the steam line and for the control logic for operating the safety and relief valves tested earlier (Wulff, 1982c; 1983a) have been implemented in HIPA-BWR/4. Models formulated and first tested separately have been implemented to simulate the control and plant protection systems and the plant components forming a closed loop through turbines, condensers and the feedwater trains. The boron tracking model (Wulff, 1983d) had been implemented first as a stand-alone module (Wulff, 1984a) and is now part of HIPA-BWR/4.

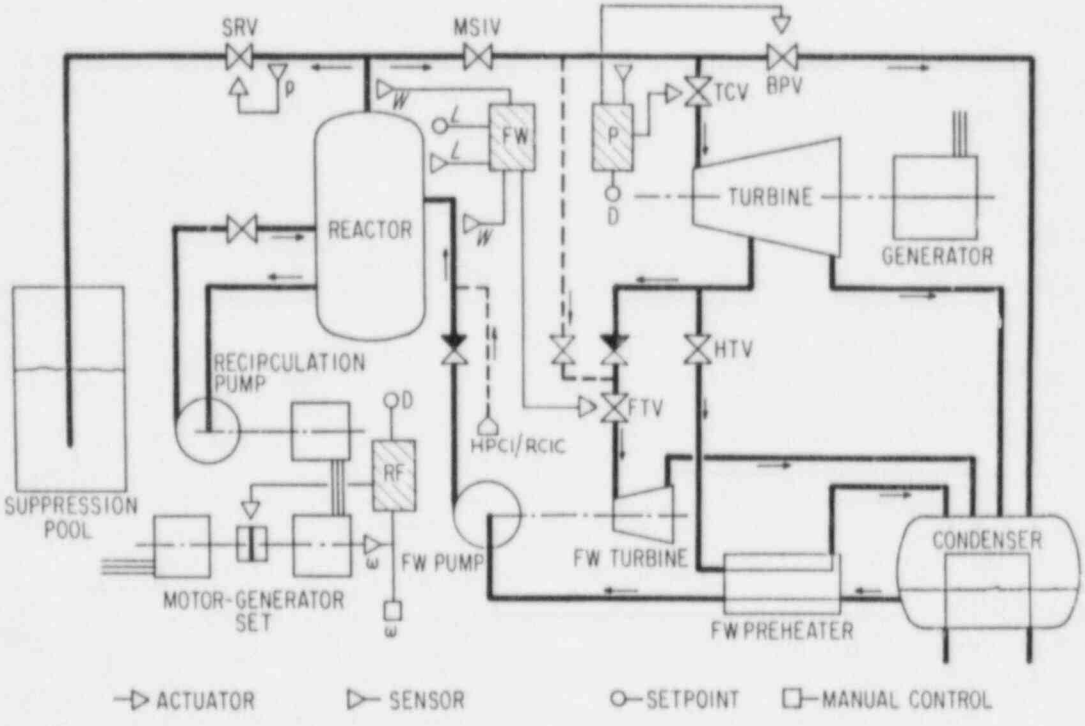

Figure 4.1 Flow Schematic and Control Blocks for BWR Simulation; FW - Feedwater Controller, P - Pressure Controller, RF - Recirculation Flow Controller

The graphics capabilities had been significantly enhanced during the second reporting period of 1984 to allow now the on-line display of two parameter variations versus time on the four-color monitor of the IBM-PC. The parameters are displayed in separate colors on labeled diagrams. Also, a Local Area Network had been assembled to display on-line simulation results from the plant analyzer in a remote conference room (Wulff, 1984a).

Earlier, we presented results from the developmental assessment of the plant analyzer. We compared plant analyzer results with GE calculations (Wulff, 1984) and with calculations from the systems codes TRAC-BD1, RELAP5 and RAMONA-3B (Wulff, 1984a). We also established proper plant analyzer performance, where no best-estimate simulations were available, by comparison with FSAR results (Wulff, 1984a). The comparisons show that the plant analyzer simulates, reliably and accurately, a large number of severe abnormal transients in a BWR power plant, and that it produces the same results as TRAC-BD1, RELAP5 and RAMONA-3B but at a considerably lower cost and in much shorter time. We have demonstrated that the BNL Plant Analyzer can simulate 37 different transients in less than four days. We have also demonstrated that the plant analyzer can now be accessed and operated remotely by using an IBM-PC and a commercial telephone line.

Specific accomplishments of the current reporting period are described below in Sections 4.5 and 4.6.

4.5 Model Developments (H.S. Cheng and W. Wulff)

The assessment of the previously documented level tracking model (Wulff, 1984c) has been continued. A number of minor improvements have been implemented. Equation 5.4 in the previous progress report (Wulff, 1984c), was recognized to have been slightly simplified by Ishii (1977) to arrive at the drift correlation used in HIPA (Wulff, Cheng, Mallen and Lekach, 1984). To achieve consistency, the drift velocity correlation was used to derive this replacement of Eq. 5.4 (Wulff, 1984c) for the prediction of the void fraction $\langle\alpha\rangle_{up}$ above the mixture level:

$$(1-\langle\alpha\rangle_{up}) \cdot f \cdot \langle j_m\rangle - (\langle\alpha\rangle_{up} + f)\langle j_\ell\rangle - \langle\alpha\rangle_{up}(1-\langle\alpha\rangle_{up})^{3/2} \cdot G = 0 , \quad (4.1)$$

where $\langle j_m\rangle$ and $\langle j_\ell\rangle$ are the given mixture and liquid volumetric fluxes, respectively, and

$$f = \sqrt{\frac{\rho_v}{\rho_\ell}} \sqrt{\frac{1+75(1-\langle\alpha\rangle_{up})}{\sqrt{\langle\alpha\rangle_{up}}}} \quad (4.2)$$

$$G = \sqrt{\frac{g d_h (\rho_\ell - \rho_v)}{0.015\ \rho_\ell}} . \quad (4.3)$$

Here ρ, g and d_h stand for density, gravitational acceleration and hydraulic diameter, while subscripts v and ℓ designate vapor and liquid, respectively. Equation 4.1 is solved iteratively. The results are pretabulated over the needed range of pressure, mixture and liquid volumetric fluxes.

4.6 Remote Access to Plant Analyzer (S. Lekach, A.N. Mallen and A. Stritar)

For the purposes of demonstrating the plant analyzer capabilities on-line anywhere, and to give any remote user access to the plant analyzer, we have developed the necessary software for operating the plant analyzer remotely from an IBM Personal Computer (PC) using a commercial telephone line.

The IBM-PC is linked, via an RS-232 serial port, a 1200 baud modem (Hayes Smartmodem is preferred) and a commercial telephone line, with the PDP-11/34 host computer at BNL. The PDP-11/34 is linked for data transmission with the AD10 peripheral processors via Digital Device Controllers (DDC). The simulation speed is governed by the data transmission speeds through the PDP-11/34 to the disc (used for data storage) and through the 1200 baud modem.

The IBM-PC controls two task executions in the PDP-11/34, one for each of the two consoles. All graphics data for the display of graphics reside in the IBM-PC. The IBM-PC converts fractional (scaled) results, obtained from the AD10 via the PDP-11/34, into engineering quantities for display in labeled diagrams.

With the IBM-PC one can:

(i) operate the plant analyzer remotely,
(ii) display data from previous simulations if they are stored on disc (REPLAY),
(iii) recall a record of input parameter changes introduced from the keyboard during the last simulation.

For the plant analyzer operation, the user may change from the keyboard any of the 230 input parameters for the specification of geometry, neutron kinetics, hydraulics, controls and operating conditions. The user may introduce, also from the keyboard, all operator actions and failure signals normally introduced as analog signals from the control panel of the plant analyzer. All available operator actions and failure signals are prompted on demand from the monitor screen. They may be introduced before or during the transient simulation, and the plant analyzer responds at once without interrupting the simulation.

During the transient simulation, there are two arbitrarily selected parameters displayed on the monitor screen while the simulation is in progress. Simultaneously, there are a hundred additional parameters stored on the disc of the PDP-11/34. These parameters may be displayed in arbitrarily chosen pairs after the simulation (REPLAY). The user can display the complete list of all the parameters available for on-line display or for replay.

The user can stop the simulation any time, enter new input parameters and continue the simulation. He can also enter any operator action or malfunction without stopping the program execution.

After a transient is completed, the user may zoom and expand any time span of the display of the graphs. He may also expand or contract the scale of the ordinate axis for any parameter.

Replay of previously stored data is carried out by selecting pairs of parameters and by scale zooming, if desirable, as during normal operation. All data are deleted from disc storage during a subsequent simulation unless they are saved from the IBM-PC keyboard. Data can also be stored locally in PC memory. Replay from PC memory is much faster than from the PDP-11/34 disc.

If a printer is connected to the IBM-PC then one can generate a permanent black on white copy of the monitor screen image, be it a graph or text.

Input parameter changes, reflecting operation actions and failure signals (pump or valve trips, regulator failures, etc.), are being logged at the start of, and during, every transient. Keyboard activities are recorded together with the time, after start of transient at which they were introduced.

Conclusion. A readily available IBM Personal Computer can now be used to access the plant analyzer at BNL from anywhere via a noise-free telephone line. All analog signals normally introduced from the control panel at BNL are emulated on the IBM-PC. One can obtain instant responses to input parameter changes and perform a large number of transients with greater ease, in short time and at low cost. A segment of a newly drafted User Guide is attached as an appendix to show the simplicity of operating the plant analyzer via remote telephone link.

4.7 Future Plans

Assessment and model improvement will continue. Methods will be developed to display plant mimics and continuous data trends indefinitely. Work will be started to develop the new simulation technique also for PWR plants.

The plant analyzer will be presented and demonstrated to domestic industries and foreign institutions interested in nuclear power plant simulation for the purpose of developing cooperative programs directed toward PWR simulations.

REFERENCE

CHENG, H. S. and WULFF, W., (1981), "A PWR Training Simulator Comparison with RETRAN for a Reactor Trip from Full Power," Informal Report, BNL-NUREG-30602, Brookhaven National Laboratory, September 1981.

CHEXAL, B., et al., (1984), "Reducing BWR Power by Water Level Control During an ATWS - A Quasi-Static Analysis," Nuclear Safety Analysis Center, Electric Power Research Institute , NSAC-69, May 1984.

ISHII, M. (1977), "One-Dimensional Drift-Flux Model and Constitutive Equations for Relative Motion Between Phases in Various Two-Phase Flow Regimes," Argonne National Laboratory, Argonne, IL., ANL-77-47.

WULFF, W., (1980), "PWR Training Simulator, An Evaluation of the Thermohydraulic Models for its Main Steam Supply System," Informal Report, BNL-NUREG-28955, September 1980.

WULFF, W., (1981a), "BWR Training Simulator, An Evaluation of the Thermohydraulic Models for its Main Steam Supply System," Informal Report, BNL-NUREG-29815, Brookhaven National Laboratory, July 1981.

WULFF, W., (1981b), "LWR Plant Analyzer Development Program," Ch. 6 in Safety Research Programs Sponsored by the Office of Nuclear Regulatory Research, Quarterly Progress Report, April 1-June 30, 1981; A. J. Romano, Editor, NUREG/CR-2231, BNL-NUREG-51454, Vol. 1, No. 1-2, 1980.

WULFF, W., CHENG, H. S., DIAMOND, D. J. and KHATIB-RAHBAR, M., (1981c), "A Description and Assessment of RAMONA-3B MOD.0 CYCLE4: A Computer Code with Three-Dimensional Neutron Kinetics for BWR Systems Transients," NUREG/CR-3664, BNL-NUREG-51746, Manuscript completed 1981, published 1984.

WULFF, W., CHENG, H. S., LEKACH, S. V. and MALLEN, A. N., (1984), "The BWR Plant Analyzer," Final Report, BNL-NUREG-51812, NUREG/CR-3943.

WULFF, W., (1982a), "LWR Plant Analyzer Development Program," Ch. 5 in Safety Research Programs Sponsored by the Office of Nuclear Regulatory Research, Quarterly Progress Report, January 1-March 31, 1982; A. J. Romano, Editor, NUREG/CR-2331, BNL-NUREG-51454, Vol. 2, No. 1, 1982.

WULFF, W., (1982b), "LWR Plant Analyzer Development Program," Ch. 5 in Safety Research Programs Sponsored by the Office of Nuclear Regulatory Research, Quarterly Progress Report, July 1-September 30, 1982; compiled by Allen J. Weiss, NUREG/CR-2331, BNL-NUREG-51454, Vol. 2, No. 3, 1982.

WULFF, W., (1982c), "LWR Plant Analyzer Development Program," Ch. 5 in Safety Research Programs Sponsored by the Office of Nuclear Regulatory Research, Quarterly Progress Report, October 1-December 31, 1982; compiled by Allen J. Weiss, NUREG/CR-2331, BNL-NUREG-51454, Vol. 2, No. 4, 1982.

WULFF, W., (1983a), "LWR Plant Analyzer Development Program," Ch. 5 in Safety Research Programs Sponsored by the Office of Nuclear Regulatory Research, Quarterly Progress Report, January 1-March 31, 1983; compiled by Allen J. Weiss, NUREG/CR-2331, BNL-NUREG-51454, Vol. 3, No. 1, 1983.

WULFF, W., (1983b), "LWR Plant Analyzer Development Program," Ch. 5 in Safety Research Programs Sponsored by the Office of Nuclear Regulatory Research, Quarterly Progress Report, July 1-September 30, 1983; compiled by Allen J. Weiss, NUREG/CR-2331, BNL-NUREG-51454, Vol. 3, No. 3, 1983.

WULFF, W., (1983c), "NRC Plant Analyzer Development," Proc. Eleventh Water Reactor Safety Research Information Meeting, held at National Bureau of Standards, Gaithersburg, MD, Oct. 24-28, 1983, U.S. Nuclear Regulatory Commission. To be published.

WULFF, W., (1983d), "LWR Plant Analyzer Development Program," Ch. 5 in Safety Research Programs Sponsored by the Office of Nuclear Regulatory Research, Quarterly Progress Report, October 1-December 31, 1983; compiled by Allen J. Weiss, NUREG/CR-2331, BNL-NUREG-51454, Vol. 3, No. 4, 1983.

WULFF, W., (1984a), "LWR Plant Analyzer Development Program," Ch. 5 in Safety Research Programs Sponsored by the Office of Nuclear Regulatory Research, Quarterly Progress Report, January 1-March 31, 1984; compiled by Allen J. Weiss, NUREG/CR-2331, BNL-NUREG-51454, Vol. 4, No. 1, 1984.

WULFF, W., (1984b), "LWR Plant Analyzer Development Program," Ch. 5 in Safety Research Programs Sponsored by the Office of Nuclear Regulatory Research, Quarterly Progress Report, April 1-June 30, 1984; compiled by Allen J. Weiss, NUREG/CR-2331, BNL-NUREG-51454, Vol. 4, No. 2, 1984.

WULFF, W., (1984c), "LWR Plant Analyzer Development Program," Ch. 5 in Safety-Research Programs Sponsored by the Office of Nuclear Regulatory Research, Quarterly Progress Report, July 1-September 30, 1984; compiled by Allen J. Weiss, NUREG/CR-2331, BNL-NUREG-51454, Vol. 4, No. 3, 1984.

APPENDIX

SHORT USER GUIDE FOR PLANT ANALYZER

This appendix briefly describes what one has to do to operate the plant analyzer. Chapter references made below in parentheses refer to the more detailed descriptions in the User Guide soon to be published.

1.0 Starting the Program

1.0.1 System with Hard Disc (IBM-PC/XT)

One must have the program loaded on the hard disc according to Appendix C of the User Guide.

(i) Switch on the power on your IBM-PC/XT and wait until the system is ready.

(ii) Enter the correct time and date if the system prompts you for it.

(iii) Type in the following DOS comment:

C> cd /rem<CR>

(iv) Type in:

C/REM> rhip<CR>

The title page of the program will appear on the screen.

(v) Hit any key, and the Main Menu of the program will appear on the screen (Chapter 2). Then go to Section 1.1 below.

1.0.2 System with Floppy Disc

(i) Insert the floppy disc with the RHIP program into the Floppy Disc Drive A (the left one).

(ii) Switch on the power on your IBM-PC and wait until the system is ready.

(iii) Follow the steps (ii) to (v) above in Chapter 1.0.1.

1.1 Running the Transient

In Main Menu (Chapter 2), enter 1 to get into the Terminal Emulation Mode (Chapter 2.1).

In Terminal Emulation Mode, hit <F10> (Chapter 2.1.3).

Enter the two names of the variables to be plotted. You may type help<CR> first, to get the list of available variables. Enter the set of input parameters for operator actions and desired malfunctions to be set before the start of simulation (Chapter 2.1.3.1), in accordance with instructions displayed on the monitor screen.

Wait for the frame to be plotted. Enter C to start the transient (Chapter 2.1.3.2).

Refer to the top line of the screen (or to Chapter 2.1.3.2) for all available options. You may halt and continue the simulation. You may also change malfunction and operator action inputs during the simulation.

Hit H three times to get back into the Terminal Emulation Mode.

1.2 Replaying the Transient

You may start from two different modes:

(i) From the Main Menu (Chapter 2), enter 1 to come to the Terminal Emulation Mode (Chapter 2.1). Hit the <F3> key (Chapter 2.1.3) and choose the transient you want to replay.

(ii) From Run Transient Mode (Chapter 2.1.3 and 2.1.3.1), enter R after you have stopped the simulation with H, H. You will replay the transient you have just run. If you want to replay any other transient from that point, you must return to the Terminal Emulation mode by hitting H and then start replay by hitting the <F3> key (Chapter 2.1.4).

Choose the two variables you want to display and start the replay (Chapter 2.1.4.1) by hitting the <CR> key.

1.3 Storing the Transient

In the Terminal Emulation Mode (Chapter 2.1), hit the <F8> key and enter the "name" (Chapter 2.1.6) for the permanent storage file.

1.4 Getting the List of Input Actions for the Transient

In Terminal Emulation Mode (Chapter 2.1), hit the <F8> key (Chapter 2.1.5), and you get two tables on the monitor screen; the first showing the initial conditions, the second one showing the time log of all actions taken during the simulation.

1.5 Zooming into the Plot

From your current position in the program, return to the Main Menu (Chapter 2). Enter 2 and the name of the stored data file defined in 1.3 (Chapter 2.2 and 2.2.1). When the plot is replotted, enter Z and new axis parameters in accordance with the instructions displayed at the top of the monitor screen.

1.6 Printing the Plot on the Printer

From your current position in the program return to the Main Menu (Chapter 2), enter 2 and choose the name of the stored data file (Chapter 2.2 and 2.2.2). When the plot is replotted, enter P, wait until the red part of the plot colored in yellow and hit the Shft PrtSc key to start the printer.

1.7 Storing of Results Locally

From your current position return to the Main Menu (Chapter 2), enter 3, and then a new "name" (Chapter 2.3) for the local data file.

1.8 Terminating the Program

From your current position return to the Main Menu and hit 4 (Chapter 2.4).

5. Code Assessment and Application

(P. Saha, J. H. Jo, H. R. Connell, U. S. Rohatgi and C. Yuelys-Miksis)

This project includes the independent assessment of the latest released versions of LWR safety codes such as TRAC, RELAP5, and RAMONA-3B, and their application to the full-scale plant accident and/or transient simulation. In the past, the TRAC-P1A, TRAC-PD2, TRAC-PF1, RELAP5/MOD1 and TRAC-BD1 codes were assessed at BNL primarily through various separate-effects experiments. Also, the code application task at BNL included (i) determination of Appendix K conservatism for a Westinghouse RESAR-3S 4-loop PWR using the TRAC-PD2/MOD1 code, and (ii) comparative analysis of TRAC-BD1 and RAMONA-3B calculations for a typical BWR/4 MSIV closure ATWS. At present, emphasis is placed on the assessment of TRAC-BD1/MOD1 and RAMONA-3B codes.

The major activities performed during the reporting period of October to December 1984 are described below.

5.1 Code Assessment

5.1.1 Simulation of FIST Experiments with TRAC-BD1/MOD1
(J. H. Jo and H. R. Connell)

The effort has been continuing to simulate the FIST test 4PMC1 (BWR/4 MSIV closure ATWS) using the TRAC-BD1/MOD1 code.

Figure 5.1 shows the VESSEL nodalization being used to represent the FIST facility. It consists of 12 axial levels, 2 radial rings and 2 azimuthal sectors. In a BWR, there is a relatively narrow annular region between the vessel wall and the dryer skirt outside the separator (Figure 5.2). If this annular region was linearly scaled in FIST based on the volume scale (1:624), it would result in an annular region with very narrow gap and the resulting boundary layer effects may significantly alter the system parameters such as water level movement. For this reason, in the FIST facility, this region was represented with an annular sector of 76° containing the same volume and flow area as that of ideally scaled annular region as shown in Figure 5.2. This FIST design of the separator-dryer-dryer skirt region can be better represented by the 2-ring and 2-azimuthal sector nodalization.

Test 4PMC1 is a power transient simulation test for a BWR/4 with MSIV closure and without power scram. The bundle power in this test was electrically provided based on an analysis for a BWR/4 power transient reported in Chen (1982).

Table 5.1 compares the TRAC-BD1/MOD1 steady-state results with the test initial conditions. Good agreement was obtained except for the downcomer water level. Two downcomer levels are shown in Table 5.1 for the calculation; one is the level in the dryer-skirt region of 76° sector (Cell 3 of Level 9) and the other is the average level in the two cells of the outer ring of the separator (Cells 3 and 4 of Level 9). In the calculation there

was a large level difference between the two cells outside the separator as shown in Figure 5.3, while the water levels in these two cells were about the same as in the test. This unexpected anomaly is under further investigation.

The TRAC-BD1/MOD1 transient calculation has been run up to 28 seconds. Table 5.2 compares the timings of the major events in the calculation and the test. Figures 5.4 and 5.5 show the system pressure and the steam line mass flow rate of the test and the calculation up to 28 seconds. They generally show very good agreement except the magnitude and timing of the peak pressure. It should be noted that the TRAC-BD1/MOD1 code predicts the magnitude of the steam flow and timing of the SRV opening and closing very well. It appears that the reported timing of the peak pressure was inconsistent with the bundle power provided in the test. Notice that the peak bundle power was reached at approximately 5 seconds (Figure 5.6). Therefore, the system pressure can be expected to continue to increase during this period and the peak pressure to reach sometime after 5 seconds. So the calculated timing of the peak pressure of 8.5 seconds appears to be reasonable.

The calculation was terminated at approximately 28 seconds due to very small time steps taken by the code. This appeared to be caused by flow oscillations between two radial rings in the bypass region. It is planned to modify the nodalization of the VESSEL using only one cell for the bypass region to prevent the oscillation. Further work is also planned to improve the steady-state including the downcomer water level. The transient calculation will then be repeated.

5.2 Code Application

5.2.1 Analysis of Westinghouse RESAR-3S Plants
(U. S. Rohatgi and C. Yuelys-Miksis)

The BNL best-estimate (BE) and two evaluation type (EM) calculations for a 200% cold leg break in a Westinghouse 4-loop RESAR-3S plant have been completed using the TRAC-PD2/MOD1 code. Results of the estimate and the first EM type calculations were reported in previous quarterly reports (Rohatgi, 1984a and 1984b).

The second EM type calculation was performed to account for the effect of locked rotor resistance of the reactor coolant pumps. Appendix K of 10 CFR 50 states that locked rotor resistance should be considered in the reflood phase if it results in a higher peak clad temperature (PCT). This calculation was started at 48.5 seconds from the first EM type calculation with the reactor coolant pump (RCP) speed set to zero. The vapor flow rate through the broken hot leg decreased due to additional pump resistance. This also slowed down the liquid penetration in the downcomer and the core, and diminished the core cooling. The fuel clad started to heat up faster than in the previous EM calculation as shown in Figure 5.7. The peak clad temperature of 1153°K occurred at 100 seconds into the transient. Both of the EM type calculations were qualitatively similar. The calculation was terminated when the clad started to cool down.

Besides these three BNL calculations, results of a fourth calculation performed by Westinghouse (Fujita, 1983) with the licensing or evaluation model type boundary and operating conditions and physical models were also available. The clad temperatures for hot rods in these calculations have been compared in Figure 5.7.

A comparison between the Westinghouse EM and the BNL BE calculations indicates that the licensing or Appendix K requirements contribute to a total conservatism of approximately 664°K in the PCT prediction. A comparison of the BNL EM type calculation (EM/BNL/locked rotor) with these two bounding calculations indicates that the licensing type operating and boundary conditions and scenarios are responsible for ~353°K conservatism in PCT while the Appendix K required physical models contribute ~311°K to the conservatism of PCT estimation. The peak clad temperature in the best-estimate calculation occurred very early in the transient, and was not affected by the ECC system. On the other hand, the ECC system did affect the other calculations. A comparison of the two EM type BNL calculations indicates that the PCT is affected by locked rotor resistance and the effect is on the order of ~81°K.

This study indicates that there is a large safety margin in the licensing or Appendix K requirements. The contribution to this safety margin due to the required physical models such as subtraction of safety injection fluid collected during the blowdown phase from coolant inventory and restrictions on the return to nucleate boiling in the core before the reflood phase, etc. are of the same order of magnitude as due to the boundary conditions, operating conditions, and scenario. The Appendix K guideline of setting the reactor coolant pumps to locked rotor condition also contributes significantly to the conservatism in PCT.

REFERENCES

CHEN, W.M., (1982), "Design Analysis and SAR Inputs for ATWS Performance and Standby Liquid Control System - Susquehanna 1 and 2 Plants," NEDE-25458, Class II, Rev. 1, April 1982.

FUJITA, R.J., et al (1983), "Comparison Between a Most-Probable and a Licensing Calculation of a 200% LOCA in a Four Loop 17 x 17 Westinghouse PWR," National Heat Transfer Conference, Niagara Falls, N.Y., August 5-8, 1983.

ROHATGI, U.S. and YUELYS-MIKSIS, C., (1984a), "LOCA Analysis of Westinghouse RESAR-3S Plants," in BNL Quarterly Progress Report for October 1 - December 31, 1983, NUREG/CR-2331, BNL-NUREG-51454, Vol. 3, No. 4, May 1984, Section 6.2.1.

ROHATGI, U.S. and YUELYS-MIKSIS, C., (1984b), "LOCA Analysis of Westinghouse RESAR-3S Plants," in BNL Quarterly Progress Report for January 1 - March 31, 1984, NUREG/CR-2331, BNL-NUREG-51454, Vol. 4, No. 1, August 1984, Section 6.2.1.

Table 5.1 Comparison of TRAC-BD1/MOD1 Steady-State Results With Initial Conditions of Test 4PMC1

PARAMETER	TEST	TRAC-BD1/MOD1
Power, kW	4346	4346 *
Feedwater Flow, kg/sec	2.14	2.26 *
Feedwater Temp., °K	473.2	473.2 *
Steam Flow, kg/sec	2.25	2.26
Steamdome Pressure, bar	70.33	70.48
Core Inlet Flow, kg/sec	17.8	18.1
Core Inlet Temp., °K	550.8	552.5
Downcomer Level, m	13.35	12.30 **
		13.64 ***

* Boundary Condition
** Dryer Skirt Region
*** Downcomer Average

Table 5.2 Sequence of Events for Test 4PMC1

EVENT	TEST (sec)	TRAC-BD1/MOD1 (sec)	
Start of programmed power	0	0	*
MSIV closure	2	2	*
Pump trip	3	3	*
First opening of SRV	3	3.5	
Maximum pressure in vessel	4	8.5	
Feedwater termination			
Hot	5	5	*
Cold	8	8	*
Opening of all 5 SRVs	~5	5.5	
SRV setting switched to low/low setting	10	10	*
Closing of 5th SRV	~20	19	
Recirculation loops isolation	20	20	*
Closing of 4th SRV	~23	23	
Level 2	2º	33	**

* Boundary condition

** Extrapolated based on the average level change.

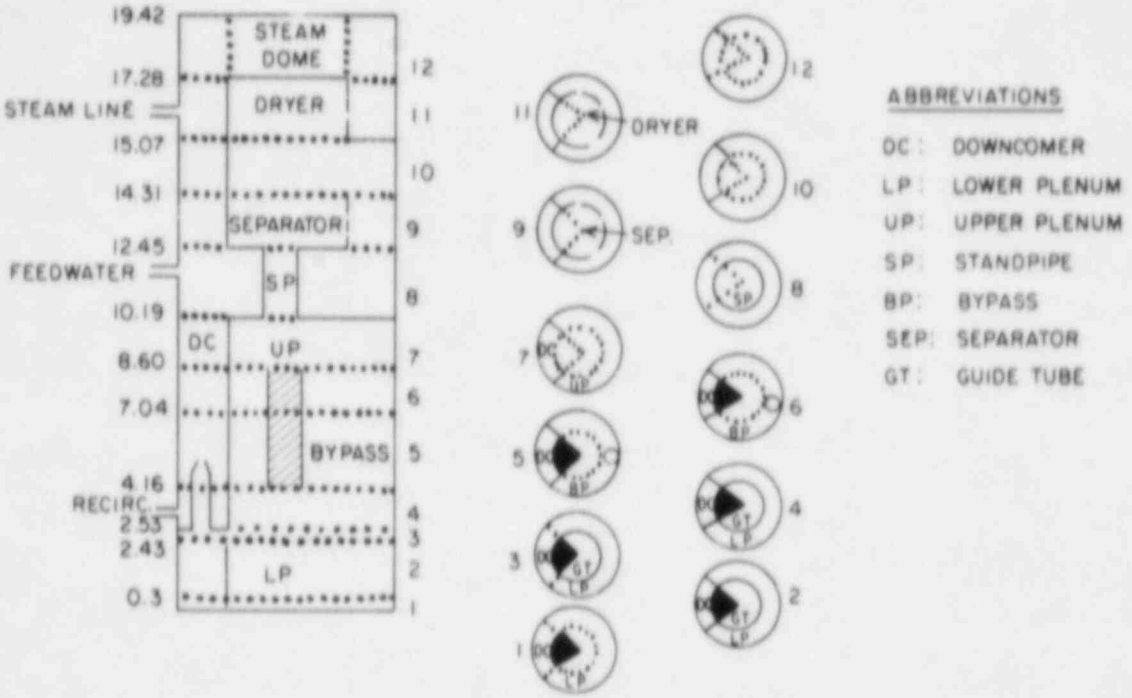

Figure 5.1 Vessel Nodalization for the FIST Facility.
(BNL Neg. No. 2-414-85)

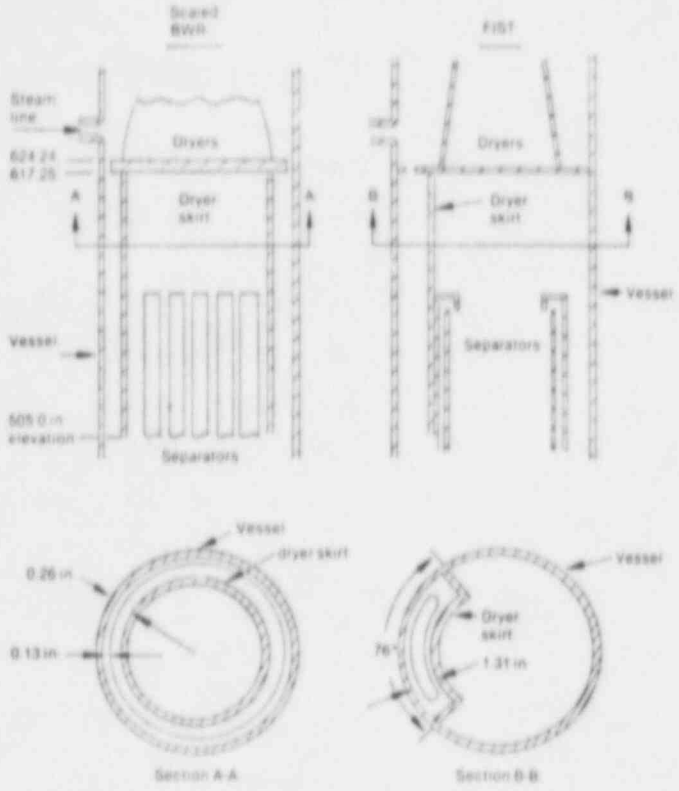

Figure 5.2 Dryer Skirt Simulation of the FIST Facility.

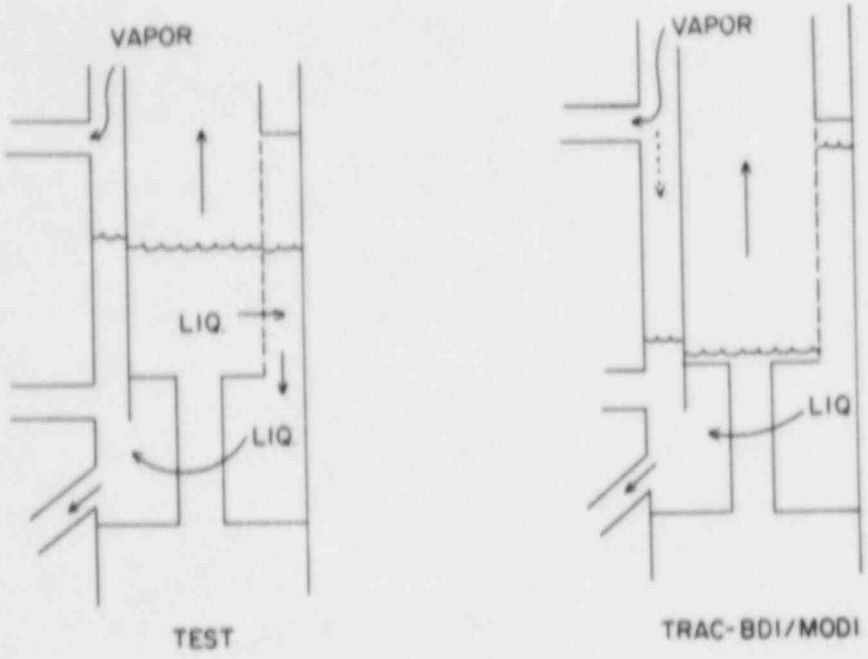

Figure 5.3 Comparison of the Water Level in the Dryer Skirt Region. (BNL Neg. No. 2-416-85)

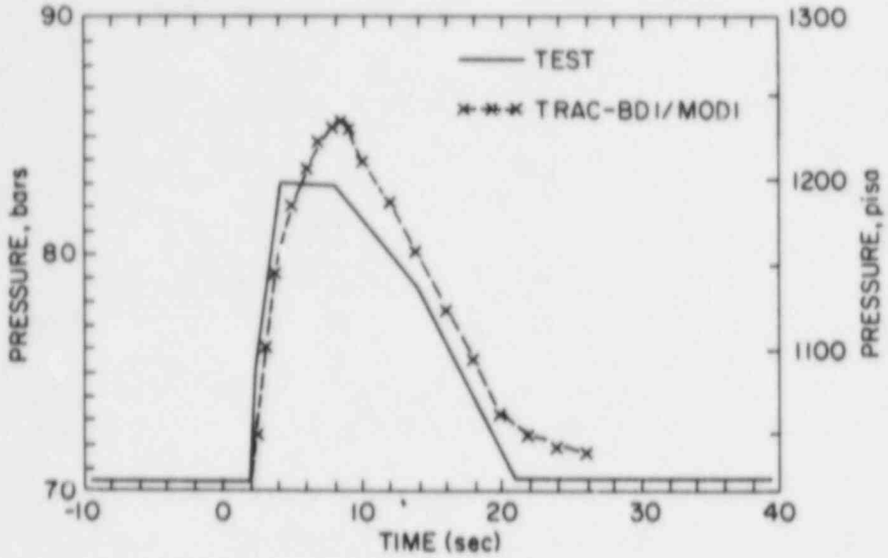

Figure 5.4 Comparison Between the Predicted and Measured System Pressure for FIST Test 4PMC1.
(BNL Neg. No. 2-417-85)

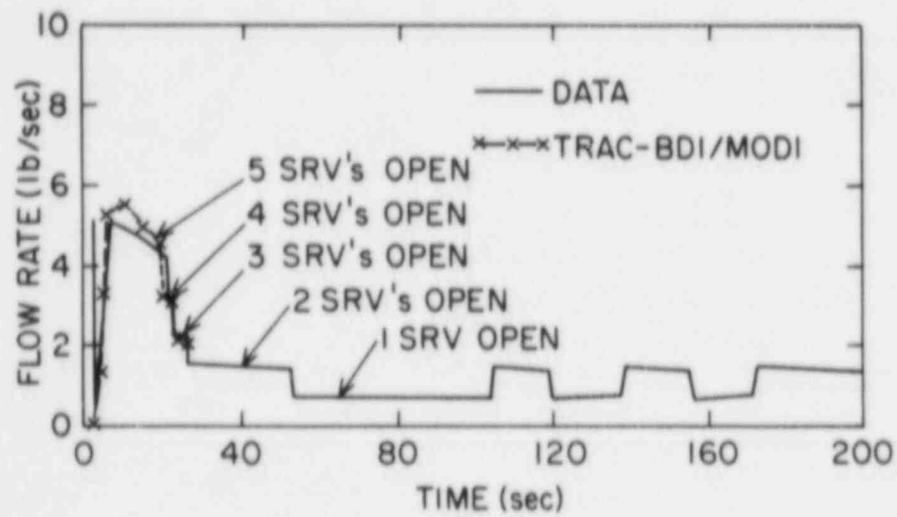

Figure 5.5 Comparison Between the Predicted and Measured Steam Line Mass Flow Rate for FIST Test 4PMC1.
(BNL Neg. No. 2-419-85)

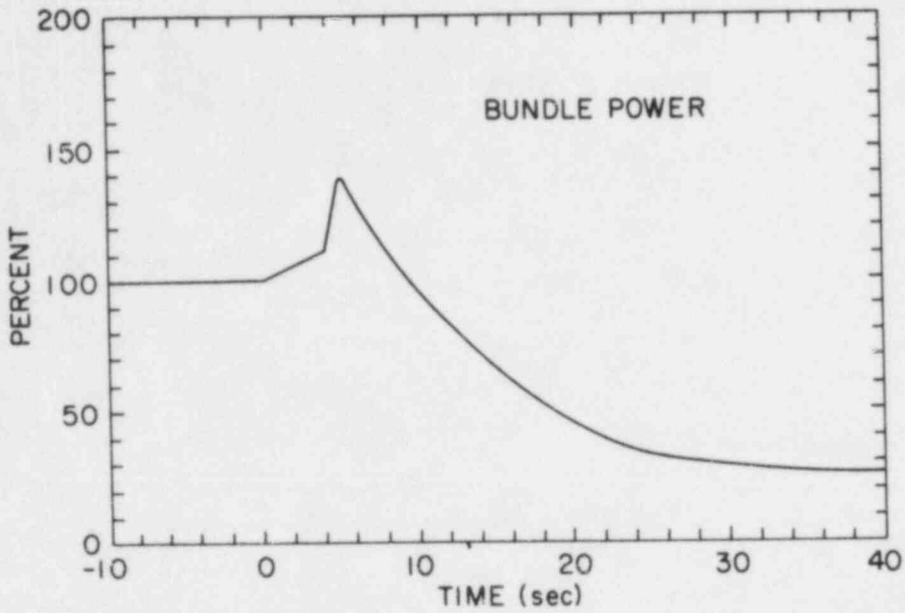

Figure 5.6 The Imposed Bundle Power During FIST Test 4PMC1. (BNL Neg. No. 2-420-85)

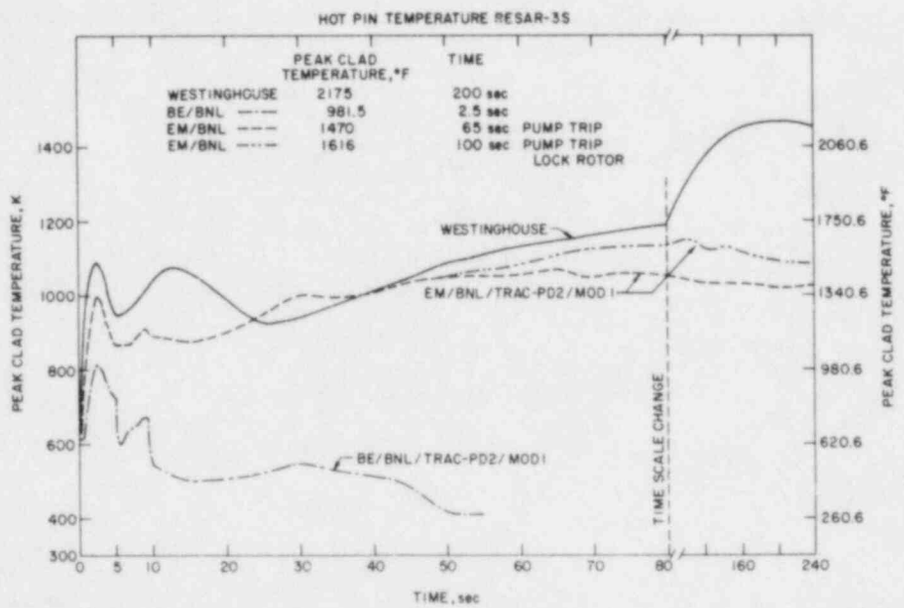

Figure 5.7 Comparison of Clad Temperatures for Hot Rods in BNL and Westinghouse Calculations for RESAR-3S Large Break LOCA. (BNL Neg. No. 2-418- 85)

6. Code Maintenance (RAMONA-3B)

(P. Saha, L. Neymotin, G. C. Slovik, and H. R. Connell)

This project consists of improvement and maintenance of the BWR plant transient code RAMONA-3B. The code employs three-dimensional neutron kinetics coupled with parallel hydraulic core channels and is complete with jet pump, recirculation pump, steam separator, steam line with all necessary valves, safety injection system and limited plant control and protection system. The code is most suitable for analyzing the BWR core and systems transients where the coupling between neutron kinetics and thermal hydraulics is important (e.g., ATWS, CRDA, etc.). The code is available to any U.S. organization, on a royalty-free basis, for the analysis of U.S. reactors.

The details of the progress achieved during the reporting period of October to December 1984 are described below.

6.1 New Cycle of the RAMONA-3B Code (H. R. Connell)

Since the creation of Cycle 7 in February 1984, a significant number of additions and changes have been made to the RAMONA-3B code and these changes have been tested and analyzed in a series of preliminary Cycle 8 versions. The new coding encompassing changes for hydraulic calculations, neutronic calculations and general code improvement, has been brought together to form the Cycle 8 version of the RAMONA-3B/MOD0 code.

The main features of Cycle 8 are: (1) the interface with the auxiliary code FRAM used for cross section collapsing to 1-D, (2) corrections to the reactivity edit calculation, (3) improvement in the input scheme for assigning the cross section data in the core representation, (4) the feedwater control system, (5) the improved recirculation pump model, (6) revisions to the condensation model and level tracking, (7) various improvements in the logics for reverse flow situations, (8) improved convergence tests and time step choice, (9) a message file which provides a running commentary of the salient events in a transient calculation, and (10) the activation of an option to perform only the thermal hydraulic transient calculations in which the detailed neutronic calculation is bypassed and the core power is imposed as a boundary condition.

6.2 3-D to 1-D Collapsing Procedure (G. C. Slovik and H. R. Connell)

Modifications to RAMONA-3B required to generate 1-D cross sections have been implemented during the reporting quarter. This work is the beginning of the BNL effort to provide the INEL TRAC-BF1 code with a 1-D cross section set. In addition to the modifications to RAMONA-3B, the FRAM code will be used to collapse the nodal distribution of cross section data to average axial plane data.

FRAM is an auxiliary code to RAMONA-3B to provide a 1-D core model corresponding to a 3-D neutronic core by collapsing the RAMONA-3B nodal distribution of cross section data with corresponding void, fuel and coolant temperature from static calculations to average axial plane data and then fitting these 1-D data sets to polynomials in void, fuel and coolant temperature dependence for input into a 1-D RAMONA-3B calculation. In this application, the FRAM 1-D cross sections including the diffusion parameters will be provided to INEL for possible use with the TRAC-BF1 code.

6.3 Improvements for Reverse Flow (L. Y. Neymotin and H. R. Connell)

A "test" calculation (with no neutronic calculation) has been run to 65 seconds in the transient time when a reverse flow situation at the bypass core channel exit began to develop. This state is being used as a starting point for check-out calculations intended for verification of the reverse flow code modifications.

Work on the modifications was started from re-evaluation of the currently used boundary conditions coupling the one-dimensional components (lower plenum and riser) with the multi-channel core component. The next task is the proper coupling of the one-dimensional components between themselves, and finally, proper treatment of the counter-current and reverse flow situations inside the core heated channels and one-dimensional components.

7. Calculational Quality Assurance in Support of PTS

(P. Saha, J. H. Jo, U. S. Rohatgi and C. Yuelys-Miksis)

The objective of this project is to provide a peer review of the thermal-hydraulic calculations that have been performed at LANL (using the TRAC-PWR code) and INEL (using the RELAP5 code) for the NRC Pressurized Thermal Shock (PTS) study. Specifically, this includes a review of the plant input decks, the steady-state and transient calculations, and an assessment of the reasonableness of the results.

The BNL staff has already completed assessment of PTS thermal-hydraulic calculations for the Oconee-1 and Calvert Cliffs nuclear power plants. The assessment results have been documented in two separate topical reports (Rohatgi, 1984; Jo, 1985). The RELAP5 calculations for the H. B. Robinson Unit 2 have also been reviewed, and the results are being documented (Yuelys-Miksis, 1985a).

This quarterly report covering the work performed during October to December, 1984 is the last segment of the BNL assignment under the NRC PTS program.

7.1 Assessment of RELAP5 Thermal-Hydraulic Analysis of PTS Transients of H. B. Robinson Unit 2

(C. Yuelys-Miksis, J. H. Jo and U. S. Rohatgi)

Several transient scenarios, specified by Oak Ridge National Laboratory, were simulated by INEL (Fletcher, 1983) for the H. B. Robinson-2 PWR plant. Six of these transients were selected for quantitative in-depth review using a simple method developed at BNL. Four of these transients were reviewed in the previous quarter and reported earlier (Yuelys-Miksis, 1985b). The remaining two transients (Transients 9 and 11) were reviewed by the end of December 1984 and are summarized in this section.

Transient 9: Steam Generator Tube Rupture at Hot Zero Power Conditions

This transient was initiated from hot standby conditions by a double-ended rupture of the cold leg end of a steam generator tube. There were no equipment failures but the operator failed to follow the correct procedures for recovery from a steam generator tube rupture. Instead, the operator responded as if it were a small break LOCA. The transient scenario is shown in Table 7.1. The transient was calculated up to 7200 seconds; so there was no need for extrapolation.

Figure 7.1 shows the downcomer fluid temperatures as calculated by RELAP5 with two different safety injection locations. Also shown are the BNL calculated system average temperature and the saturation temperature corresponding to the RELAP5 calculated downcomer pressure. The RELAP5 downcomer temperature for the base case (solid line in Figure 7.1) showed large oscillations in the later portion of the transient which were attributed to code limitations. Since this phenomenon probably was not physical, a second

RELAP5 calculation was performed during this later part of the transient to remove the oscillations. This was done by injecting the cold high pressure injection (HPI) and make-up directly into the vessel. The temperature calculated in this way was referred to as the adjusted temperature. However, although this adjustment succeeded in damping out the oscillations, it neglected the slight warming of the cold injected water due to heat transfer from the cold leg walls.

It can be seen from Figure 7.1 that the saturation temperature corresponding to the RELAP5 calculated downcomer pressure is much higher than the BNL average system temperature. This could mean that voiding in the upper head was maintaining high temperature and pressure. Since the BNL temperature is a system average temperature it should fall between this saturation temperature, which should be the highest system temperature and the downcomer temperature, as it does. Thus, the RELAP5 results appear reasonable for this transient.

The pressurizer normalized levels calculated by RELAP5 and the simple method of BNL are shown in Figure 7.2. In both calculations there was a rapid inventory loss through the break. During this time the downcomer pressure also rapidly decreased, as can be seen in Figure 7.3. Soon after the HPI flow started and the reactor coolant pump was tripped, the pressure increased and stabilized at just below the HPI shutoff head. At this time the pressurizer was empty and the break and injection volumetric flows were nearly equal. The break flow was maintained by the pressure differential between the downcomer and the affected steam generator (SGA). As can be seen in Figure 7.4, the SGA pressure remained elevated at the steam dump valve set point and this affected steam generator was the heat sink in the early portion of the transient. By 200 seconds the pressurizer emptied, and at 276 seconds, auxiliary feedwater (AFW) was received by the other two steam generators, SGB and SGC. After the AFW to SGB and SGC was terminated at approximately 600 seconds, the secondary pressures dropped as these two steam generators became the primary heat sources. During this time the mass inventory of SGA increased and since the liquid in this steam generator is subcooled, some nonequilibrium effects could be expected.

In summary, the RELAP5 calculated results for this transient seem reasonable and the calculated sequence of events appear to follow the expected trends.

Transient 11: Loss of Secondary Heat Sink With Primary System Feed-and-Bleed Recovery at Hot Full Power Conditions

This transient was initiated from hot full power conditions by a manual trip of the main feedwater pumps. This trip occurred when the water level in one of the three steam generators decreased below 5% of full range resulting in a loss of the secondary heat sink. As a result, the temperature differential between the minimum and current temperature at the inlet of SGA increased. When this hot leg temperature increased by 5°F, the operator initiated the high pressure injection and opened both of the pressurizer power-operated relief valves (PORVs) to attempt a feed-and-bleed recovery. In

addition, the auxiliary feedwater pumps failed to start. The description of the scenario is given in Table 7.2. The RELAP5 calculation was run up to 8100 seconds and several key parameters were extrapolated up to 11000 seconds.

Figure 7.5 shows the downcomer and the Loop A hot leg temperatures calculated by RELAP5 and the BNL system average temperature. The sudden downcomer temperature drop in RELAP5 occurred after the high pressure injection was initiated and the PORVs were opened. In response to the decreasing primary temperature, the steam dump valves (SDVs) closed. The downcomer temperature showed the sudden effect of the HPI whereas the hot leg temperature experienced a more gradual decrease. In Figure 7.5, the BNL system average temperature falls between these two values, as would be expected. The RELAP5 calculated temperature drop occurs soon after the reactor coolant pumps are tripped in response to the low SG level at 3600 seconds. Assuming that the fluid flowing through the SDV was all vapor, it would have taken approximately 4700 seconds to reach this condition. This indicates that there is water entrained in the fluid during this period. Calculations showed that for the SGA level to reach 5% of full range at 3600 seconds, the average void fraction of the fluid flowing out of the SDV would have to be approximately 98% during this period. This agrees with the value predicted by RELAP5.

The INEL downcomer temperature extrapolation and the BNL system average temperature are shown in Figure 7.6. As can be seen, both temperatures steadily decline at about the same rate. This decrease is due to the energy loss from the PORV and the cooling effects of the HPI, make-up flow and accumulator flow, which are greater than the heat addition due to the core decay power. The two temperatures are in good agreement although the lower RELAP5 temperature indicates that stagnation continues throughout the transient. The RELAP5 calculated downcomer pressure and the saturation pressure corresponding to the BNL system average temperature are shown in Figure 7.7. Since the BNL system average temperature is slightly lower than the RELAP5 hot leg temperature, it is expected that the saturation pressure corresponding to the BNL system average temperature will also be slightly lower than the downcomer pressure, as is the case. Both pressures follow the same trend and the INEL pressure prediction appears reasonable. In summary, the primary system temperatures and pressures calculated by RELAP5 generally follow the expected trends and the results are reasonable.

REFERENCES

FLETCHER, C.D., et al., (1983), "RELAP5 Thermal-Hydraulic Analyses of Pressurized Thermal Shock Sequences for the H. B. Robinson Unit 2 Pressurized Water Reactor," EGG-SAAM-6476, December 1983.

JO, J.H. and ROHATGI, U.S., (1985), "Review of TRAC Calculations for Calvert Cliffs PTS Study," BNL-NUREG Report in publication.

ROHATGI, U.S., et al., (1984), "Assessment of Selected TRAC and RELAP5 Calculations for Oconee-1 Pressurized Thermal Shock Study," NUREG/CR-3703, BNL-NUREG-51750, in press.

YUELYS-MIKSIS, C., JO, J.H. and ROHATGI, U.S., (1985a), "Review of RELAP5 Calculations for H. B. Robinson Unit 2 PTS Study," BNL-NUREG Report to be published.

YUELYS-MIKSIS, C., et al., (1985b), "Assessment of RELAP5 Thermal-Hydraulic Analysis of PTS Transients of H. B. Robinson Unit 2," in BNL Quarterly Progress Report for July 1 - September 30, 1984, NUREG/CR-2331, BNL-NUREG 51454, Vol. 4, No. 3, Section 8.1.

Table 7.1 Scenario for Transient No. 9

Plant Initial State - Just prior to transient initiator.

General Description: Hot 0% Power, 0% Power after 100 hrs of shutdown
System Status
- Turbine: Not latched, TSVs closed
- Secondary PORV: Automatic control
- Steam Dump Valves (SDVs): Automatic control
- Charging System: Automatic control
- Pressurizer: Automatic control
- Engineering Safety Features: Automatic control
- PORVs: Automatic control
- Reactor Control: Manual
- Main Feedwater: In bypass mode, manual control to provide zero power level in S/Gs; 1 condensate pump, 1 MFWP operating.
- Aux Feedwater: Automatic control
- MSIVs: Open, Automatic control
- MFIVs: Closed, Automatic control

Transient Initiator - A steam generator tube rupture on the cold leg side of tube sheet of SGA.

Equipment Failures which occur during the transient if the equipment is demanded.

None

Operator Reactions to Reported Information

1. If SIAS signal is generated, the operator will trip the reactor coolant pumps when RCS pressure reaches 1300 psig.

2. The operator will restart reactor coolant pumps 10 minutes after all the following criteria are met.

   A. > 40°F subcooled
   B. Pressurizer level $\geq$ 20% or increasing
   C. R.C. pressure > 325 psig

3. The operator will throttle AFW flow to maintain 40% S/G level.

Table 7.2 Scenario for Transient 11

Plant Initial State - Just prior to transient initiator.

General Description: 100% power steady state
System Status
- Turbine: Not latched, TSVs closed
- Secondary PORV: Automatic control
- Steam Dump Valves (SDVs): Automatic control
- Charging System: Automatic control
- Engineering Safety Features: Automatic control
- Pressurizer PORVs: Automatic control
- Reactor Control: Automatic control
- Main Feedwater: Automatic control
- Auxiliary Feedwater: Automatic control
- Main Steam Isolation Valves (MSIVs): Automatic control
- Main Feedwater Isolation Valves (MFIVs): Automatic control

Transient Initiator - Both Main Feedwater pumps trip simultaneously.

Equipment Failures that occur during the transient if the equipment is demanded.

Auxiliary Feedwater pumps fail to start.

Operator Reactions to Reported Information

1. Operator trips reactor coolant pumps (RCPs) when 1/3 Steam Generator (S/G) wide range (WR) levels decrease below 5%.

2. Operator initiates safety injection (HPI) and opens the pressurizer PORVs after RCP trip and when the A Loop hot leg temperature has increased 5°F.

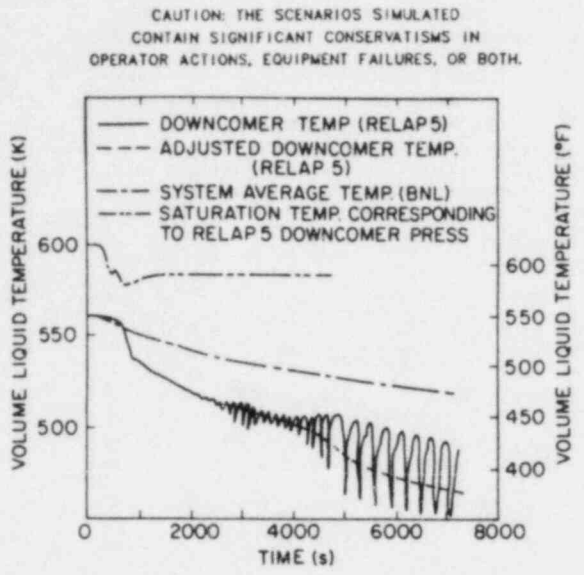

Figure 7.1 Comparison Between RELAP5 Downcomer Fluid Temperature and BNL System Average Temperature for Transient 9. (BNL Neg. No. 1-342-85)

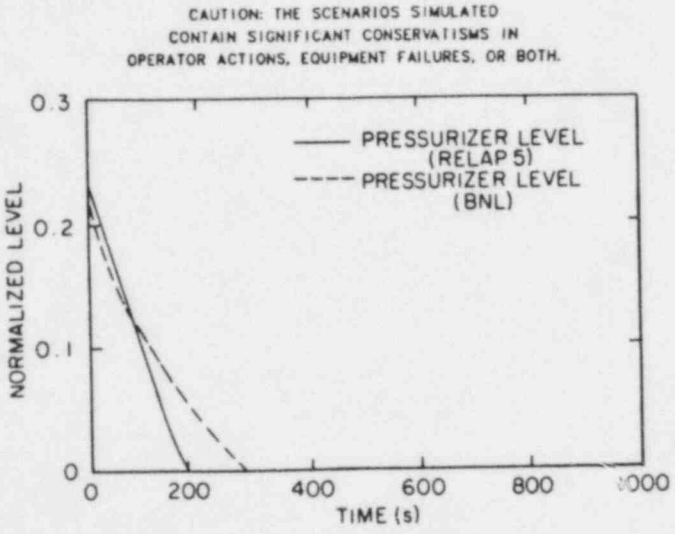

Figure 7.2 RELAP5 and BNL Pressurizer Levels for Transient 9. (BNL Neg. No. 1-340-85)

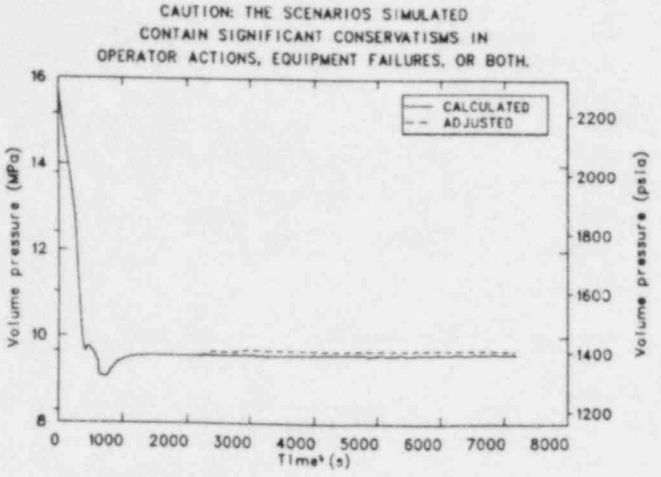

Figure 7.3 Reactor Vessel Pressure as Calculated by RELAP5 for Transient 9. (BNL Neg. No. 2-573-85)

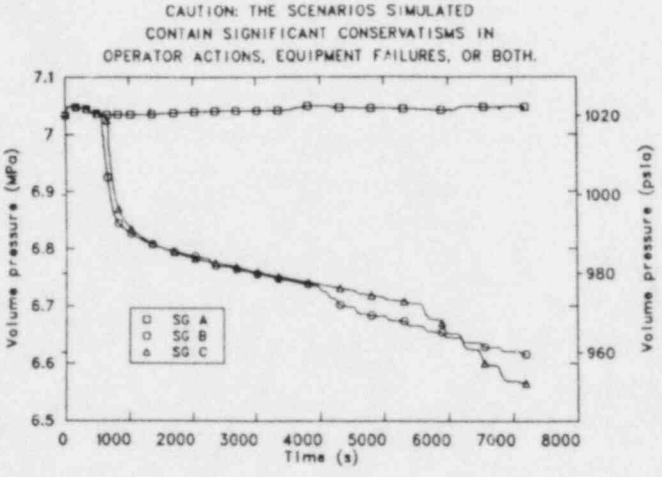

Figure 7.4 Steam Generator Secondary Side Pressures as Calculated by RELAP5 for Transient 9. (BNL Neg. No. 2-574-85)

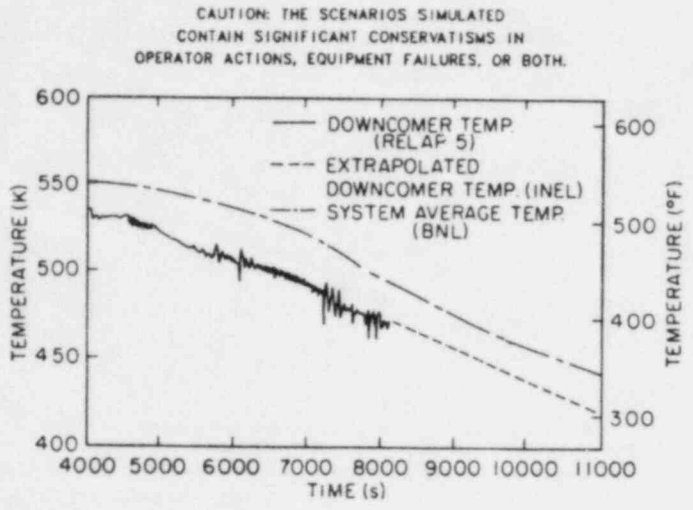

Figure 7.5 Comparison Among the RELAP5 Downcomer Fluid Temperature, RELAP5 Hot Leg Fluid Temperature and the BNL System Average Temperature for Transient 11. (BNL Neg. No. 1-341-85)

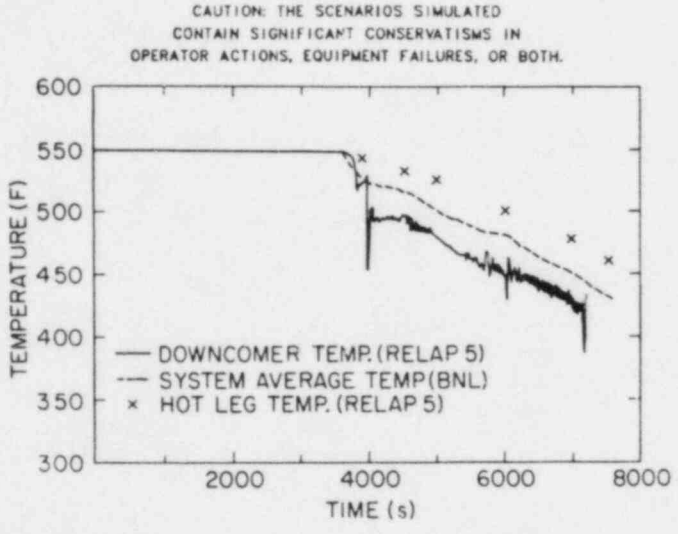

Figure 7.6 Comparison of the Long Term RELAP5 Downcomer Fluid Temperature With the BNL System Average Temperature for Transient 11. (BNL Neg. No. 1-339-85)

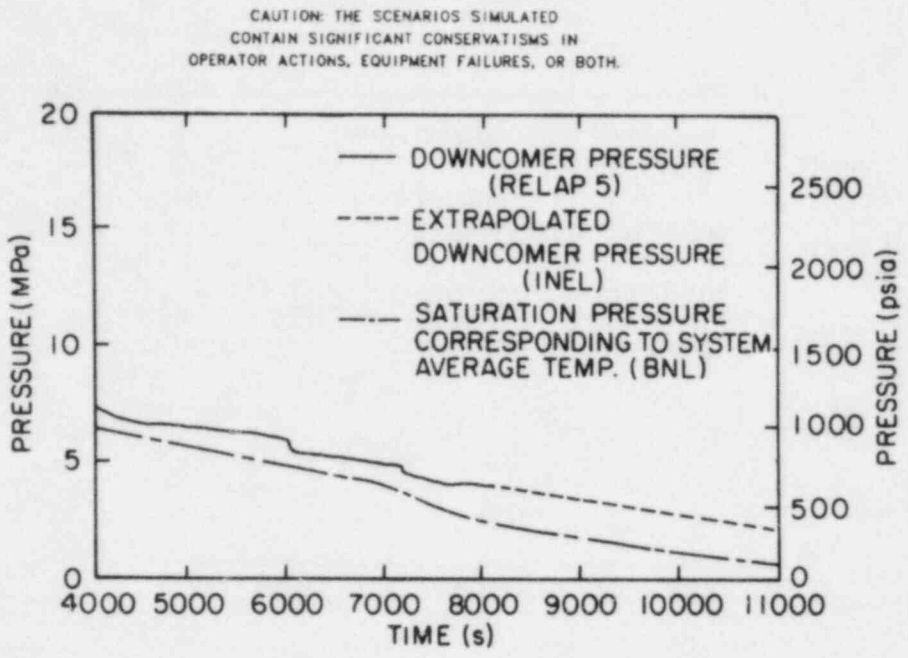

Figure 7.7 Comparison of RELAP5 Pressure and BNL Saturation Pressure for Transient 11. (BNL Neg. No. 1-343-85)

II. DIVISION OF ENGINEERING TECHNOLOGY

SUMMARY

Stress Corrosion Cracking of PWR Steam Generator Tubing

The experimental program on stress corrosion cracking (SCC) at Brookhaven National Laboratory (BNL) is aimed at the development of a quantitative model for predicting the behavior of Inconel 600 tubing in high temperature aqueous media, with special reference to its use in nuclear plant steam generators. Empirical relationships are being established between SCC failure time, crack velocity and factors influencing cracking.

Tests continued during this period with U-bends exposed to water without oxygen at high temperatures in order to establish a formula for extrapolating failure times from accelerated tests to operating conditions. Variables in the formula were correlated with the nature of specific tube parameters. Reliable SCC initiation data already exist for some heats of tubing.

Improvements were made in the quantitative relationship between stress level and SCC initiation.

Crack propagation rates have to be established with greater accuracy, requiring funding not available in FY 1984 and FY 1985. Similarly, funding was not available for the verification of the model; samples have yet to be provided from the Surry steam generator now at PNL for this purpose.

Probability Based Load Combinations for Design of Category I Structures

A tangential shear limit state for reinforced concrete containments has been established. On the basis of this limit state, the reliability analysis of Indian Point Unit 3 containment has been carried out.

A reliability analysis method for shear walls has been developed and applied to typical shear walls. This reliability analysis method can be used to evaluate the reliability level in existing structures and to derive load factors for design of shear walls.

Soil-Structure Interaction Evaluations

Lift-off capability has been implemented into the SIM computer code. A soil-structure interaction model has been used to predict uplift and is being correlated with the SIMQUAKE data. Results from Phase I dealing with layering effects have been obtained. Currently, the influence of the foundation layer-

ing on floor response spectra is being investigated. Finally, the development of a computer program with the capability of predicting soil-fluid coupled behavior is underway. Preliminary numerical evaluations indicate that pore water effects could have significant impact on response of nuclear facilities.

Identification of Age Related Failure Modes

This report provides an aging assessment of electric motors and was conducted under the auspices of the NRC Nuclear Plant Aging Research Program (NPAR). The objectives of this program are to identify concerns related to the aging and service wear of equipment operating in nuclear power plants, to assess their possible impact on plant safety, to identify effective inspection surveillance and monitoring methods and to recommend suitable maintenance practices for mitigating aging related concerns and diminish the rate of degradation due to aging and service wear.

Motor design and materials of construction are reviewed to identify age-sensitive components. Operational and accidental stressors are determined, and their effect on promoting aging,degradation is assessed. Failure modes, mechanisms, and causes have been reviewed from operating experiences and existing data banks. The study has also included consideration for the seismic correlation of age-degraded motor components.

The aforementioned reviews and assessments were assimilated to characterize the dielectric, rotational, and mechanical hazards on motor performance and operational readiness. The functional indicators which can be monitored to assess motor component deterioration due to aging or other accidental stressors are identified. Conforming with the NPAR strategy as outlined in the program plan, the study also includes a preliminary discussion of current standards and guides, maintenance programs, and research activities pertaining to nuclear power plant safety-related electric motors.

8. Stress Corrosion Cracking of PWR Steam Generator Tubing

(D. van Rooyen)

The objective of this program is to develop quantitative data to serve as a basis for determining the useful life of Alloy 600 tubing in service from accelerated test data.

The present experimental program addresses two specific conditions, i.e., 1) residual stress conditions where deformation occurs but is no longer active, such as when denting is stopped and 2) where plastic deformation of the metal continues.

8.1 Constant Load

During this quarter our work has led to a refined log-log curve for SCC under constant load. At high stress, failure time is proportional to the -4th power of stress; this value may tend to become more negative when stress is lowered towards yield (see Figures 8.1 and 8.2).

8.2 CERT

It is essential for the completion of the program that a better distinction between the initiation and propagation stages is achieved in the CERT. These corrections are needed to improve the quantitative determination of SCC induction times and SCC growth rates. New data confirm an activation energy of 33 Kcal/mole for crack growth, but are based on estimated induction times. Funding for this, as well as for verification of the model and samples from the Surry steam generator (at PNL) for doing so have not been made available yet.

As opposed to other alloy systems described in the literature, crack growth rates of Inconel 600 in high temperature water without oxygen, seem to be relatively insensitive to strain rate.

The plotting of percentage of fracture surfaces that exhibit SCC has proven a good way of studying the strain rate effects at various temperatures. We have established ranges that are and are not suitable for one heat of material (Figures 8.3-8.6).

8.3 Dents

Static "dents" continue in test, and are due for re-examination in the next quarter. No cracks have been seen so far.

8.4 U-bends

For .01% carbon, split type tube U-bend tests are practically complete at 315°C, and several cracks have also occurred at .02 and .03% carbon. Activation energy still appears to increase with increasing carbon content but less strongly in the .02-.03% range of carbon. No cracks have been seen yet at any carbon level at 290°C. Activation energy values fall between about 40 Kcal/mole and >60 Kcal/mole for the various carbon levels in our tests. See also Figures 8.7-8.12.

8.5 Future Work

Future work will be the continuation of long-term tests. However, it is strongly recommended that work on the model, especially in crack propagation rates, be re-started to complete the quantitative relationships. Without this additional effort the work to date may lose much of its potential application. Surry and/or other "known" steam generator tubes are needed for model verification, and can be tested readily in the laboratory areas that have been especially equipped for such work. U-bends, CERT and constant load experiments can be performed.

Computer programs are in existence, and will be refined, for data analysis and for use in making a variety of performance predictions from accelerated laboratory data.

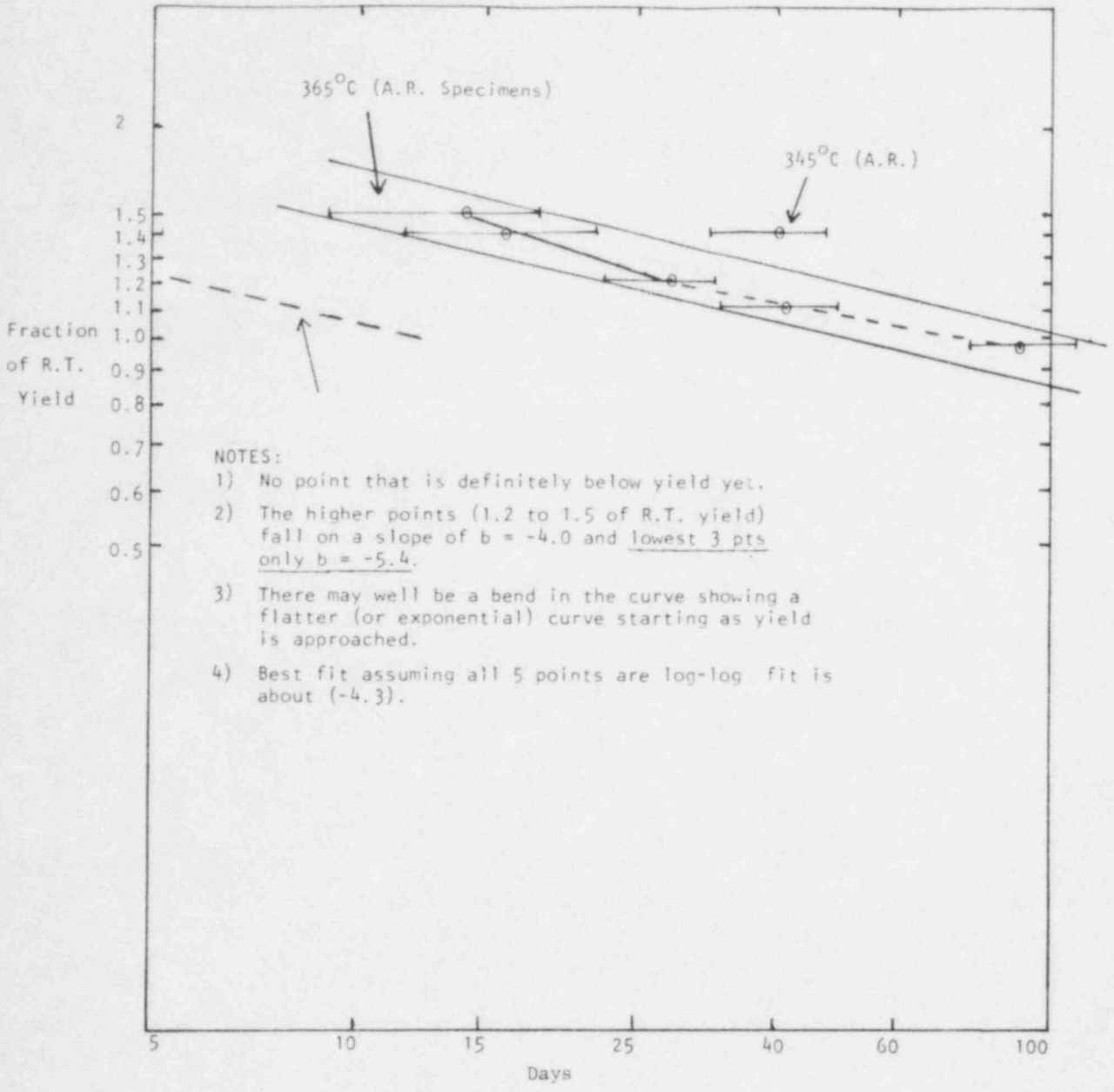

Figure 8.1 Log-Log Plot of Stress vs. Time to SCC Inconel 600. Pure H_2O . 365°C

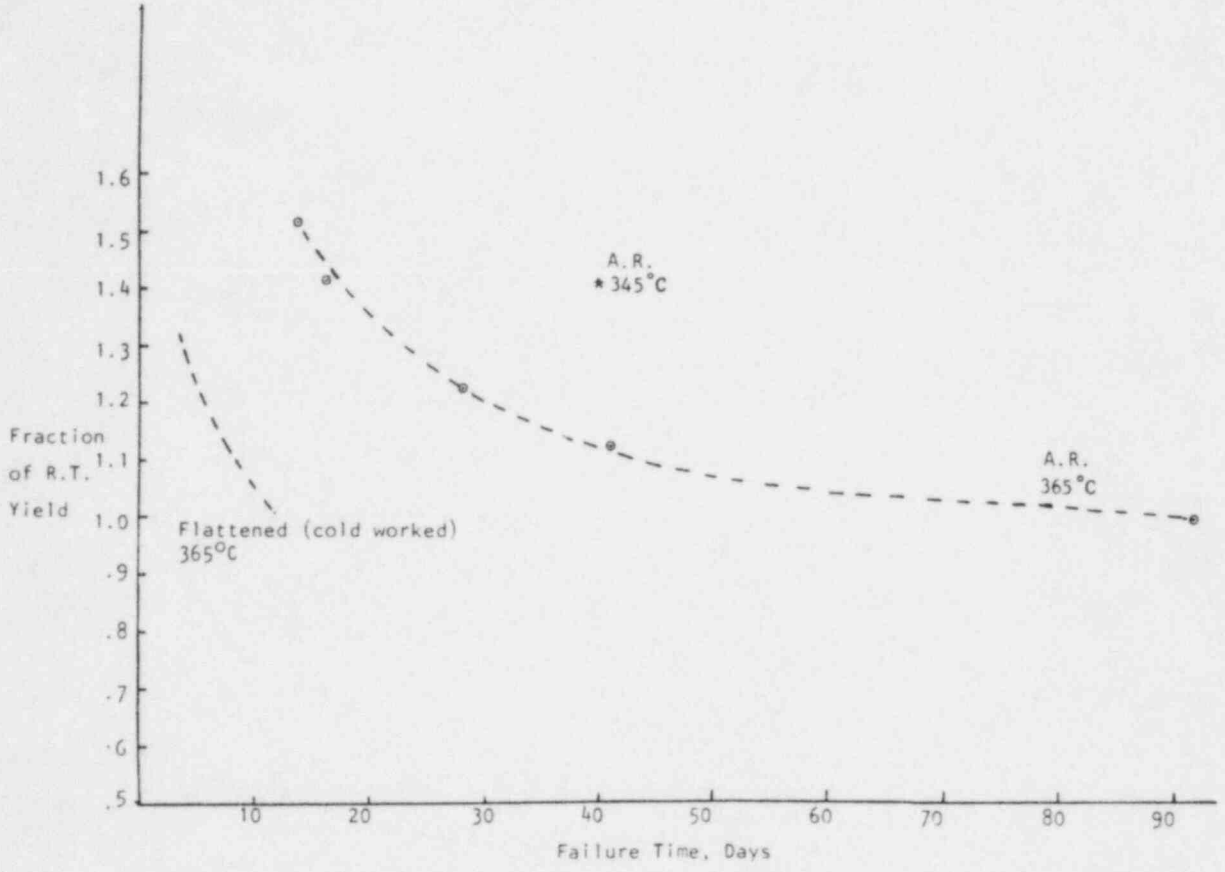

Figure 8.2 Linear Plot of SCC Fracture Time vs. Stress Constant Load Tests in Pure H_2O . 365°C Tensile Specimens. Ht #4 0.01% C

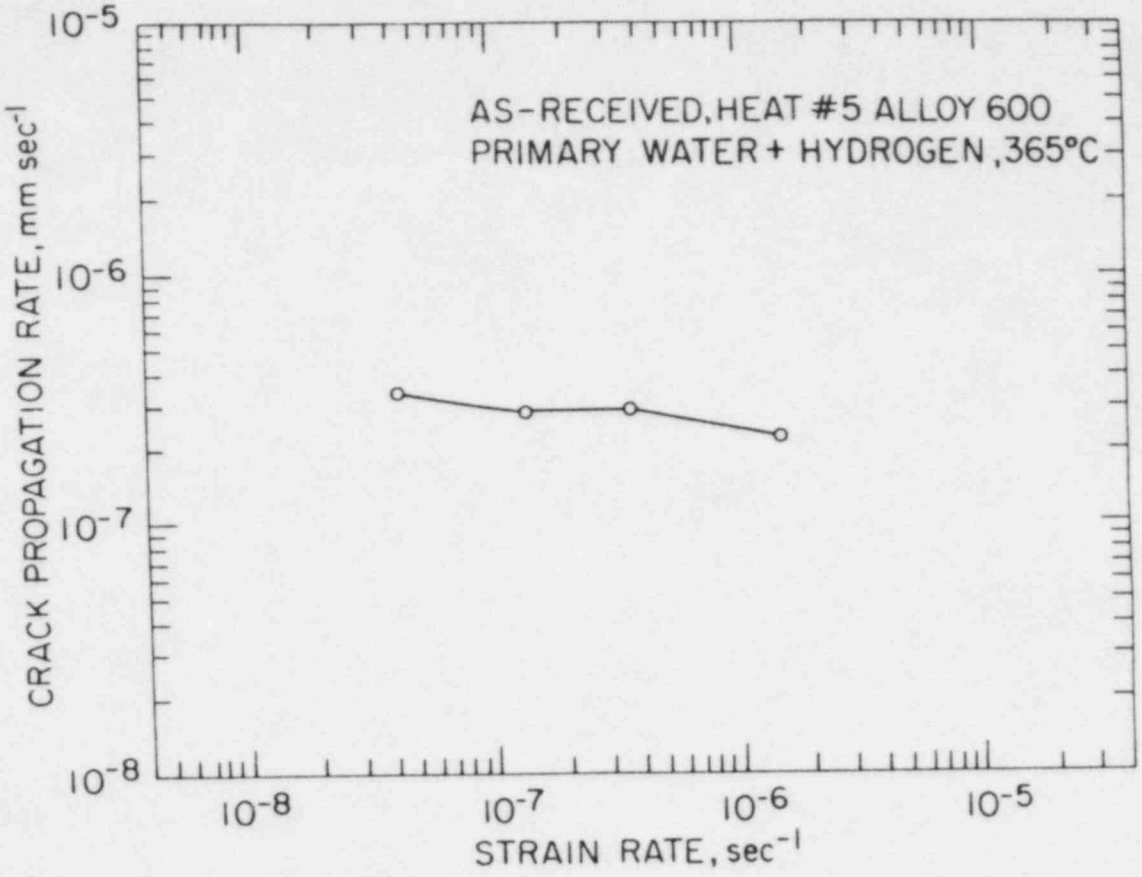

Figure 8.3 Strain Rate Effect on Average Crack Propagation Rate for BNL Heat #5 Alloy 600 Tubing.

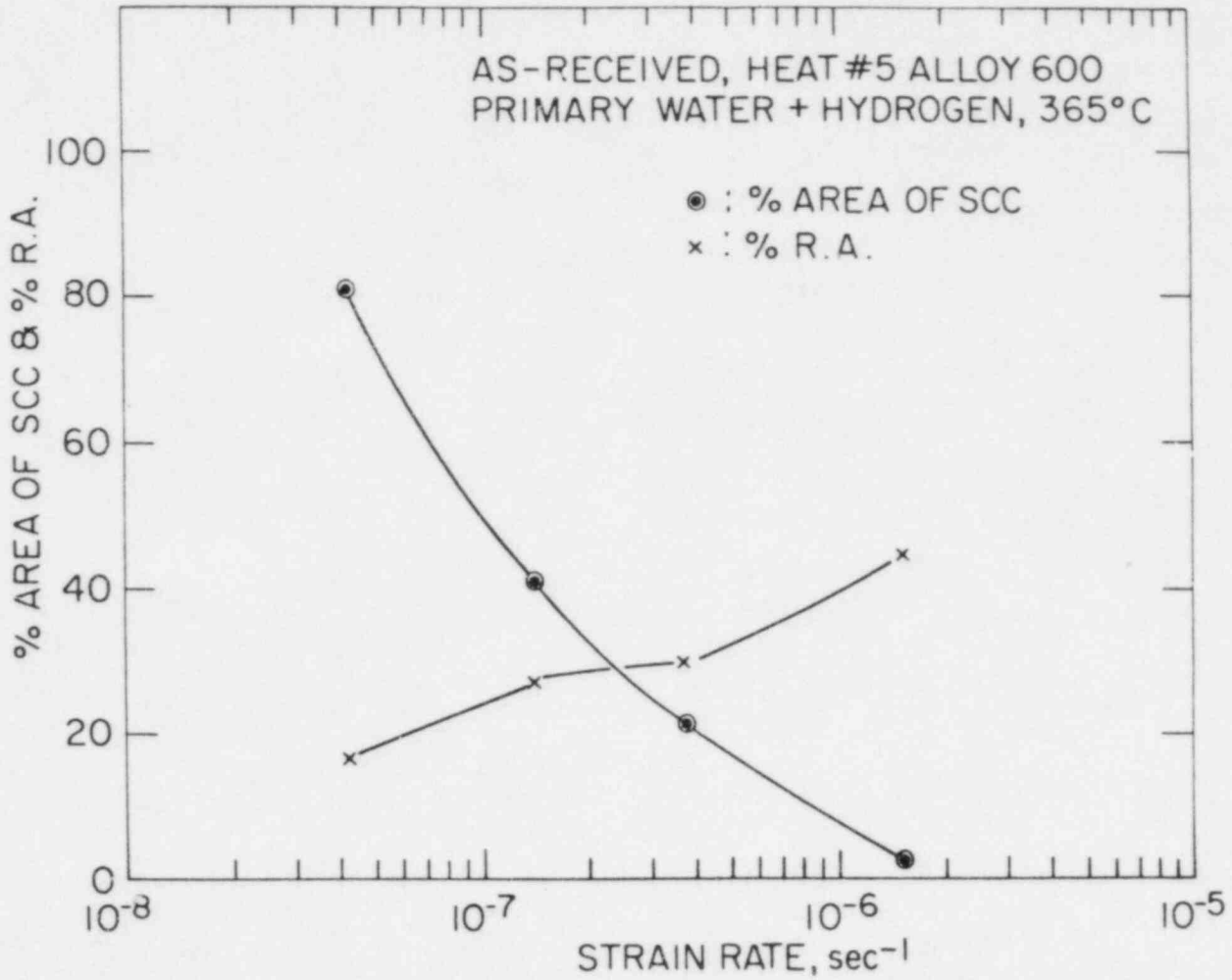

Figure 8.4 % Area of SCC and % Reduction Area Versus Strain Rate for BNL Heat #5 Alloy 600 Tubing.

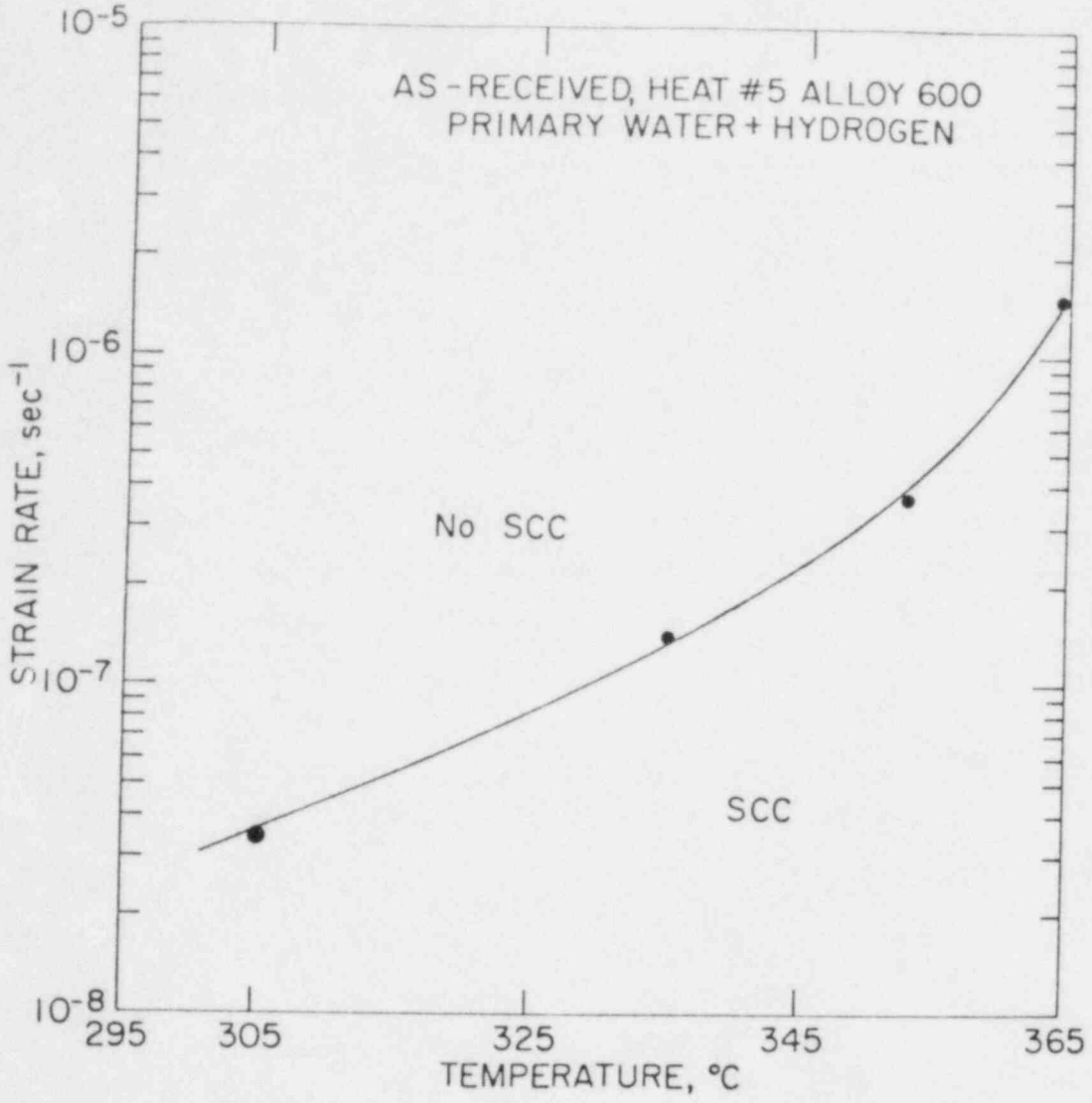

Figure 8.5 Temperature Effect on Limiting Strain Rate Below Which SCC is Observed for BNL Heat #5 Alloy 600 Tubing.

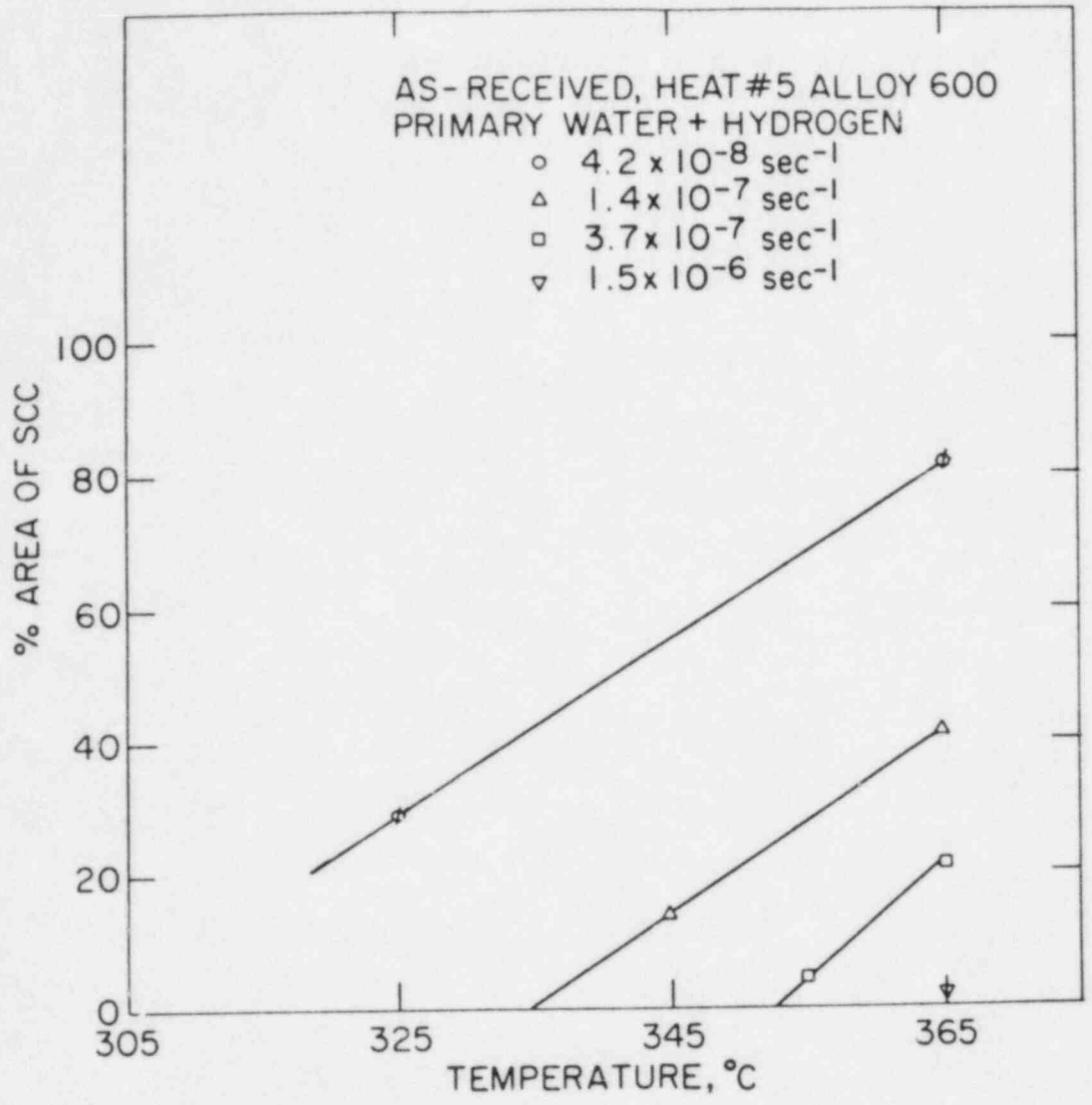

Figure 8.6 Temperature Effect on % Area of SCC for BNL Heat #5 Alloy 600 Tubing at Constant Strain Rates.

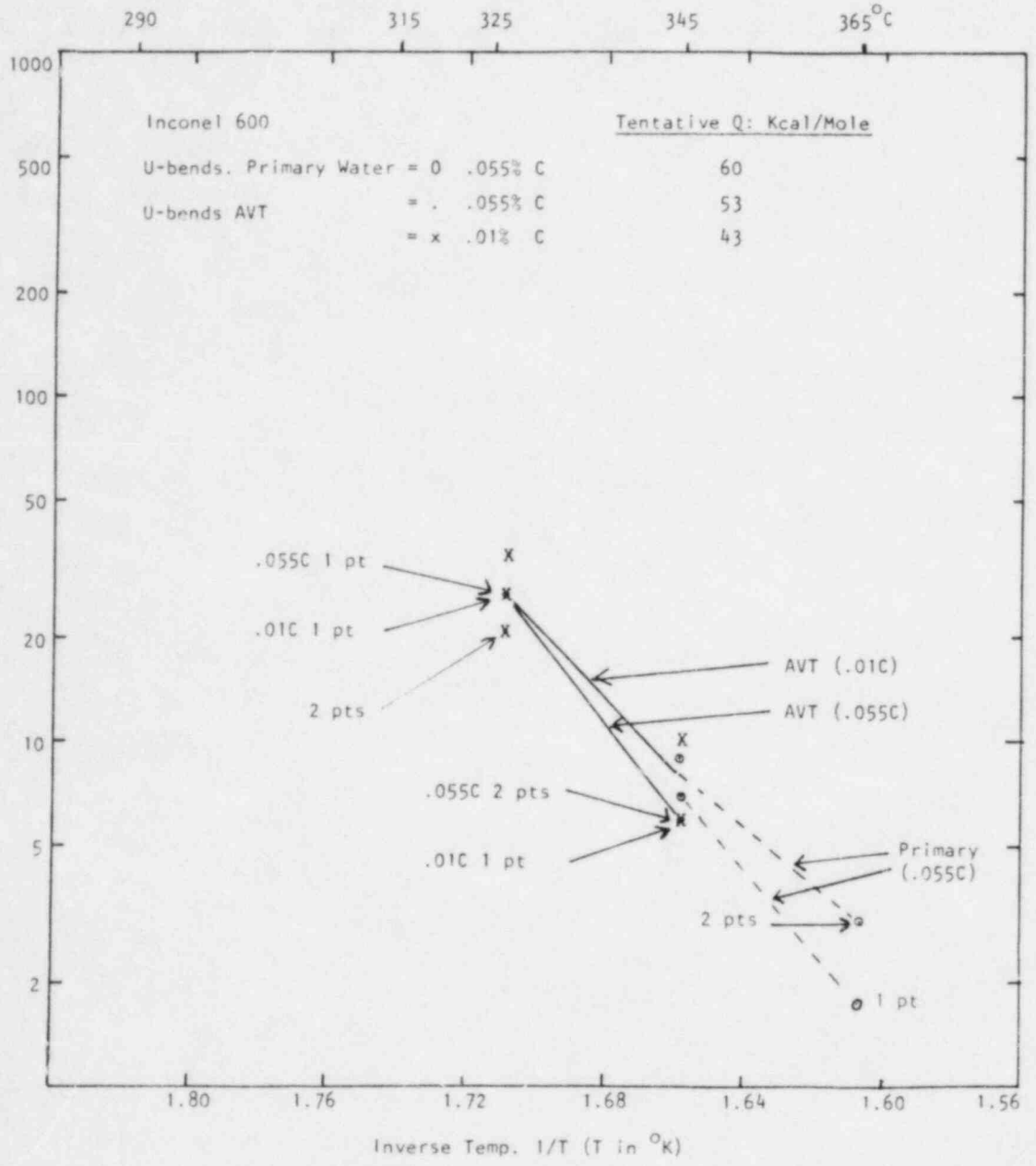

Figure 8.7 U-bends of Inconel 600 Primary H_2O and AVT

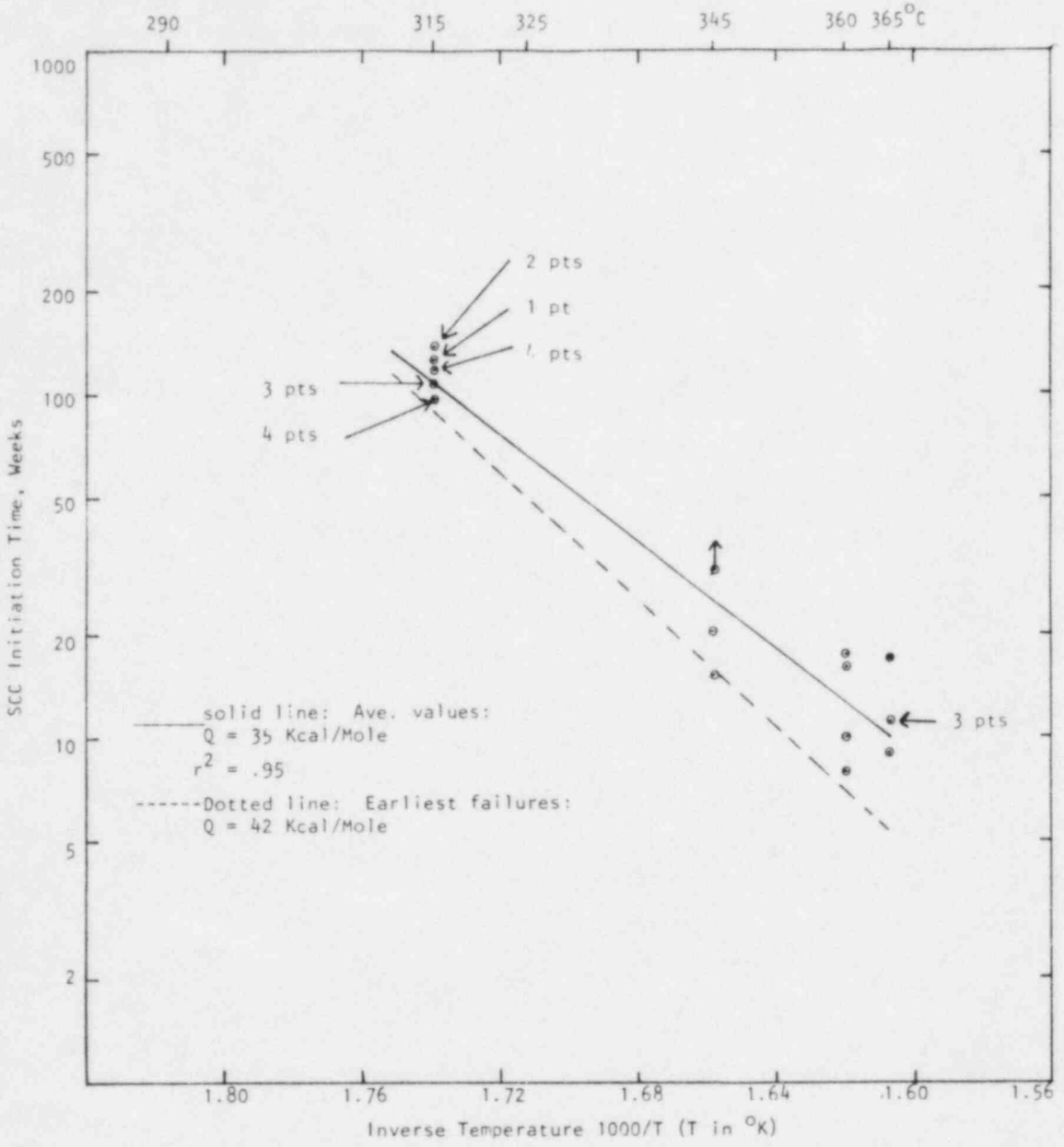

Figure 8.8 For Inconel 600 . U-bends
Pure H_2O . 0.01% C

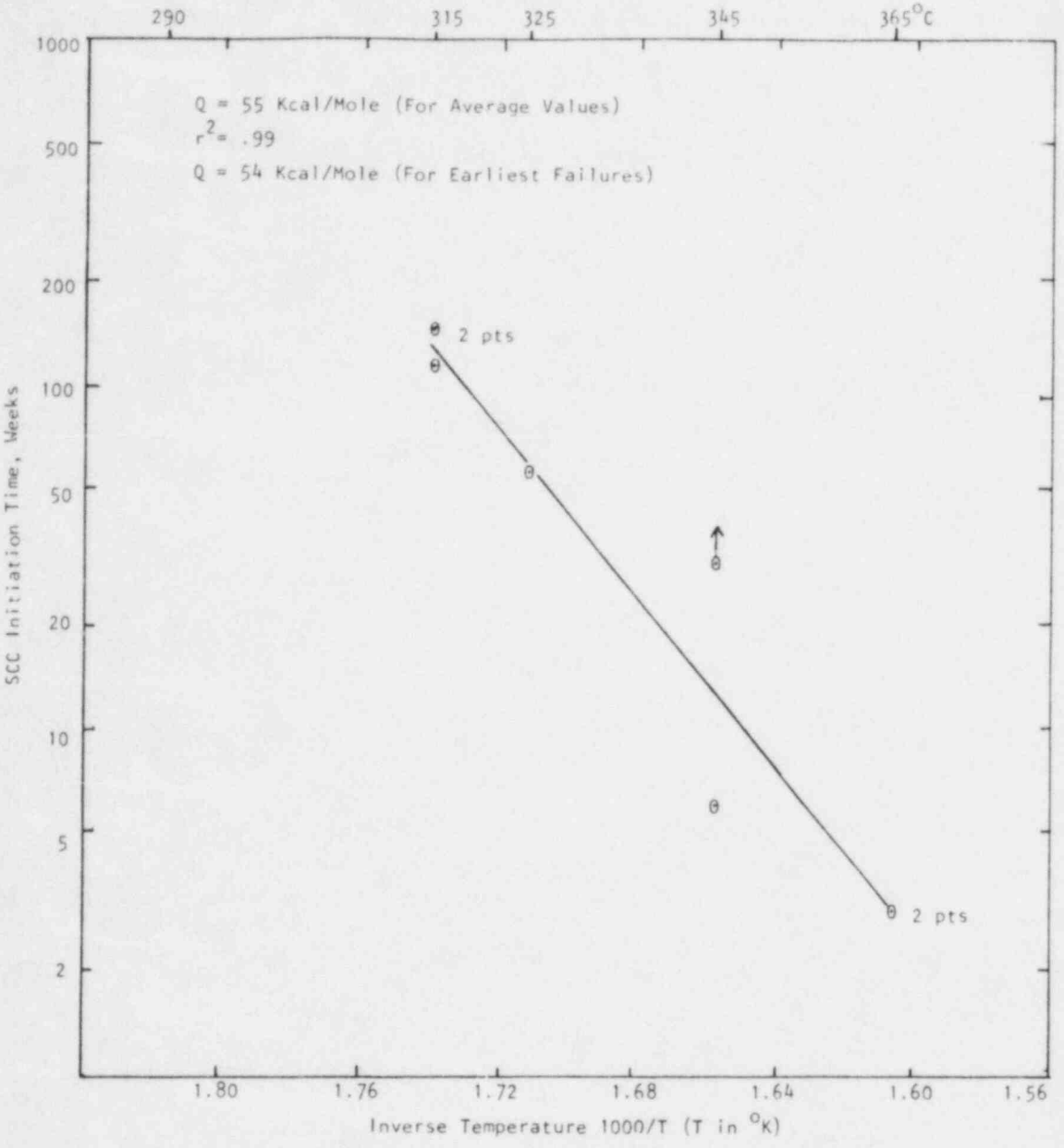

Figure 8.9 For Inconel 600 . U-bends (More Tests Continue)
Pure H_2O . 0.02% C

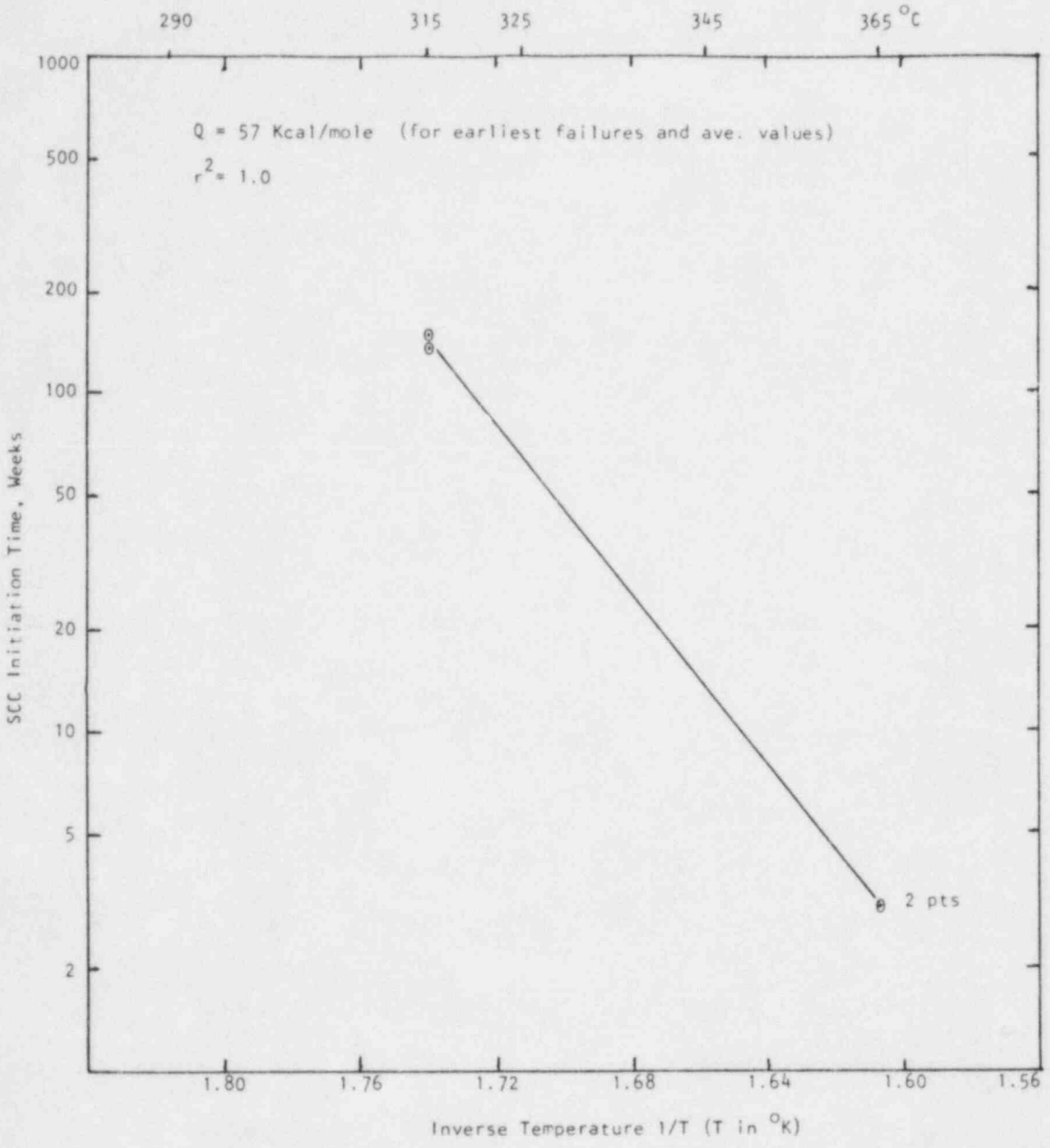

Figure 8.10 For Inconel 600 . U-bends (More Tests Continue)
Pure H_2O 0.03% C

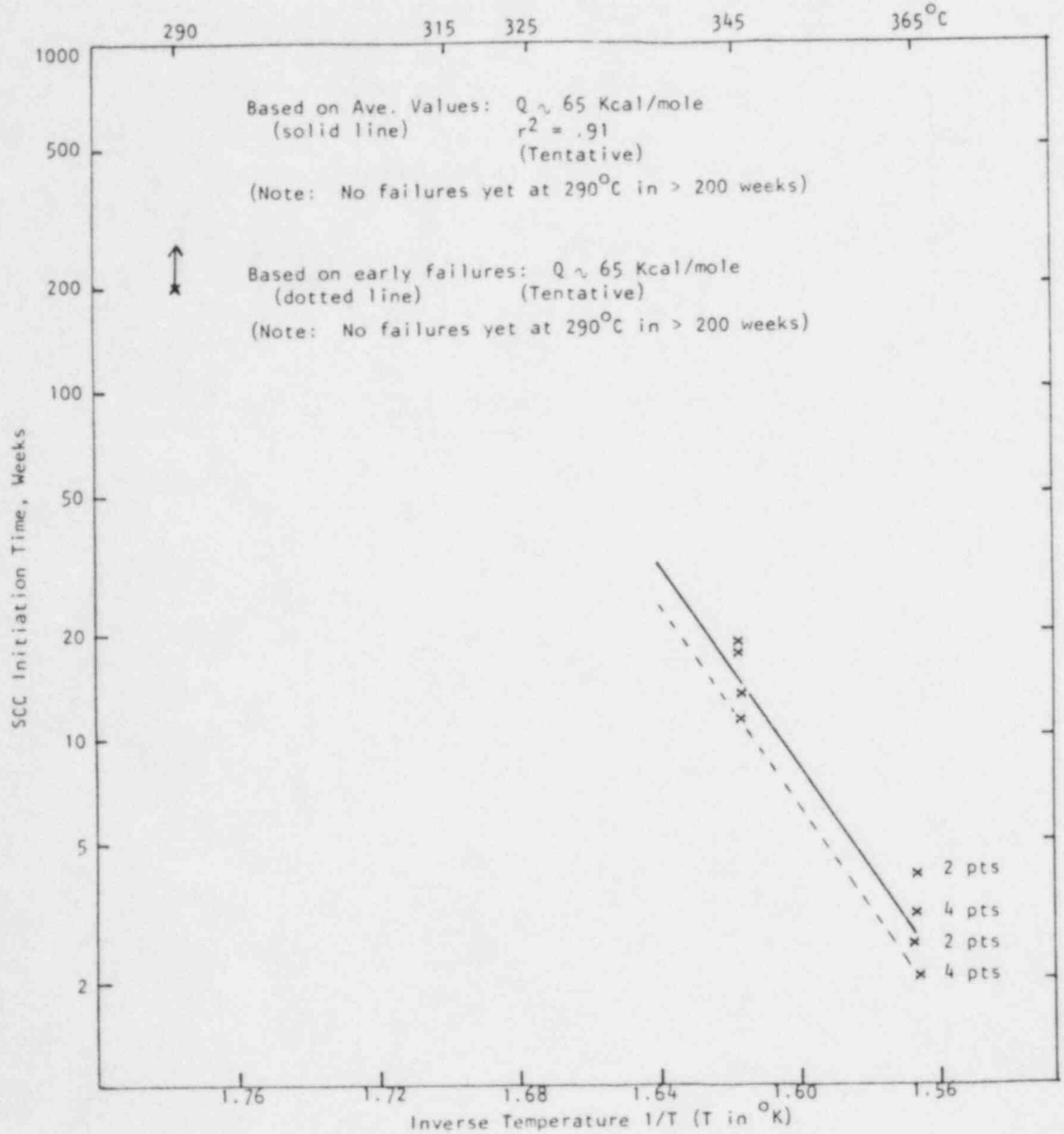

Figure 8.11 For Inconel 600 . U-bends . Pure H_2O. 0.055% C

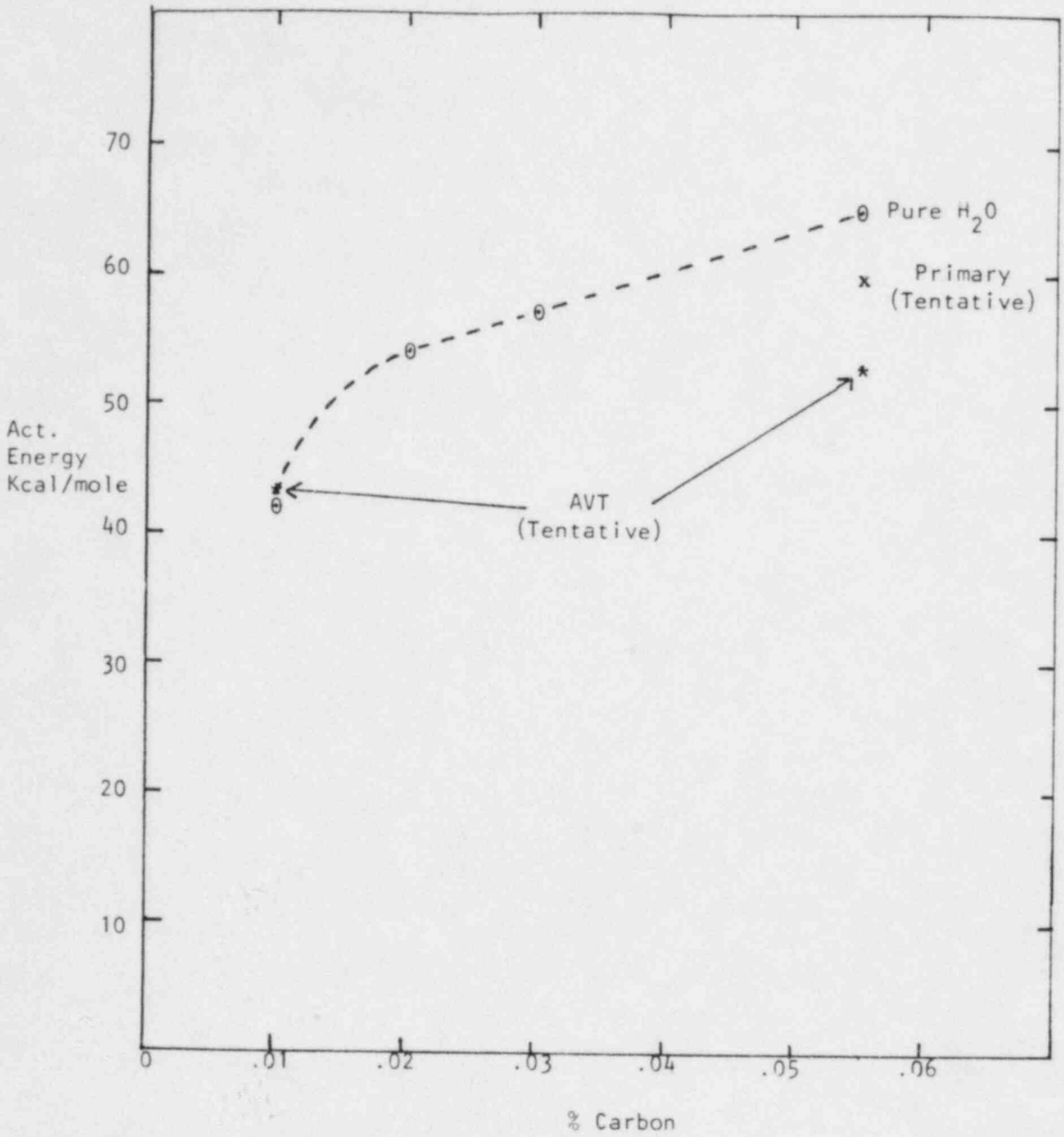

Figure 8.12 Inconel 600 . U-bends . Pure Water, Primary Water and AVT Based on First Observed SCC Initiation

9. Probability Based Load Combinations for Design of Category I Structures

(H. Hwang, M. Reich, J. Pires, P. C. Wang, M. Shinozuka, B. Ellingwood and S. Pepper)

9.1 Tangential Shear Limit State for Concrete Containments

A tangential shear limit state for reinforced concrete containments has been established. This limit state is described as follows:

The total ultimate tangential shear strength, V_u, has the following expression

$$V_u = V_c + V_{so} + V_{si}$$

where

V_u = total tangential shear strength of a wall element.
V_c = tangential shear strength provided by concrete.
V_{so} = tangential shear strength provided by orthogonal (hoop and meridional) reinforcement.
V_{si} = tangential shear strength provided by diagonal reinforcement.

The unit ultimate tangential shear strength, v_u, is obtained from V_u divided by the cross-sectional area, i.e.,

$$v_u = v_c + v_{so} + v_{si} = \frac{1}{bt}\left[V_c + V_{so} + V_{si}\right]$$

where b is the unit length and t is the wall thickness. The ultimate unit tangential shear strength, based on the test results as described by Oesterle, is summarized as follows:

$$v_c = 0$$

$$v_{so} = \begin{cases} \rho_o f_y (1 - f_s/f_y) & \sigma_{xx}, \text{ or } \sigma_{yy} > 0 \text{ (tension is)} \\ \rho_o f_y & \sigma_{xx}, \text{ or } \sigma_{yy} \leq 0 \text{ positive} \end{cases}$$

$$v_i = \rho_i f_y$$

where

f_s = tensile membrane stress in orthogonal reinforcement.
f_y = yield strength of reinforcement.
ρ_o = orthogonal reinforcement ratio, $\rho_o = A_{so}/bt$.
ρ_i = diagonal reinforcement ratio, $\rho_i = A_{si}/bt$.

A_{so} = area of reinforcing steel in each orthogonal direction (in^2/ft) or (in^2/in).

A_{si} = area of reinforcing steel in the inclined diagonal direction (with 45° inclined bars) (in^2/ft), or (in^2/in).

on the basis of this limit state, a limit state surface can be constructed for each cross section of an element. A typical limit state surface is shown in Fig. 9.1.

A reliability analysis of the Indian Point Unit 3 containment structure has been performed based on the above tangential shear limit state. Under the combination of dead load and earthquakes, the limit state probability for 40 years is 1.68×10^{-10}. This value is smaller than a previous value obtained by Kawakami, et al. based on flexture limit state. It is believed that the differences are due to the more conservative design critieria used for the tangential shear limit state.

9.2 Reliability Analysis Method for Shear Wall Structures

A reliability analysis method for shear walls has also been developed. In this method, the shear wall is modelled by beam elements. The limit state for flexure is defined according to the ACI strength design for combined axial forces and bending moments. The shear limit state is established from test results reported by Barda. At present, three loads, i.e., dead load, live load and earthquake ground acceleration, are considered in the reliabillity analysis. Dead load is assumed to be Gaussian distributed, while the live load is assumed to follow gamma distribution. The probabilistic model for earthquakes is the same as that used in the concrete containment reliability analysis. Based on the above information, the limit state probabilistics for flexure and/or shear during the lifetime of a shear wall can be computed. This reliability analysis method has been used to evaluate the reliabilities of several typical shear walls. The details of the methodology and the numerical examples will be described in a forthcoming technical report.

This reliability analysis method can be used to evaluate the reliability level of an existing shear wall, and to derive load factors for design of shear walls.

REFERENCES

OESTERLE, R.G., "Tangential Shear Design in Reinforced Concrete Containments Research Results and Applications", Nucl. Engr. Des., 79, 1984, pp. 161-168.

KAWAKAMI, H., HWANG, H., CHANG, M.T., REICH, M., "Reliability Assessment of Indian Point Unit 3 Containment Structure", BNL-NUREG-51740, NUREG/CR-3641, January 1984.

BARDA, F., HANSON, J.M., AND CORLEY, W.G., "Shear Strength of Low-Rise Walls With Boundary Element", Reinforced Concrete Structures in Seismic Zones, ACI SP-53, American Concrete Institute, Detroit, MI, 1977.

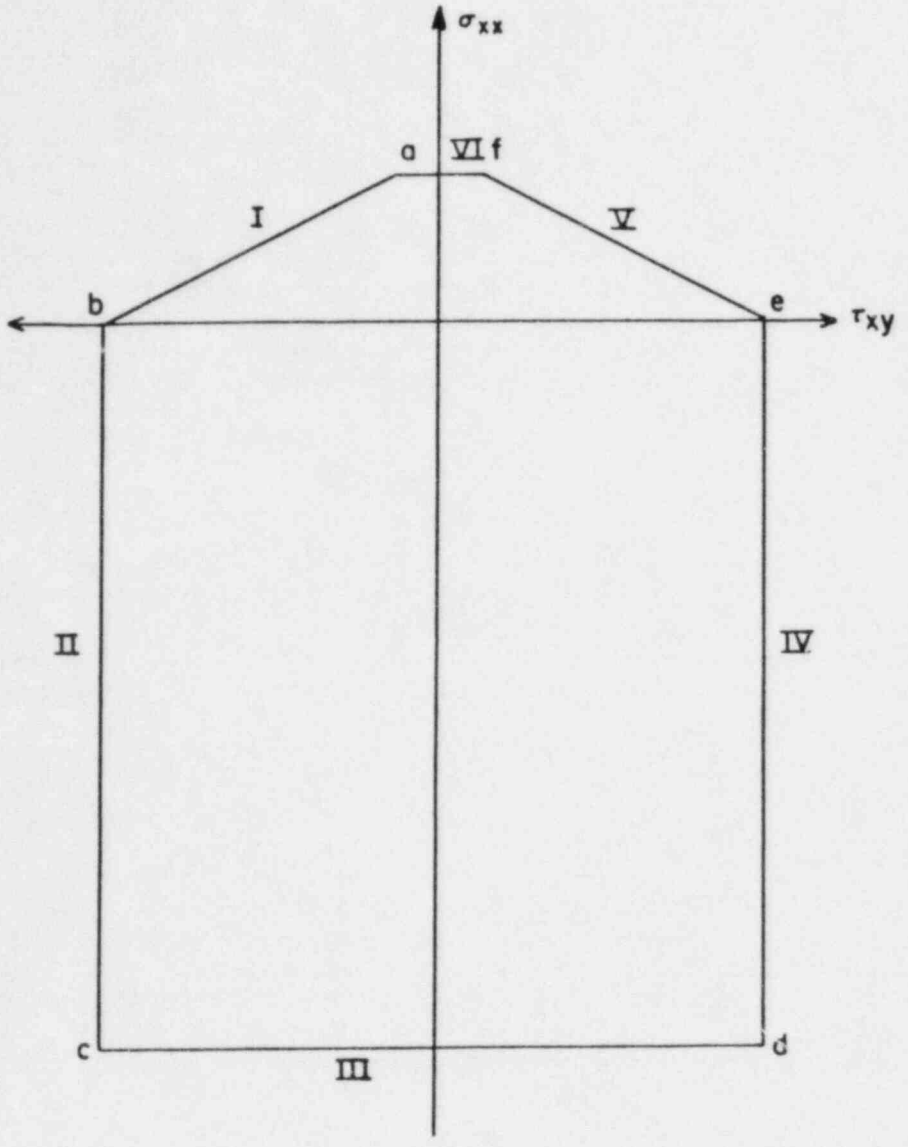

Figure 9.1 - Tangential Shear Limit State Surface

9A. Soil-Structure Interaction Evaluations

(A. J. Philippacopoulos, C. A. Miller,
C. J. Costantino, Q. Liu and M. Reich)

9A.1 Introduction

Brookhaven National Laboratory (BNL) is carrying out an investigation to determine the ranges of validity of the methods currently used to predict soil-structure interaction (SSI) effects in nuclear power plant facilities during earthquakes. In previous studies, BNL performed an evaluation of SSI methods by comparing analytical predictions versus experimental data. A draft report describing the results of these studies was submitted to the Nuclear Regulatory Commission (NRC). During this reporting period an investigation is carried out with the objective to establish criteria regarding the significance of special effects such as lifting-off, layering and water table effects.

9A.2 Lift-off Effects

The SIM Code has been modified to include liftoff effects. This was done by converting the base interaction springs and dampers to foundation modulii springs and dampers (i.e., distributed over the base of the structure). The springs and dampers are taken to be nonlinear in that a threshold cutoff is established equal to the dead weight bearing pressure under the foundation.

This modified code was then used to predict the uplift effects which were observed in the SIMQUAKE experiment. The correlation between the predicted and measured data was found to be better than was found when liftoff effects were neglected.

The liftoff interaction model is being developed further to improve this correlation with the SIMQUAKE data. In particular, the effect of impact as the foundation comes back into contact with the ground after separation is being considered. As this impact occurs, a sudden change in foundation velocity must occur if the total momentum of the system is maintained. An impulsive force is applied to the foundation to account for this velocity change. Results obtained with this model are now being correlated with the SIMQUAKE data.

Work has been initiated to establish structure, soil and earthquake parameters required to have liftoff occur. Typical structures have been selected which are representative of nuclear power plant facilities. These structures are founded on three different soil types (soft, medium and hard) and subjected to an earthquake. The intensity of the earthquake (defined by peak acceleration) is increased until liftoff occurs. Several different actual earthquake records will be used to assess the importance of wave form.

Once the above work, establishing the earthquake intensities required to have liftoff occur, has been completed the task of establishing the

significance of liftoff effects will be started. The typical structures will be subjected to earthquake intensities larger than required to have liftoff occur. Floor response spectra will be generated based on the linear interaction model where liftoff effects are neglected and the nonlinear model including liftoff effect. A comparison of these two spectra will then indicate the magnitude of the errors which could occur when liftoff effects are neglected.

9A.3 Layering Effects

The soil-structure interaction problem for uniform foundations is often treated by the half-space impedances. Previous studies have shown that in this case this problem can be further simplified by the use of frequency-independent springs and dashpots. Such approximation is usually accepted because the frequency dependence of the half-space impedances is rather weak in the frequency range of interest for nuclear plant evaluations. When, however, the foundation is layered, the corresponding impedances demonstrate a rather strong frequency-dependence. Thus the known standard spring-dashpot solutions may not be appropriate. Rather, a frequency domain solution is used, which takes into account the variation of the impedance functions.

The objective of this program is to investigate layering effects on the soil-structure system characteristics and particularly on floor response spectra. For this purpose our activities are subdivided into two phases. During the phase I, layering effects are investigated using simplified soil-structure interaction models. Such models allow for a wide variation of parameters required for a good understanding of the physical problem. These results will be then used in the phase II of the program in which a benchmarking of complex models representing typical nuclear plant structures will be carried out.

During this reporting period, our efforts were concentrated on the phase I of the program. Layering effects are being investigated using simple models. Transfer functions were obtained in closed form and implemented into a computer program. Numerical solutions were obtained using different foundation layering properties. Structural parameters were also varied. From the results obtained thus far, it is concluded that layering effects can be important in SSI evaluations. Changes in frequencies and amplitudes were observed for the sliding, rocking and flexural motions. Currently, layering effects on floor response spectra are investigated. Again, a variation of layering parameters is used: layer thickness, shear wave velocity, etc.

After the completion of the phase I work, criteria establishing the significance of layering effects will be obtained. These criteria will be then utilized in phase II in order to set up benchmark problems for typical nuclear power plant structures.

9A.4 Water Table Effects

Interaction between structures and surrounding soil is of considerable interest in the design/analysis of nuclear facilities. Earthquake analysis of

structures built on either dry or saturated soils requires special consideration due to the interaction between the structure and the soil. For a number of years, extensive studies have been made of the seismic response of structures built on single-phased, non-saturated, soils. Typical studies represent the soil as a linear (elastic or viscoelastic) medium, and use extensive numerical computations to evaluate the influence of soil/structure interaction on structural response. In a few cases, the soil is represented as a nonlinear medium. In these cases, however, the soil is treated as a single-phased medium, and no account is taken of the influence of entrapped pore fluid (ground water) on the response, although it is known that its effect could be considerable.

The purpose of this task is to treat the true two-phased structure of most foundation soils, suitably accounting for the ability of the ground water to move separately from the soil solids. Some attempts have been made to treat soil saturation effects or response without including soil mobility properties. However, no studies of the impact of two-phased properties of soil/water systems on soil/structure interaction has yet appeared in the literature.

The goal of this task is to develop such a computer program to treat the coupled response of both the solid and fluid phases of the soil system, and also to determine the impact of this coupling on soil/structure interaction. To date, a finite element computer program has been developed and is being debugged. Following this task, numerical studies will begin and interacation parameters developed and compared to the results typically used in SSI.

10. Identification of Age Related Failure Modes
(J. H. Taylor)

An aging assessment of electric motors was conducted under the auspices of the NRC Nuclear Plant Aging Research (NPAR) Program. The goals of this program are to resolve issues related to the aging and service wear of equipment and systems at operating reactor facilities and to assess their possible impact on plant safety.

10.1 Electric Motors

10.1.1 Operating Data Review (M. Subudhi, W. Gunther)

Only a few categories of electric motors are of direct safety significance in nuclear power plants: 1) three phase induction motors, 2) Direct Current (DC) motors, and 3) three-phase synchronous motors. The squirrel cage induction motor is the "work-horse" of the nuclear industry, comprising nearly 90% of the total population. Synchronous and DC motors constitute an additional 9% with the balance comprised of specialty applications. The percentage of motor failures of the total population in each category ranges from 2.4% for synchronous motors to 6.3% for DC motors. The DC motor failure rate is higher than normal and attributable to commutator related problems. One of the data bases indicated that motors with ratings of 1 - 99.9 horsepower (HP) represent nearly 47% of the total motor population. Fractional HP (< 1.0 HP) motors and motors with ratings of 100 - 999 HP represent another 41% of the total population while large motors (> 1000 HP) essentially making up the balance. It can be deduced from the data analysis that failure rate typically increases with horsepower rating even though large motors are often equipped with sophisticated surveillance, monitoring and protection systems.

Three-phase induction motors are versatile and reliable, and speed can vary based on applied voltage and loading. DC motors are reliable and have accurate speed control as well as efficient performance over the entire speed range but commonly require more maintenance. Where constant speed is an absolute necessity, the synchronous motor is available.

In regard to motor applications, valves and pumps constitute nearly 95% of the total motor population.

An analysis of the major motor components and their respective materials of construction are summarized in the following table:

Motor Components	Materials	Relationship With Aging
Stator	Copper, Steel, Aluminium	Minimal
	Insulating Materials	Significant
Rotor	Copper, Steel	Minimal
	Insulating materials	Significant
	Graphite	Significant
Bearings	Steel, Brass, Bronze	Moderate
	Grease, Lube oil	Significant
Accessories	Steel, Cast Iron, Brass, Copper	Minimal
	Seals and Gaskets	Significant
	Mica, Plastics	Significant
	High temperature PVC for Cables	Moderate

The insulating system of a typical electric motor consists of various materials in association with conducters and supporting structural parts. Insulating systems are NEMA designated as A, B, F and H, in ascending order of thermal endurance capability. Class B insulation systems are consistently in the highest failure category while Class F and H exhibit significantly lower failures.

10.1.2 Stressors - Operational and Accident Related

Motors are subjected to various operational stressors which originate both from system-level effects and from the environment, and as a result individual motor components are required to endure numerous types of service wear conditions. Abnormal or accident events tend to worsen these conditions while potentially introducing additional stressing effects. The selection of a particular motor type and rating for the performance of a specific system function therefore requires consideration of the predominate mode of system operation, whether continuous or intermittent, and prediction of the expected mild or harsh environment. System considerations are extremely important in motor specification and failure to adequately consider these aspects can result in excessive loading and premature aging.

The Residual Heat Removal Systems, Service Water Systems, and High Pressure Coolant Injection Systems were noted to experience the majority of motorized system failures.

All motors components are susceptible to degradation including the stator, rotor, bearings, and accessories. The two most significant stressors in motors are heat and vibration-related, and while the potential for the occurrence of these stressors is multiple in nature, thermal effects commonly result from excessive current which imposes self-heating and thereby insulation failure, and vibrational effects which can originate from internal and external abnormalities.

Predominant failure modes for motors are associated with the stator and bearings. Stator related failures are the highest having nearly equal probability of occurrance for both pump and valve applications, whereas bearing failures are significantly higher for pump motors. Stators are highly inclined towards ground insulation burnout due to overheating and corresponding material degradation which occurs normally as well as at an accelerated rate under harsh environment conditions. Bearing failures result primarily from the deterioration of lubrication properties in grease or oil caused by high temperatures and foreign materials.

The stresses caused by normal as well as misoperation also degrade motors. Excessive starts and stops and backseating of valves are the two most common forms of operational stressors.

Environmental parameters that are resultant aging mechanisms and therefore influence the degradation of insulation, lubrication, gaskets and seals, and other components made of organic materials are predominately electrical, mechanical, chemical, thermal, moisture-related, and radiation. In order to fully assess the effect of aging degradation on motor components it was important that the material behavior of the various organic or inorganic components be characterized.

The extent of aging degradation for insulating materials is indexed by evaluating dielectric and mechanical properties: dielectric properties include dielectric strength, dielectric constant, dissipation factor, and volume/surface resistivity; mechanical strength is characterized by resistance to tensile or shear stress and the corresponding amount of material elongation. The dielectric characteristics of most materials declines with temperature, time, and thickness. Changes in the normal values of these can be indicative of abnormal conditions such as the presence of moisture, short circuiting of condenser sections in a bushing, or the grounding of terminal leads.

One of the most critical mechanical loads which can promote degradation is vibration and is often caused by coupling misalignment, rotor imbalance, loose parts, and seismic events.

Remaining stresses to be discussed have their most significant effects on insulation and therefore motor dielectric integrity. Chemical oxidation reduces the tensile strength of insulation while also making it brittle. High temperatures and moisture concentration reduces both electrical insulating properties and insulation tensile strength. Exposure to radiation adversely affects electrical and mechanical insulation properties by causing embrittlement.

Potential seismic damage to motor components are primarily mechanical and inertia-related. Inertial failures are always associated with the size of the mass and the vibration acceleration and consequently many small components of a motor can be excluded from seismic consideration. However, damage can also be caused by seismically-provoked conditions such as dislodged objects falling on the motor. Sinc aging-related degradation is complex in nature, the correlation of aging with seismic effects is difficult to qualify and quantify. A method has been suggested based on the mechanical failure of weak link motor components in consideration of the environmental, service wear, and cyclic mechanisms. Based on the review of seismic test data and actual earthquake effects it appears that for electric motors, seismic effects should be minimal providing motor dielectric, rotational, and mechanical integrities have been properly maintained.

10.1.3 Data Evaluation and Assessments

Licensee Event Report (LER), In-Plant reliability Data System (IPRDS), and Nuclear Plant Reliability Data System (NPRDS) data provide the most complete information available to date on actual nuclear power plant motor failure and therefore provide the primary basis for the assessment of common failure modes, mechanisms, causes, and the associated frequency. Other sources of information utilized include Nuclear Power Experience (NPE), Edison Electric Institute (EEI), and Electric Power Research Institute (EPRI) reports as well as actual experience relayed by motor maintenance and design specialists. A thorough analysis of operating experience necessarily requires a review of incipient, partially degraded, and catastrophic losses of motor integrity.

Analysis of the LER data provided the following:

- Motor failures that occur inside of the defined boundary are significantly greater in number than those that occur outside the boundary.

- PWR systems apparently experience higher motor reliability than BWR systems.

- For BWR systems, pump and valve motors are equally prone to failure during normal plant operation, whereas for PWR systems pump failures are more likely to occur.

An IPRDS data review revealed the following:

- Pump motor failures are often control related.

- Continuous operation causes less stress in a motor than intermittent or infrequent operation.

- Vibration and moisture in-leakage are the prime causes of motor failure.

- Most reported pump and valve motor failures are catastrophic (Note: This indicated that incipient failures are not being identified.)

A comparison of NRC licensee SALP (Systematic Assessment of Licensee Performance) ratings with LER motor failures indicates that licensees receiving below average maintenance ratings also experienced a comparatively higher number of motor failures. This condition demonstrates that improved preventative maintenance and increased management attention could prolong motor life and reduce the overall number of failures.

A review of additional data sources utilized served to reinforce foregoing conclusions:

- Motor failures typically occur, and are detected, while the machine is in the operational modes.

- Most degraded motor conditions are either in advanced stages or have resulted in catastrophic failures.

- Stator grounding and bearing related problems are the primary causes of motor failures.

10.1.4 Conclusions

During motorized system operation various parameters such as temperature, vibration, current, voltage, and application equipment output can be utilized to generally assess motor integrity. Various performance or functionalindicators serve to characterize the behavior of any electric motor, and when normal values for these parameters are observed to adversely change, theincipient stage of degradation potentially leading to ultimate failure is occurring. Therefore, characteristic parameter performance can be linked to failure modes, mechanisms, and causes that are representative for all types of motors.

Predominant motor failure modes are associated with the stator insulation system and the bearings. The failure mechanisms for stator insulation include degraded mechanical and electrical strength, shorted windings, loose laminations, wedges (etc.), overheating and burned windings, corona or ionization,

and corrosion of electrical connections. Failure mechanisms for bearings are overheating, cracking, scoring, corrosion, and lubrication problems (i.e., too much, too little, loss of properties).

The performance or functional indicators and stressors for stator insulation are temperature, humidity, radiation, vibration, current, voltage, power factor, condition of windings, modes of operation (number of starts, overload conditions), and insulation resistance. The performance or functional indicator and stressors for bearings are vibration, moisture, proper cooling, and lubrication properties (by analysis).

Another area of failures can be classified as miscellaneous. The items to be observed in this category include loose bolts, coupling or anchor bolts which could cause vibration, environmental contamination, damaged seals or gaskets which lead to oil or water leaks, faulty protective equipment settings which could cause overloading or overheating, malfunctioning space heaters which would allow moisture buildup, poor operation, and worn commutator brushes.

It has been established through analysis and independent testing that for at least certain small induction motors (approximately 10 HP), seismic effects should be minimal providing motor dielectric, rotational, and mechanical integrity have been properly maintained. However, the definition of proper maintenance remains as an area requiring further research and more extensive determination of motor aging-seismic susceptibility.

10.1.5 Future Work

As a natural outgrowth of the work performed to date, and in accordance with the NPAR program strategy, the following future work is planned:

- To identify and recommend acceptable motor maintenance practices which can be undertaken to mitigate the effects of aging.
- To review advanced inservice inspection, surveillance and monitoring techniques and finalize the identification of critical performance indicators.
- To develop service life predictions.
- To establish in-situ testing methods as necessary to corroborate other related findings.
- To expand Aging-Seismic correlation studies to assess all sizes and types of motors.
- To provide recommendations for standards and guides, with specific emphasis on IEEE Std. 323, 344 and 627.

10.1.6 Aging-Seismic Correlation (M. Subudhi, J. Curreri)

One of the elements of the study involves an understanding of the significance of aging as a potential mechanism for degrading the functional capability of electric motors to withstand stresses generated by trigger events such as seismic disturbances.

In order to address the above goals, Brookhaven National Laboratory (BNL) obtained two 10 horsepower (HP), 480 Volt (V) gas turbine fan cooler motors from a northeastern nuclear power plant. Both motors were about 12 years old and were in continuous service outside of the plant. These motors were catalogue purchased items and were not subjected to any qualification testing prior to initial installation. They are Westinghouse Life Line-A drip-proof motors with Class B insulation.

Each motor was first tested to determine its dynamic characteristics, including natural frequencies and mode shapes. These tests established that the first fundamental frequency of the motors is well above 250 Hz. Therefore single frequency and single axis seismic testing was found to be suitable.

Both motors were then subjected to a seismic excitation level with a peak required response spectra (RRS) level of 23.88 g acceleration. Relevent operating parameters such as current, voltage, and temperatures were monitored during the seismic excitations.

10.1.7 Motor Descriptions and Correlation Discussion

Both motors were manufactured by Westinghouse and are rated as 10 HP, 440 V, 60 Hz, 3-phase, fan-cooled induction motors with drip-proof enclosures. They are commercial grade Life-Line A series motors.

These motors were not specified for nor used for safety related applications during their service life. However, their design and construction is similar in almost all aspects to motors of similar size used in contemporary nuclear plant safety systems. This holds true for the motor frame and housing, winding construction, bearing design and load coupling arrangements. One difference is the insulation class. These motors have class B insulation, whereas higher class insulations (F or H) are usually specified for nuclear safety related applications.

Another difference relates to the motor's actual environmental exposure. These motors were not subjected to radiation or any harsh environment inside the reactor building. However, the vast majority of the motors in nuclear plants are likewise not located in environments with adverse radiation fields or temperatures. The outdoor environment in the northeast, to which these motors were exposed, is quite harsh with respect to the humidity, dust and other age related stressors, as compared to the typical motor service environment inside a power plant.

10.1.8 Test Procedure

The testing program was organized in a manner such that the electrical performance of the naturally aged motors could be assessed prior to seismic testing, during the seismic testing, and after the seismic tests were completed.

The pre-seismic testing consisted of visual examinations and insulation resistance checks. These were followed by operating tests at no load and full load. The following parameters were monitored during the operating tests:

voltage, speed of rotation, bearing and winding temperatures, current, and bearing vibration. These are also the parameters identified in the motor operating experience study as functional performance indicators for motors.

Each motor was rigidly bolted to the shaker table for the seismic testing. First, an exploratory resonance search was conducted to determine the dynamic characteristics of the motors. The seismic dynamic loading, consisting of a test response spectra defined by the Generic Floor Response Spectra (GFRS) based on NUREG/CR-3466 was performed. It should be noted that the development of GFRS was not part of NPAR program, but was based on a previous study performed for the Equipment Qualification Branch of the NRC. During the seismic loading single axis, single-frequency excitation was applied in various stages with continuous monitoring of a number of important parameters of the motors.

After the seismic testing was completed, the pre-seismic electrical tests were repeated to determine if there was any notable difference in the motor's condition or operation.

This testing established a baseline condition for the motors and then evaluated the effect of the seismic testing both during and after the tests. Line voltage, current, and temperatures at various locations of the motor were used to monitor the operating conditions of the motors.

The pre-seismic testing consisted of visual examinations and insulation resistance checks. These were followed by operating tests at no load and full load. The following parameters were monitored during the operating tests: voltage, speed of rotation, bearing and winding temperatures, current, and bearing vibration.

10.1.9 Test Results

The motors were partially disassembled and visually inspected. They both were in reasonably good condition except for the following noted items. Both motor terminal boxes were severely corroded. This was most likely caused by improper sealing of the cover gaskets. This condition is not deleterious in itself, but could eventually lead to cable termination corrosion and overheating. Motor No. 1 also had deterioration in a small portion of the stator winding, consisting of a partial breakdown in the varnish and insulation. Additionally, it had a noisy inboard bearing, caused by wear and inadequate lubrication. Neither of these observed conditions were corrected prior to seismic loading.

No aberrations in motor performance were observed during testing. Visual inspections subsequent to seismic testing revealed that none of the observed deficiencies had deteriorated as a result of the "imposed" seismic events.

All recorded parameters were in the normal range. Horsepower values were slightly below nameplate, bearing temperatures were about 120°F, and no significant vibration was present. There were no significant variations of any electrical parameters between the motor phases.

10.1.10 Conclusions

In conclusion, both naturally aged motors indicated no trend of degradations in their functional indicators even after being subjected to the most severe seismic excitation of 23.88g peak acceleration per the GFRS. Existing age-related deficiencies in one bearing and in the stator winding of motor 1 were not magnified by the seismic excitation. This indicates that these small commercial grade motors are built ruggedly and do not appear to have component aging related degradations which could be further deteriorated during a seismic event. However, since the present study was limited to two identical motors driving fan coolers, a general conclusion on motors with regards to aging-seismic correlation cannot be established. In order to achieve this, additional tests on motors of various sizes and applications would have to be performed. Also, the hostile reactor environment in a nuclear power plant containment during post-accident conditions including irradiation and chemical spray was not addressed in this study, and no testing based conclusions regarding harsh environment qualification can be made.

REFERENCES

1. "Nuclear Plant Aging Research for Operating Reactors Inspection, Surveillance, and Maintenance: Program Plan," U.S. NRC Report, Rev. 1, July 1984.

2. "Program Plan for Aging and Seismic Interaction Studies of Electrical/Mechanical Components in Nuclear Power Plants," BNL Report, Rev. 2, June 1984.

10.2 Battery Chargers and Inverters (W. Gunther and M. Subudhi)

A preliminary review of the operating failure characteristics of the equipment was initiated with the LER data sources. Other efforts are made to obtain additional data bases for identifying the failure modes, causes and mechanisms associated with battery chargers/inverters. Trips to the manufacturing companies were made to better understand the design, manufacturing and construction of the equipment. It is expected that a comprehensive aging assessment of this component will be achieved during the next quarter.

Further analysis of the operating failure characteristics of this equipment was accomplished. LER and IPRDs data sources were reviewed in depth and exhibited a failure-age correlation which is being further examined for subcomponent failure trends. Initial emphasis has been placed on the failure analysis of inverters since it became apparent from the data review that the failure of an inverter can have a major impact on plant performance and has initiated significant challenges to safety systems. For instance, at least twenty seven reactor trips occurred from 1976 to 1984 directly attributable to inverter failures. Safety system injections, loss of shutdown cooling systems, and loss of high pressure injection systems also resulted directly from inverter failure.

III. DIVISION OF RISK ANALYSIS AND OPERATIONS

SUMMARY

Application of HRA/PRA Results to Resolve Human Reliability and Human Factors Safety Issues

Brookhaven National Laboratory has been tasked in this program to identify approaches for using anticipated Human Reliability Analysis (HRA)/Probabilistic Risk Assessment (PRA) data to resolve human reliability/human factors issues of interest, and development of techniques for implementing those approaches.

The initial research in this project involved a comparison of the data needed to address human performance regulatory issues and the data currently available from PRA. To accomplish this, two separate efforts were undertaken: (1) identifying, collecting, and storing all quantitative human performance data contained in all PRAs done to date and (2) listing all human performance regulatory issues and systematically deriving from the issues the data needed to address them.

As a result of these efforts, BNL is developing the following document which reports on the findings in the above program.

- Uses of Human Reliability Analysis Probabilistic Risk Assessment Results to Resolve Human Performance Issues That Could Affect Safety (NUREG/CR-4103).

PRA Technology Transfer Program

This program has been an ongoing NRC program since 1982. However, it is a new program for BNL, which was initiated this fiscal year. The program is designed to provide research support to transfer the technology of Probabilistic Risk Assessment (PRA) to the NRC staff. This will be accomplished through conducting pre-established courses, formulating curriculum changes and additions based on the needs of the NRC staff, and the publication of textboks on the subject for future NRC usage.

The purpose of this program is, therefore, to provide the NRC with an adequate PRA resource capability with which independent validations of the effectiveness of regulatory, risk-related programs can be performed and rom which risk and reliability methods can be applied to inspection and enforcement decisions.

During this quarter preliminary progress has been made in the management of the overall program. Scoping documents have been prepared describing the

technical content that each textbook should contain. Planning documents were also prepared detailing the purpose/objective, and scope of a new PRA FUNDAMENTALS course which will be given to the "Regions." A Regional Steering Committee has been established to oversee this course. A team of instructors has been presented to the NRC Program Manager for final recommendations. The most likely instructors have been notified and a course schedule for final approval has been submitted.

Emergency Action Levels

Brookhaven National Laboratory has been tasked in this program to develop guidance for Emergency Action Levels (EALs) that can be integrated into Emergency Operating Procedure (EOP) guidelines. From this guidance, a method will be developed that can be applied by licensees to verfiy that the EALs incorporated into their EOPs are usable in the control room under accident conditions. This should result in a reliable and timely basis for declaring emergencies without being too complex or burdensome to those who are trying to safely mitigate an accident. Thus far, a preliminary assessment has been made to integrate EALs and EOPs based on the degradation of the fission product barrier criteria.

Protective Action Decisionmaking

In this program, BNL staff are developing a technical basis for NRC guidance on protective action decisionmaking based on an evaluation of the consequences of nuclear power plant accidents. Potential actions under consideration include sheltering, evacuation, and relocation. In the past, specific recommendations have proven to be difficult to justify because of uncertainties in potential accident sequences. Consequently, BNL will establish strategies appropriate to those sequences for which emergency planning is necessary, emphasizing credible failure modes, links to emergency action levels based on in-plant observables and containment status, and other factors such as weather.

11. Application of HRA/PRA Results to Resolve Human Reliability and Human Factors Safety Issues

(J. N. O'Brien and C. M. Spettell)

Brookhaven National Laboratory has been tasked in this program to identify approaches for using anticipated Human Reliability Analysis (HRA)/Probabilistic Risk Assessment (PRA) data to resolve human reliability/human factors issues of interest and development of techniques for implementing these approaches.

The initial research in this project involved a comparison of the data needed to address human performance regulatory issues and the data currently available from PRAs. To accomplish this, two separate efforts were undertaken: (1) identifying, collecting, and storing all quantitative human performance data contained in all PRAs done to date and (2) listing all human performancr regulatory issues and systematically deriving from the issues the data needed to address them. Each of these efforts is described below.

11.1 Identifying, Collecting, and Storing all HRA/PRA Data

Every volume of all 19 currently available PRAs were collected and placed in a dedicated library. Technical readers closely examined every page of every PRA volume in order to identify the presence of any a set of approximately 20 key words relating to human reliability or performance. After these key words were identified, experienced human reliability analysts examined each key word to determine if any HRA/PRA data were present. If so, the particular datum was entered into a computer data base as a single data record along with any information pertinent to it including the type of datum (i.e., human error or system unavailability due to testing and maintenance), confidence or uncertainty bounds, factors affecting human performance (e.g., stress, time available, training), the situation involved (e.g., LOCA, transient, external event), the plant system involved, the type of error (i.e., omission or commission), the particular human action involved, and the particular personnel involved (e.g., operator, maintenance, I&C). In most cases all of this information was not available from the PRA so that most data records are not complete. Each PRA is a separate file in the data base so that comparisons between PRAs, as well as among the data generally, are possible.

11.2 Listing of Human Performance Regulatory Issues and Data Needs

It was recognized that the issues facing NRC are somewhat different at any given time. As a result, an effort was made to systematically generate a representative list of human performance regulatory issues. First, each Generic Safety Issue (i.e., TMI Action items, Task Action items, and New Generic Issues) was examined and the human performance issues attendant upon it listed. Second, to refine and clarify these issues, NRC planning documents were reviewed and over 25 NRC personnel with cognizance over the issues were interviewed. This resulted in a refined list of human performance regulatory

issues. Each issue was broken down into a set of data records which would address the issue in question. Each data record includes the personnel involved, the actions involved, the presence of factors affecting performance, the situation involved, and the plant system involved.

11.3 Comparison of HRA/PRA Data Records and Issues Data Records

In order to assess the usefulness of HRA/PRA data with regard to human performance regulatory issues a comparison of HRA/PRA data records and a issue data records was made. The cases where HRA/PRA data records existed to address issues data records were noted. This project is in the process of being documented in a NUREG/CR-4103 entitled "Uses of Human Reliability Analysis Probabilistic Risk Assessment Results to Resolve Human Performance Issues That Could Affect Safety." This document is currently under review in the Office of Nuclear Regulatory Research and is expected to be published shortly.

12. PRA Technology Transfer Program

(J.L. Boccio and R.E. Hall)

12.1 Objectives

The purpose of the PRA Technology Transfer Program (PRATTP), originally established by the NRC four years ago, has been to formulate a curriculum for training select NRC staff members in the use of probabilistic risk assessment (PRA) techniques. To support this mission, NRC developed training aids, conducted courses, and provided course notebooks to supplement the lectures and to use later as reference material.

As the needs of the NRC staff changed, and as the use of PRA techniques increased in the licensing and inspection areas, the curriculum required change. Also as a result of this teaching experience, the responses of the students to the courses and requests by them for examples of applications of PRA of the type the staff may use itself or be called upon to evaluate, this program is now structured to address the lessons learned and deal with the recent developments.

Accordingly, BNL has been tasked to provide research support to transfer the technology of PRA and PRA techniques to the NRC staff. This is to be accomplished by conducting pre-established courses, formulating curriculum changes and additions based on the needs of the NRC, developing training aids, and publishing a series of textbooks on the subject for future NRC use.

12.2 Major Tasks

To conduct this program, five major tasks have been identified, viz.,

- Program Management - to manage, coordinate, and assure overall program performance
- Course Presentation - to provide instructors, training aids, and teaching facilities to teach a series of nine courses.
- Documentation/External Peer Review - to provide a review process to assure the quality and technical validity of the documentation.
- Text Preparation for Publication - to prepare the course documentation for publication as course manuals and bound text.
- New Curriculum Development - to develop and teach a new course design to introduce the NRC Regional and Inspection and Enforcement (I&E) staff to the basic concepts and terminology of PRAs and to familiarize them with the available tools to understand its potential use in inspection and general plant review.

12.3 Work Performed During Period

Under Task 1, Program Management, work performed entailed the participating in two Regional Steering Committee meetings to review the materials to be prepared and the presentation to be given. A working draft was developed describing the course outline for the PRA class to be offered in Region III. Five NRC/RES planning meetings were attended, and contracts were initiated to procure the services of JRB, BCL, EI, and SAIC personnel. A program team was assembled, and a draft program plan was developed with milestones, an interface chart, and a costing schedule.

Under Task 2, Course Presentation, work performed included scheduling the PRA Fundamentals course, assigning instructors, and preparing course material. In addition the Data Development course was scheduled, instructors were assigned, and course material was prepared. Tentative dates have been established for the remaining courses, subject to change due to instructor availability.

Work under Task 3, External Peer Review, included preparation for NRC approval of a list of individuals to act as external peer reviewers of documentation prepared under this program. A review of existing course notes was initiated to assess their use in the Regional program and their incorporation into the planned textbooks.

Work under Task 4, Text Preparation for Publication, entailed making initial contact with editors, printers, and publishers to discuss various strategies in publishing the texts and to establish costs and time requirements.

Task 5, New Curriculum Development, work included drafting an outline of the new I&E PRA Fundamentals course and sending it to the steering committee for review. Discussions have begun with I&E and the Regions as to their additional needs in technology transfer.

13. Emergency Action Levels

(W. J. Luckas, Jr.)

Brookhaven National Laboratory (BNL) has been tasked in this program to develop guidance for Emergency Action Levels (EALs) that can be integrated into Emergency Operating Procedure (EOP) guidelines. From this guidance, a method will be developed that can be applied by licensees to verify that the EALs incorporated into their EOPs are usable in the control room under accident conditions. This should result in a reliable and timely basis for declaring emergencies without being too complex or burdensome to those who are trying to safely mitigate the accident.

EALs are a plant specific, predetermined observable and/or measurable set of indications (such as a particular set of control room instrument readings having reached specific off-normal values) which are used to declare one of the Emergency Classes (Alert, Site Area Emergency, or General Emergency). A more descriptive term for EALs would be emergency declaration indicators.

After appropriate examination, an attempt is being made to utilize currently available EALs developed by utilities, such as Kansas Gas and Electric Company on their Wolf Creek Cenerating Station, that use the degradation of fission-product barrier approach as a starting point. The EAL guidance will be verified by testing it against the example initiating conditions listed in Appendix 1 of NUREG-0654.

During the first quarter of FY 1985, a preliminary assessment was reviewed for the adaptability of the BWR Owners' Group Emergency Procedure Guidelines to integrate EALs and EOPs based on the appropriate criteria.

14. Protective Action Decisionmaking

(W. T. Pratt, A. G. Tingle, H. Ludewig,
W. R. Casey*, and A. P. Hull*)

14.1 Background

NRC regulations require that, in the case of a major nuclear power plant accident, licensees recommend protective actions to reduce radiation dose to the public. When certain emergency action levels are exceeded, the licensee recommends protective actions to State and local officials. The nature of the protective actions recommended is determined by which emergency action levels are exceeded.

In practice drills, decisions on protective action recommendations have proven to be difficult. NUREG-0654 states that if containment failure is imminent, sheltering is recommended for areas that cannot be evacuated before the plume arrives, but evacuation is recommended for other areas. The assumption in NUREG-0654 is that there would be a greater dose savings if the population were sheltered during plume passage rather than evacuated, but this assumption has not been proven. Furthermore, the recommended protective actions must be based on estimated containment failure times, which are difficult to determine.

Alternatively, other NRC publications suggest that the appropriate response would be early evacuation of everyone within a distance of about 2 or 3 miles for all events that could lead to a major release even if containment failure is imminent or a release is underway. Those at greater distances should take shelter. Further, if a release occurs, the appropriate action would be for monitoring teams to find "hot spots" (radiation dose rate exceeding about 1 R/hr) and for people to evacuate these "hot spots."

14.2 Project Objectives

The objectives of the activities to be performed in this project are to:

(1) characterize the family of potential accident sequence for which emergency planning is necessary,

(2) establish strategies appropriate to these sequences, emphasizing credible failure modes,

(3) identify those factors which would influence the implementation of these strategies,

(4) determine how these factors should be incorporated into the decisionmaking process, and

---

*BNL Safety and Environmental Protection Division

(5) develop a guidance report on the protective actions to be recommended for combinations of these factors.

14.3 Technical Approach

The technical approach is based on an evaluation of the consequences of nuclear power plant accidents as they relate to protective action decision-making. The evaluation includes a careful review of previous work (e.g. NUREG/CR-2339, NUREG-0654, NUREG/CR-2025, NUREG-0396, and reports and memoranda by the NRC staff) and its applicability to protective action decision-making. The approach is also based on a consideration of a wide range of potential accident sequences and on up-to-date assessments of containment performance. Thus the technical basis will reflect the new fission product source term information under development by the NRC/RES Accident Source Term Program Office (ASTPO). BNL staff are closely following the activities of ASTPO and, in addition, are participating in the SARP Containment Loads Working Group and in the Containment Performance Working Group. The work of these groups will be integrated into our development of protective action strategies.

The evaluation will be based in large part on results obtained from the CRAC2 computer code (Consequence of Reactor Accident Code, version 2). The output is being analyzed for a variety of release characterizations, weather sequences, and protective action strategies.

In accordance with the above, we have selected the following six facilities to represent the range of U.S. reactor and containment designs:

Zion: PWR with a large dry containment
Surry: PWR with a subatmospheric containment
Sequoyah: PWR with an ice condenser containment
Brown's Ferry: BWR with a Mark I containment
Limerick: BWR with a Mark II containment
Grand Gulf: BWR with a Mark III containment

14.4 Project Status

14.4.1 Summary of Activities

Several source terms calculated by ASTPO were used to evaluate potential protective action strategies. A draft report which includes the following elements was prepared:

1) a general discussion of the consequences of radiation releases,

2) a discussion of boiling water and pressurized water reactor containment designs and pertinent accident release characterizations,

3) a discussion of protective action strategies for a range of source terms based on ASTPO methodology.

NRC staff visited BNL in December to discuss progress and the format of the draft report.

14.4.2 Preliminary Conclusions

The results of the analyses to date have supported certain preliminary conclusions reached last quarter.

(1) In-plant conditions: BNL staff have continued evaluating specific accident sequences to determine if readily identifiable plant conditions exist which permit selection of appropriate protection action strategies. Results indicate that such links do exist and that protective action strategies can be based on in-plant observables for those accident sequences examined to this point.

(2) Warning time: BNL staff analysis of severe accidents indicates that warning times of several hours or more can be expected for the more probable accident sequences, e.g. small break LOCA or transients. Short warning times of 1 hour or less are associated only with less probable accident sequences which should be readily identifiable by the operator.

(3) Weather: The importance of weather in defining the consequences of a radioactive release has been convincingly reconfirmed in our analyses of different accident scenarios.

(4) Plume rise: The energy of release is an important parameter since it could influence the dose to individuals downwind.

NRC FORM 335 (11 81)

U.S. NUCLEAR REGULATORY COMMISSION

BIBLIOGRAPHIC DATA SHEET

1. REPORT NUMBER (Assigned by DDC)
NUREG/CR-2331
BNL-NUREG-51454, Vol. 4, No.4

4. TITLE AND SUBTITLE (Add Volume No., if appropriate)
Safety Research Programs Sponsored by Office of Nuclear Regulatory Research, Quarterly Progress Report October 1 - December 31, 1984.

2. (Leave blank)

3. RECIPIENT'S ACCESSION NO.

7. AUTHOR(S)
Compiled by Allen J. Weiss

5. DATE REPORT COMPLETED
MONTH: March | YEAR: 1985

9. PERFORMING ORGANIZATION NAME AND MAILING ADDRESS (Include Zip Code)
Brookhaven National Laboratory
Department of Nuclear Energy
Upton, New York 11973

DATE REPORT ISSUED
MONTH: May | YEAR: 1985

6. (Leave blank)

8. (Leave blank)

12. SPONSORING ORGANIZATION NAME AND MAILING ADDRESS (Include Zip Code)
U. S. Nuclear Regulatory Commission
Office of Nuclear Regulatory Research
Washington, D. C. 20555

10. PROJECT/TASK/WORK UNIT NO.

11. FIN NO.
A-3014,15,16,24, A-3208,15, 26,27,42,66,68,70,71,72,74,75, 77

13. TYPE OF REPORT
Quarterly

PERIOD COVERED (Inclusive dates)
October 1 - December 31, 1984

15. SUPPLEMENTARY NOTES

14. (Leave blank)

16. ABSTRACT (200 words or less)

This progress report will describe current activities and technical progress in the programs at Brookhaven National Laboratory sponsored by the Division of Accident Evaluation, Division of Engineering Technology, and Division of Risk Analysis & Operations of the U.S. Nuclear Regulatory Commission, Office of Nuclear Regulatory Research.

The projects reported are the following: High Temperature Reactor Research, SSC/MINET Development, Validation and Application, Thermal-Hydraulic Reactor Safety Experiments, Plant Analyzer, Code Assessment and Application, Code Maintenance (RAMONA-3B), Calculational Quality Assurance in Support of PTS; Stress Corrosion Cracking of PWR Steam Generator Tubing, Probability Based Load Combinations for Design of Category I Structures, Soil-Structure Interaction Evaluations, Identification of Age-Related Failure Modes; Application of HRA/PRA Results to Resolve Human Reliability and Human Factors Safety Issues, PRA Technology Transfer Program, Emergency Action Levels, and Protective Action Decisionmaking.

17. KEY WORDS AND DOCUMENT ANALYSIS

17a. DESCRIPTORS

High Temperature Graphite Reactor
Super System Code
MINET Code
Thermal-Hydraulic Reactor Safety
Emergency Action
Plant Analyzer
RAMONA-3B
Pressurized Thermal Shock
Stress Corrosion Cracking
Protective Action
Prob. Risk Assessment
Load Combinations
Nuclear Plant Aging
Human Error
Human Factors

17b. IDENTIFIERS/OPEN-ENDED TERMS

18. AVAILABILITY STATEMENT

19. SECURITY CLASS (This report)

21. NO. OF PAGES

20. SECURITY CLASS (This page)

22. PRICE
S